Hungary-Serbia
IPA Cross-border Co-operation Programme

The project is co-financed by the
European Union

URBAN CLIMATE AND MONITORING NETWORK SYSTEM IN CENTRAL EUROPEAN CITIES

Urban-Path

Good neighbours creating common future

Novi Sad (Serbia) – Szeged (Hungary)
2014

EDITED BY
Kosztolányi Éva, project manager
Dr. Vladimir Marković, project manager

AUTHORS
Dr. János Unger, lead scientist; Dr. Stevan Savić, researcher;
Dr. Tamás Gál, researcher; MSc Dragan Milošević, researcher

PUBLISHED BY
University of Novi Sad, Faculty of Sciences (UNSPMF)
University of Szeged, Department of Climatology and Landscape Ecology (SZTE)

LAYOUT
Stojkov štamparija, Novi Sad

PRINTING AND BINDING
Stojkov štamparija, Novi Sad

ISBN
987-86-7031-341-5 (SRB)
..... (HU)

CONTACTS
www.hu-srb-ipa.com
http://urban-path.hu

EMAILS
unger@geo.u-szeged.hu (Dr. János Unger, lead scientist)
vladimir.markovic@dgt.uns.ac.rs (Dr. Vladimir Marković, project manager)

THIS PUBLICATION HAS BEEN FINANCIALLY SUPPORTED BY IPA CROSS-BORDER CO-OPERATION PROGRAMME (HUSRB/1203/122/166)

The project is co-financed by the European Union

Content

The project is co-financed by the European Union

Foreword

In the second part of the 20th century the urbanization accelerated and reached enormous magnitude. The Earth's urban population grows faster than the total population, therefore more and more people live in urbanized regions. Not only the large cities but also the smaller ones can modify almost all properties of the urban atmospheric environment compared to the natural surroundings. Thus owing to the artificial factors a local climate (*urban climate*) develops that means a modification to the pre-urban situation. This climate is a result of the changes in radiation, energy and momentum processes. These changes are caused by the artificial building-up, as well as by the emission of heat, moisture and pollution related to human activities.

In the course of urban climate development the temperature shows the most obvious modification compared to the rural area. This modification mainly consists of an increase which is manifested in the *urban heat island*.

In this study we firstly review the acceleration of urbanization. After the main reasons of the development and peculiarities of urban climate (stressing the heat island) are dealt with, then the tools of the heat island effect mitigation and the related energy-saving possibilities are discussed. In the second chapter, new methods of defining local climate zones and station locations in urban areas are presented in details. Furthermore, created urban climate monitoring network systems in Szeged (Hungary) and Novi Sad (Serbia), based on new methods, in the last two subchapters are shown. In the last part of this study, there are reviewed the five most important published scientific papers related with URBAN-PATH project issues.

Szeged – Novi Sad
May 2014

Dr. János Unger
Dr. Stevan Savić

1. Theoretical background of UHI

1.1. Acceleration of urbanization

Large development of the European settlements started at the age of the industrial revolution (17-18th centuries), while at the first half of the 20th century the development in America was the most striking. In the last decades development of different agglomerations can be detected worldwide (*Figure 1*). The largest urbanization is in the Third World, which is only partly the consequence of the industrialization, but rather the explosion-like population increment (e.g. Lagos, Mexico City, Sao Paulo, Mumbai, Dacca, Cairo).

The urbanization levels of different historical ages are clearly reflected in the ratios of the urban population compared to the total population. According to these values, 2.4%, 13.6%, 33.6%, 41% and 46.6% of the Earth's population lived in cities in the years of 1800, 1900, 1960, 1985 and 2000, respectively (*Table 1*).

Recently, the number of cities with more than one million inhabitants is over 200, the built-up areas are continually expanding and their ratios are even larger than 10% in the developed countries. Ac-

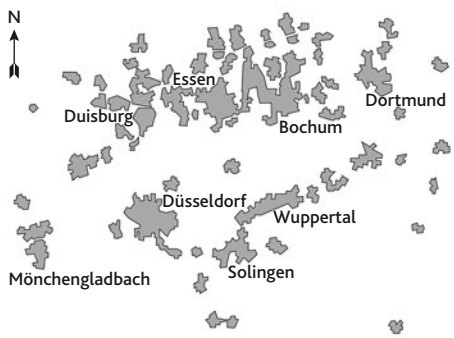

Figure 1. Agglomeration of Ruhr-area

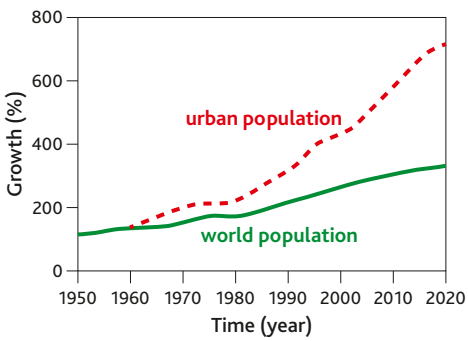

Figure 2. World and urban population growth between 1950 and 2020 (1950 = 100%)

Table 1. Number of urban population and its ratio compared to the total population

Region	1950		1985		2000	
	%	mill.	%	mill.	%	mill.
world	29.2	734.2	41.0	1982.8	46.6	2853.6
developed	53.8	447.3	71.5	838.8	74.4	949.9
developing	17.0	286.8	31.2	1144.0	39.3	1903.7

cording to the *Figure 2* the Earth's population multiplies 'only' threefold, while the urban population sevenfold by the year of 2020 compared to 1950.

1.2. Main reasons of the urban climate development

The surface and atmospheric modifications associated with the construction and operation of cities are massive. When a new city (or a neighbourhood) is developed it is apparent that a mosaic of microclimates is being created. At the scale of a person walking amongst the buildings, the spatial variation of microclimates is huge. That person can be a sunny spot or in shade, buffeted by swirling winds or becalmed, in relatively hot/dry or cool/moist surroundings, all just walking a few metres from the street into a building courtyard. However, within a neighbourhood of similar building types, the mix of microclimates tends to be repeated so that an ensemble climate at the local scale is created. In turn, when these are combined with the climates of the other urban land uses, a special climate at the city scale is produced (Oke, 1997). This is the **urban climate** which is defined as a local climate that is modified by interactions between built-up area and regional climate (WMO, 1983).

According to the preceding section about half of the human population is affected by the loads of urban environments: environmental pollution, noise, stress of the accelerated life-style and last but not least the modified parameters of the urban atmosphere compared to the natural environment. This makes study of urban impact on climate particularly important.

The location of a city in a given macro-scale climate zone, its size (population, area) and structure, economy features all have significant impacts on the magnitude of the developed urban/rural climatical differences. Certain physical geographical features of its wider environment (e.g. (a) topography – valley, basin, slope, plain, (b) coastal location – sea, large lake, and (c) surface type – wetland, desert) may intensify or moderate the changes occur by the anthropogenic impacts. The reasons of these changes are:

- Replacement of natural surfaces by buildings and impermeable surfaces (roads, pavements, parking lots) combined with sanitary and storm sewer systems.
- The geometry of the urban surface is very complex, the irregularities are varied horizontally as well as vertically (from street surfaces to different building heights) (*Figure 3*).
- Physical properties of road and building materials are different from the original natural ones. Usually they have lower albedo, higher heat conductivity and heat capacity.
- Important factors considering the radiation processes are the materials released by the heating, traffic and industrial processes, for example water vapour, gases, smoke and other solid pollutants which cover the city as a haze (*Figure 4*).
- In certain cases and periods the heat produced by human activities (industry, traffic, heating) and released into

Figure 3. Skycrapers in New York

Figure 4. Photochemical smog over Mexico City

the environment can also be significant (*Figure 5*).

Figure 6 summarizes the factors influencing the peculiarities of the urban climate. Among them there are those which can not be changed ('fixed'), others have significant role as 'modulators'. Factors related to impacts of human activities are 'controllable', that is – theoretically – they can be formed according to the demands during the processes of urban planning, building and space design.

The boundary layer over settlements is different compared to the rural one. Two layers can be recognized: one is governed by processes acting at micro-scale; the other by those at the local or meso-scale (Oke, 1976).

The first layer is termed **urban canopy layer** (UCL), which consists of the air contained between the urban roughness ele-

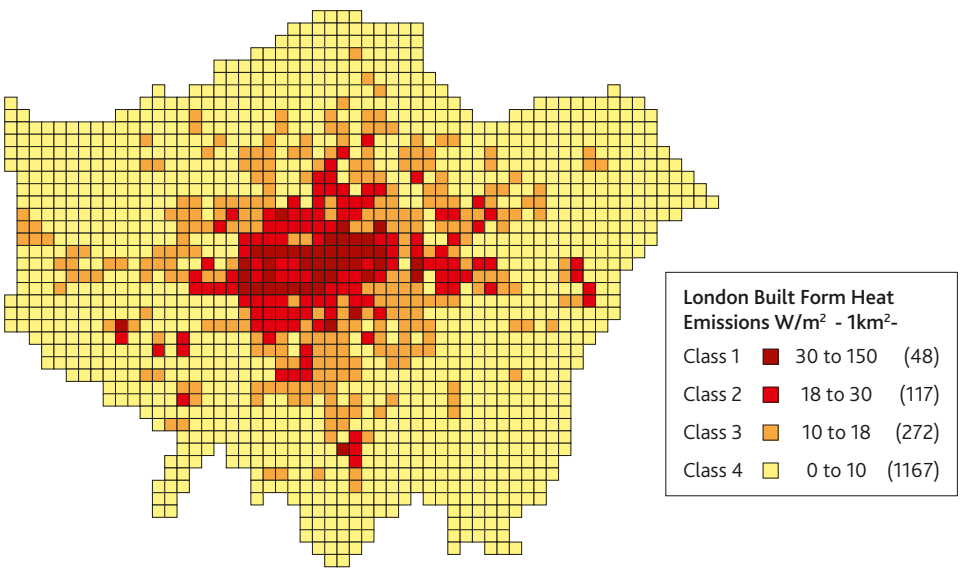

Figure 5. Annual average heat emission from buildings (1×1 km) in London (2005) (Hamilton et al., 2009)

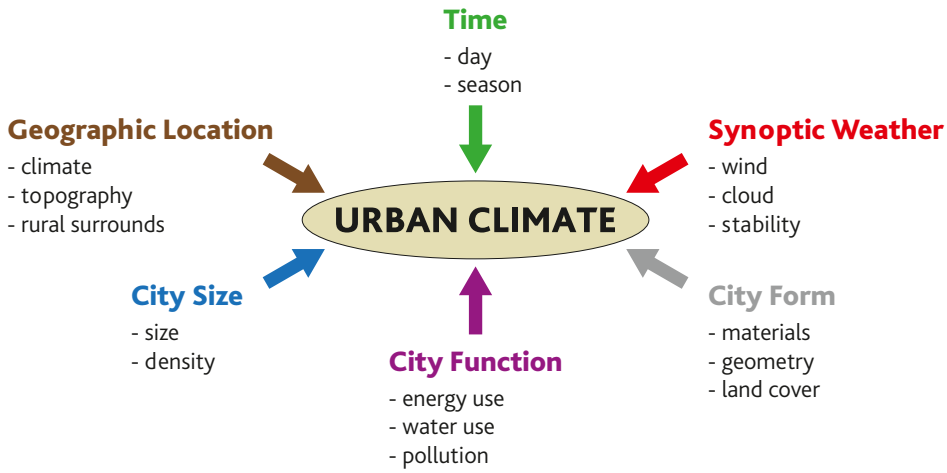

Figure 6. Factors influencing the peculiarities of the urban climate

ments (mainly buildings) (*Figure 7*). The UCL is a micro-scale concept, its climate being dominated by the nature of the immediate surroundings (especially site materials and geometry). The upper boundary of the urban canopy is likely to be imprecise because of the complexity of the urban 'surface'. In densely built-up areas the limit is near at roof level; in large open spaces it may be entirely absent.

The second layer, situated directly above the first one is called **urban boundary layer** (UBL) (*Figure 7*). This is a local to meso-scale phenomenon whose characteristics are affected by the presence of an urban area at its lower boundary. Its height depends on the roughness conditions of the underlying urban surface. In the downwind region this layer may become separated from the surface as a new rural boundary layer develops underneath, and this has been termed the **urban plume**.

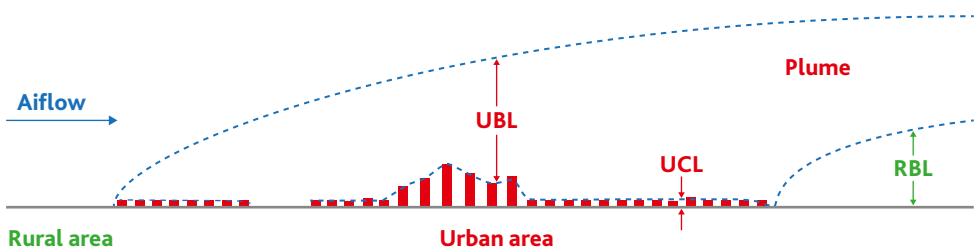

Figure 7. Schematic representation of the urban atmosphere with its two layer (the slope of the UBL is between 1:100 and 1:200 in reality) (Oke 1976)

1.3. Radiation budget and energy balance in urban areas

The city has a marked impact upon the short- and long-wave components of the net radiation budget due to the presence of the pollutants in the air and to changes in the surface radiative properties (Oke, 1982).

The incoming short-wave radiation (1) and that reflected from the city surface (3) are subjected to greater attenuation in the polluted urban air than the equivalent fluxes in the rural areas (*Figure 8*). The amount received at the surface (K↓) consists of direct-beam and diffuse (2) plus net back-scattered (4) is generally 2-10% lower in the city. Because of the intensive turbulence and mixing these values smaller in summer than in winter (Kuttler, 1998). Pollution and the associated fog (smog) used to cause some British cities to lose 25-55% of the incoming solar radiation during winter. In 1945 it was estimated that the city of Leicester lost 30% radiation in winter, as against 6% in summer (Barry and Chorley, 1982). The losses are greatest in the morning and late afternoon hours when the sun's rays travel longer path through the polluted layer because of the low solar angle. In the developing countries the loss can be increased even during a few decades as a result of explosion-like urbanization and its related processes (e.g. Cairo) (Rooba, 2006).

On the other hand the urban albedo values are typically 0.05 to 0.10 lower than for the countryside in the mid-latitudes (Oke, 1974), that is the reflected short-wave radiation (K↑) is smaller. This can be attributed partly to the colours of the building materials and to the shorter-life snow cover, partly to the beams trapped by the dissected surface.

Similar off-setting of effects occurs in the long-wave radiation budget (*Figure 8*). Because of the developed heat island

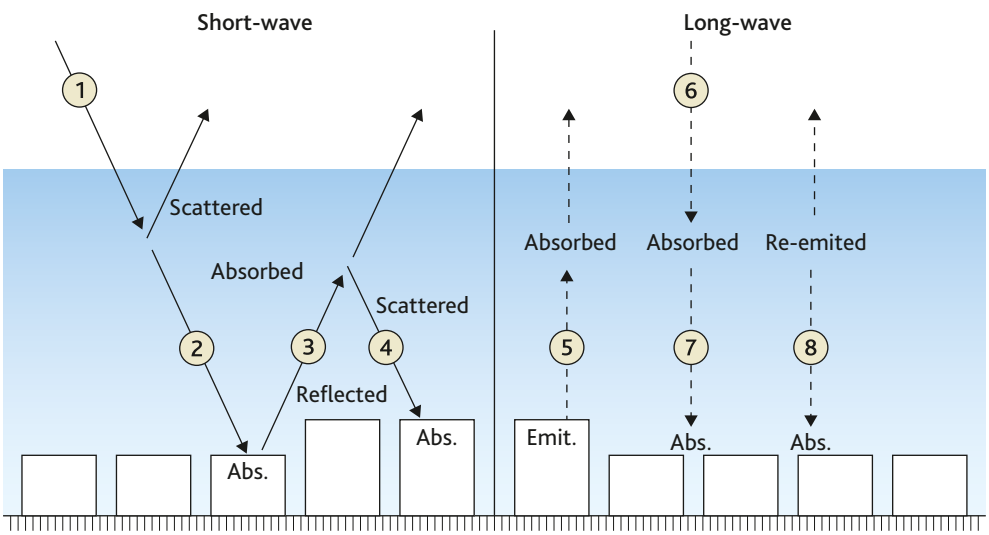

Figure 8. Schematic depiction of radiative exchanges in a polluted urban boundary layer (Oke, 1982)

Table 2. Components of radiation balance and Q_F (Wm^{-2}) in the city and its rural area at different times in summer (Cincinnati, Ohio)

	City core			Rural		
	08h	13h	20h	08h	13h	20h
K↓	288	763	-	306	813	-
K↑	42	120	-	80	159	-
L*	-61	-100	-98	-61	-67	-67
Q*	184	543	-98	165	587	-67
Q_F	36	29	26	-	-	-

(see Section 6) the higher surface temperature of the city produces an enhanced emission (5). A relative large part of this is absorbed by the polluted air layer and re-radiated back to the surface along that portion of sky radiation (6) transmitted to the surface (7), and that emitted by the warmed urban air (8). At night these combined long-wave inputs are slightly larger in the city than in rural areas, and by day the excess may be greater still, due to emission from solar heated pollutants.

In summary both long- and short-wave inputs (K↓, L↓) and outputs (K↑, L↑) are increased by urbanization so that urban/rural net all wave radiation (Q*) differences are small, probably less than 5%. Of course the anthropogenic heat (Q_F) increases the urban input. *Table 2* gives some values as examples.

At the scale of the UBL the spatially-integrated energy-exchanges between the city and its overlying air have to be considered. Here the 'surface' corresponds to the level of the UCL/UBL interface. The fluxes across this plane comprise those from the individual UCL units (such as roofs, trees, lawns, roads, etc.) integrated over larger land-use divisions. In centre of such a division, where meso-scale advective effects may be neglected, the energy balance becomes:

$$Q^* + Q_F = Q_H + Q_E + \Delta Q_S$$

where Q_F – is the anthropogenic heat flux.

The terms of a suburban energy balance and their diurnal variation are shown in *Figure 9.* Note that the sensible and latent fluxes are of similar magnitude during the daytime so the rate of evapotranspiration is far from insignificant. It is probably due to the higher ratio of (irrigated) green areas in suburbs.

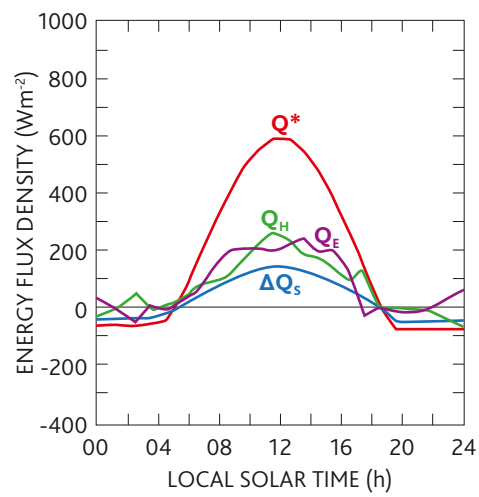

Figure 9. Daily variations of the energy balance terms in a suburban area (Vancouver, Canada) (Oke, 1982)

But, in the case of inner city it can be established that the role of the latent heat (Q_E) decreases further compared to rural areas but it is still far from negligible. However, the urban heat storage (ΔQ_S) is significantly larger than in its surrounding areas because of the greater thermal conductivity and heat capacity. Especially at night, when storage assumes a more significant role in the energy balance of both urban and rural environments, thus it may be important in maintaining higher urban temperatures.

In summary, the impact of urbanization is to favour to partitioning of energy into sensible (warming the air) rather latent heat and to increase heat storage by the system.

1.4. Water balance in urban areas

The urban (soil-building-plant-air system) water balance is expanded by new components (F, I) compared to the natural one (Oke, 1987):

$$p + F + I = E + Dr + DS (+ DA)$$

where F – water released to the atmosphere by anthropogenic processes, I – water supply piped in from rivers and reservoirs, and DA – net amount of water droplets and water vapour advection to/from the city air. This balance applies to a layer which extends to depth where vertical water (f) exchange is negligible (*Figure 10*).

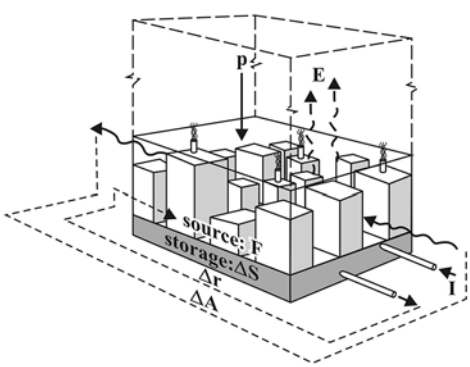

Figure 10. Components of urban water balance (Oke, 1987)

Considerable amounts of water vapour are released when fossil fuels such as natural gas, gasoline, fuel oil and coal are burnt. The use of water to absorb 'waste' heat from power plants and other industrial processes also greatly enhances vaporization from cooling towers, cooling ponds, rivers and lakes. These provide a source of vapour for the urban atmosphere and they are summarized in term F. The importation of water to the city (I) is necessary to meet demands from residential, industrial and other users. This mass input to the city system can be fairly easily monitored by the date of supplier companies. Ultimately this water is lost from the system via evapotranspiration and runoff. F and I are mass flows that are directly controlled by human decisions and respond to the daily and seasonal rhythms of human activities.

Let us compare the water balance of an urban (soil-building-plant-air) system with that of a corresponding rural (soil-plant-air) system. To simplify matters consider both to have an extensive area, so that the advective term (DA) may be neglected for both.

The water input of the urban system is greater because its precipitation (p) is aug-

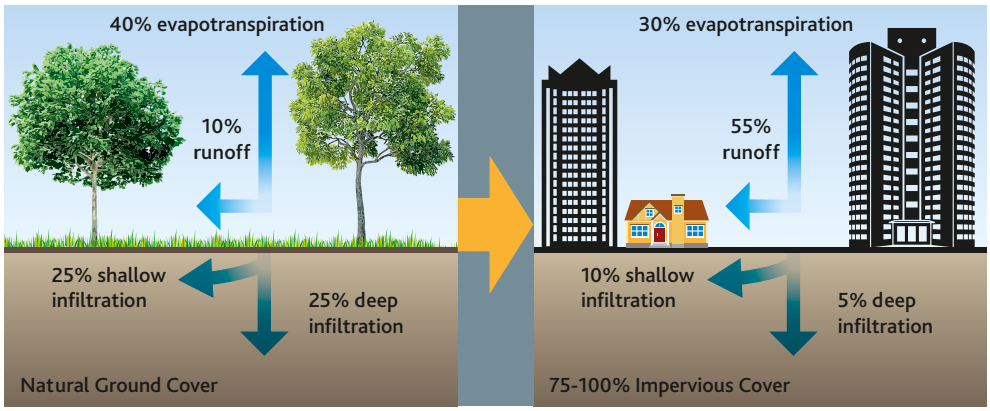

Figure 11. Partitioning of the water balance components in urban and rural areas

mented by F and I (*Figure 11*). Anyway, because of the extra condensation nuclei of anthropogenic origin the precipitation amount over and near the city may be increased, especially in the case of showers. On the other hand, usually the urban evapotranspiration (E) and DS are less because of the reduction of the original vegetation cover and its replacement by relatively impervious materials. Although the complex surface of the city presents a larger interception area for the precipitation, the poor infiltration properties of urban materials outweigh this benefit and thus water storage amount is smaller than in the rural case. It follows from these considerations that the third term on the right-hand side of the balance the runoff (Dr) is greater in urban areas. One part of this growth is due to the disposal of a portion of I as waste water via sanitary sewers, the other part is due to the waterproofing of surface building materials and artificial runoff routing (e.g. storm sewers).

1.5. Urban temperature modification

The **urban heat island** (UHI) is a thermal excess which is a result of urban/rural energy balance differences. Many kinds of UHIs can be detected according to the target medium (air, surface, sub-surface) (*Figures 12 and 13*). Of course, they are related to each other, but there are substantial differences in their generating processes and temporal dynamics. Now the discussion is concentrated on the warm urban air in which two heat islands (UCL and UBL) can be distinguished according to the layers of urban atmosphere. In the following our establishments are related to the heat island developed in the UCL.

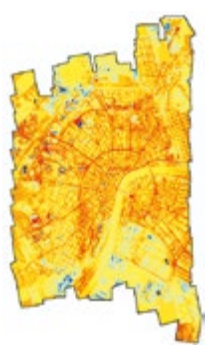

Figures 12. Nocturnal surface temperature pattern (Szeged, 14 August, 2008)

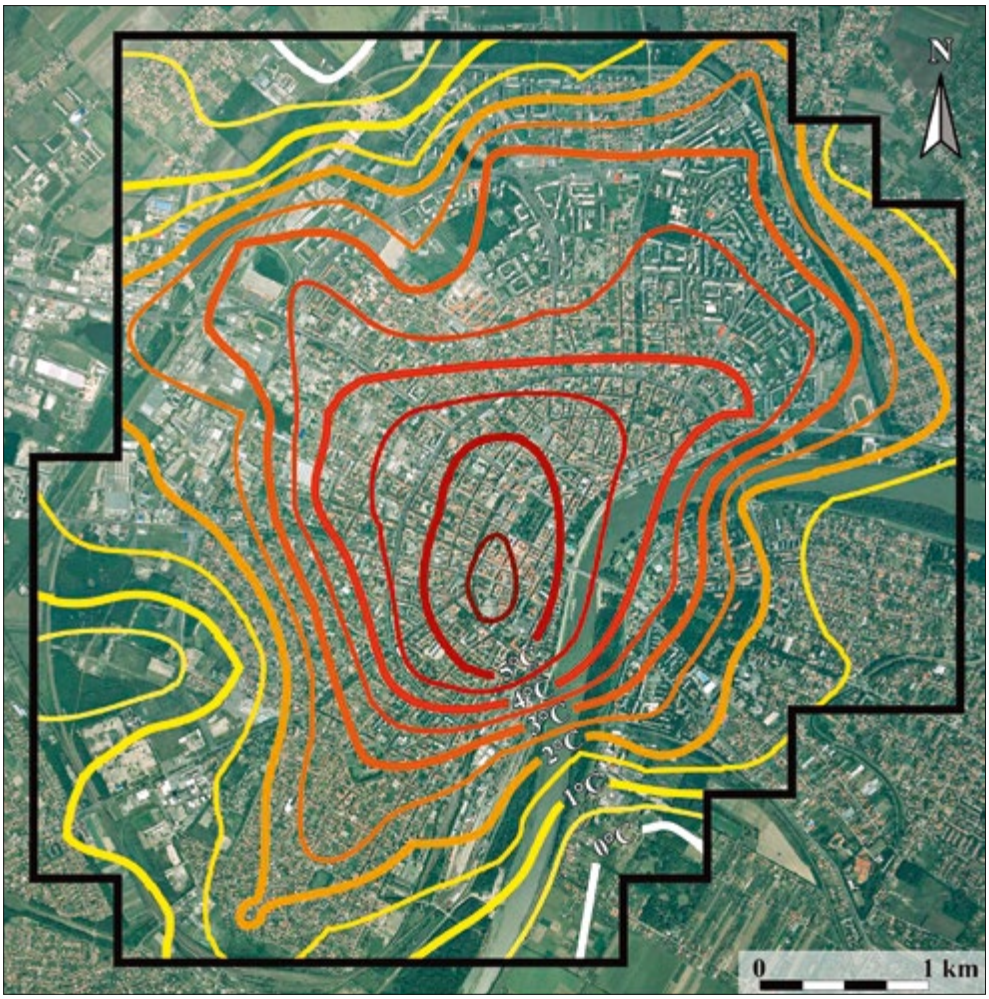

Figures 13. Nocturnal UHI intensity distribution (Szeged, 25 March 2003)

1.5.1. Spatial and temporal features of the urban heat island

Presentation of the UHI by isotherms showing the spatial distribution and magnitude of the temperature excess relative to the surroundings of the city is well illustrated: the more or less circular and closed lines remind us on the topographical appearance of islands on contour maps (*Figure 14*). At the urban/rural boundary the temperature is increased significantly ('cliff'), and much of the rest of the urban area appears as a 'plateau' of warm air with a steady but weaker horizontal gradient of increasing temperature towards the city centre. It may be interrupted by warm and cold spots associated with areas of anomalously high or low building density. A park or lake might be relatively cool whereas an industrial area

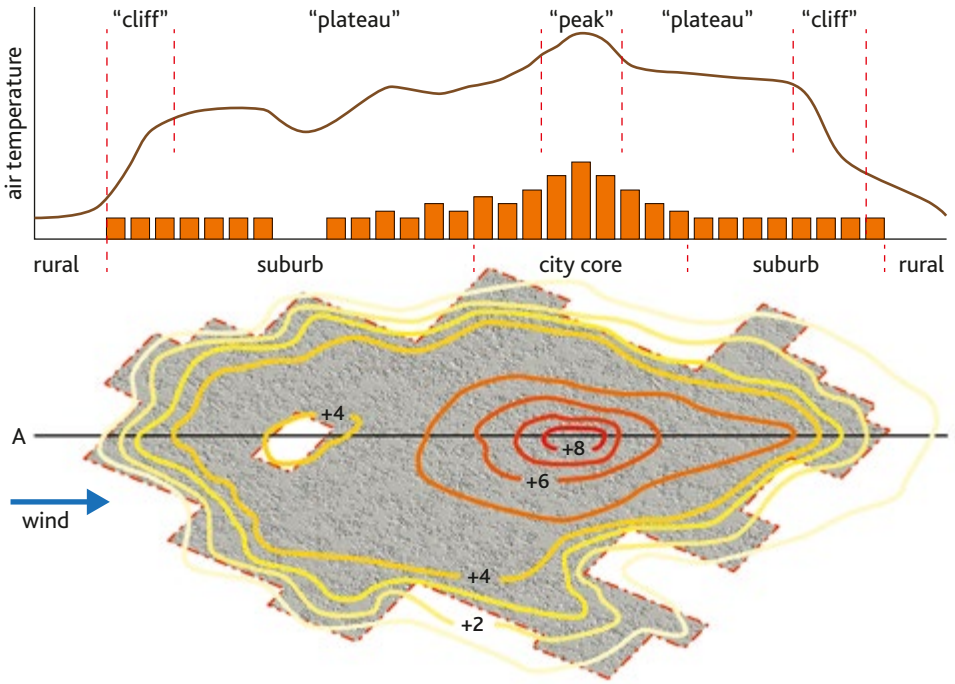

Figure 14. Spatial pattern of UHI along a cross-section (AB) and its horizontal structure (after Oke, 1982)

or a shopping centre might be relatively warm. The densely built urban core shows a final 'peak' to the heat island where the largest temperature difference is observed (Oke, 1987). This relatively regular configuration exists only during those weather situations which promote the development of microclimatic processes. The **heat island intensity** (ΔT) is defined as the difference of temperatures measured at same time over the urban and rural surfaces.

The ΔT exhibits a marked diurnal variation. Its main feature is that because of the more moderate cooling in the late afternoon and evening the minimum temperature at dawn is not so low as in rural areas (*Figure 15*). At the same time the urban atmosphere warms slowly after sunrise. As a result the intensity grows sharply around sunset to a maximum a few hours (3 to 5 h) later (Oke and Maxwell, 1975). In the remaining part of the night the temperature difference decrease slowly but steadily, then the decreasing strengthens at sunrise. So the intensity variation during the day is governed by the different cooling/warming rates between the urban and rural areas.

Diurnal and annual variations of UHI can be presented very clearly by isopleths (*Figure 16*). According to the investigation based on hourly values there are scarcely any differences between 7 and 18 hours, moreover they can be negative too. These negative values with a maximum at about noon appear during spring and summer (e.g. -1.2°C), while in autumn and winter the differences are positive all

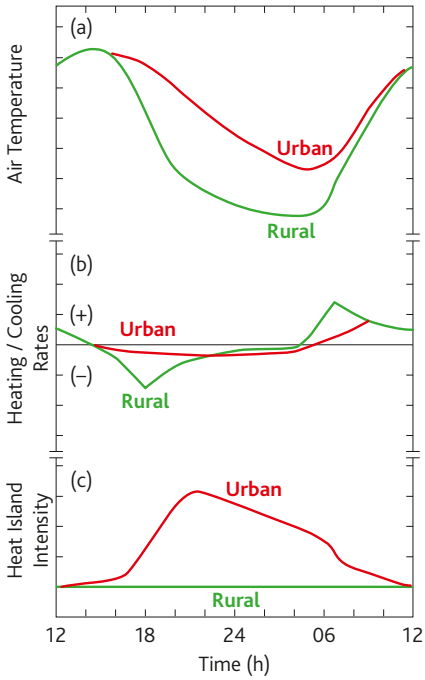

Figure 15. Temporal variation of urban and rural (a) air temperature (°C), (b) heating/cooling rates (°Ch-1) and (c) the resulting UHI intensity (°C) (Oke, 1982)

day. The positive deviations are the greatest at night and they can reach even 3.5°C in summer, while in winter the intensities are more moderate. This supports an earlier statement that the UHI is primarily an evening and nocturnal phenomenon.

1.5.2. Other heat island controls

In previous sections the main reasons forming the special climate of cities were already discussed. Now some additional factors will be mentioned which have quantitative influence on the strength of the heat island.

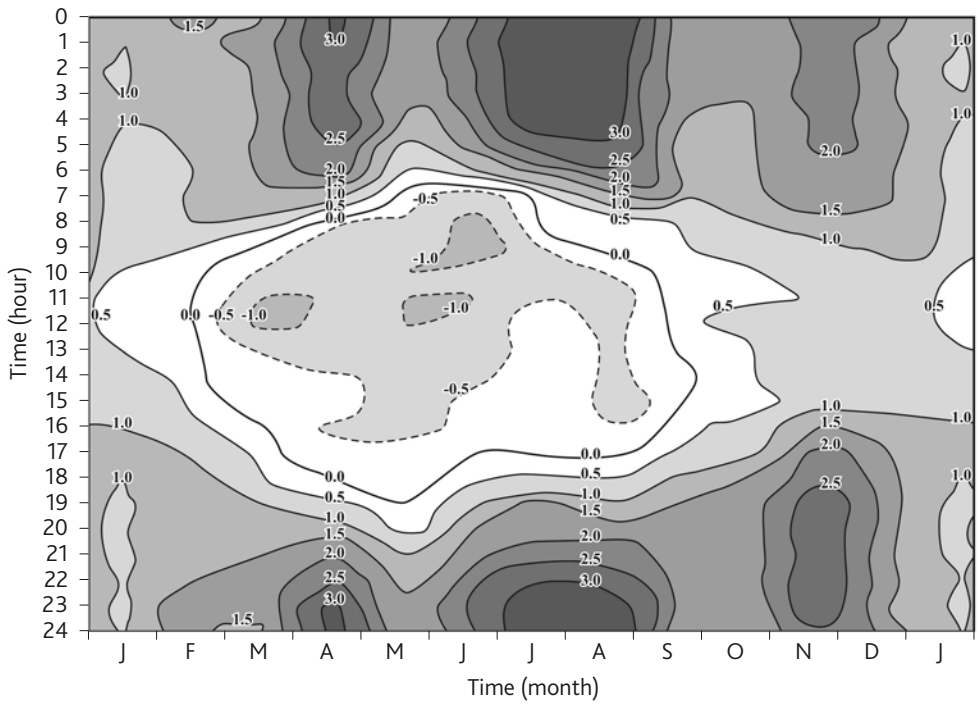

Figure 16. Annual and diurnal variation of UHI intensity

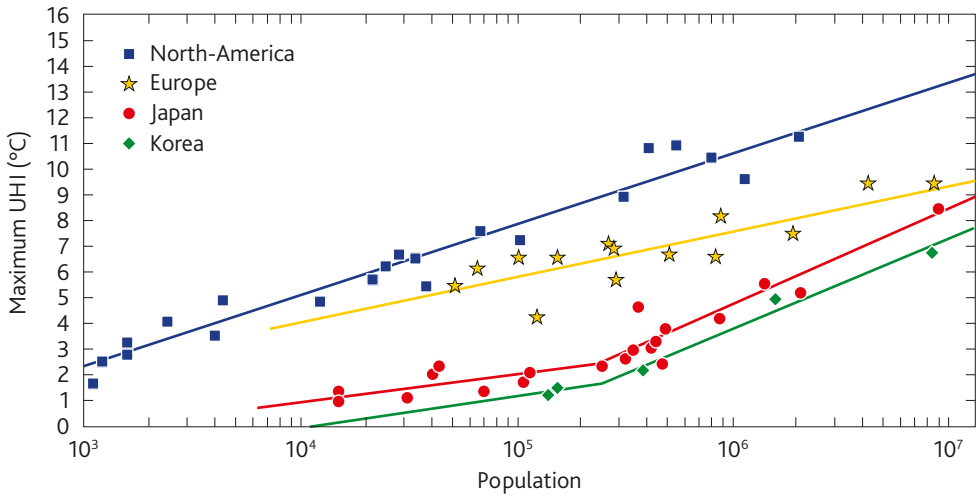

Figure 17. Relation between maximum UHI intensity and population for North-American, European, Japan and Korean settlements (Oke, 1973; Park, 1987)

The maximum heat island intensity (ΔT_{max}) is strongly related to the city size. A surrogate of city size is its population (P). The relation is found to be proportional to logP: the obtained two equations have some deviations according to the numbers of cities taking into consideration:

$$\Delta T_{max} = 2.01 \cdot \log P - 4.06 \ [^{o}C]$$

$$\Delta T_{max} = 1.92 \cdot \log P - 3.46 \ [^{o}C]$$

Figure 17 shows that even settlements with population of 1000 have a heat island and in the case of mega-cities with millions of inhabitants the possible greatest thermal modifications is about 12°C (Park, 1987; Klysik and Fortuniak, 1999). Certain difference can be seen in the slopes of North-American and European cities, as well as the Japan and Korean cities are particularly interesting because the regression lines bend. This is partly due to differences in the nature of the cities (different urban structures, traditions in building constructions, heat release) existing in different regions of the world. Therefore the characterization of city size with its population is not always satisfactory to explain the considered physical phenomenon. That is it cannot be negligible at all regarding the heat island intensity whether widely separated low buildings or compact built-up structure with tall elements is dominated in a given settlement. *Table 3* gives a few examples on the maximum temperature excess generated by cities.

Weather controls (particularly wind and clouds) on the development of heat island have significant influence on the UHI magnitude. For heat island generation the high pressure (anticyclonic) weather situations are the most favourable when the sky is clear and the air is calm. Clouds moderate the differences of radiation inputs and outputs, thus also the urban/rural temperature differences. The strong wind significantly weakens or even prohibits the heat island development. As larger cities are able to generate

Table 3. Examples on the maximum UHI intensity values (Matzarakis, 2001)

City	Investigated period	ΔTmax (°C)
Barcelona	Oct. 1985 – July 1987	8.2
Calgary	1978	8.1
Mexico City	1981	9.4
Montreal	15 Feb. 1970 (22h)	10.5
Moscow	1990	9.8
München	1982-1984	8.2
New York	July 1964 – Dec. 1966	11.6
Szeged	July 1977 – May 1981	8.2
Tokyo	14 March 1992 (3-5h)	8.1
Vancouver	4 July 1972	11.6

larger heat island, therefore the larger the settlement population the stronger wind is necessary to eliminate the formation of thermal differences. There is an empirical relation between the threshold of this limiting wind speed and the population number (Oke and Hannell, 1970):

$$v = 3{,}41 \cdot \lg P - 11{,}6 \ [ms^{-1}]$$

1.5.3. Influence of the intra-urban green areas on temperature

The intra-urban green areas (parks) have an attenuating effect on thermal load not only inside them but this effect may extend beyond the parks into their surrounding built-up areas (Oke, 1989; Eliasson and Upmanis, 2000). As a result of differently cooling green and built-up areas there is a temperature difference which induces a pressure gradient leading to a divergent outflow of cool air at a low level from the park. This is the **park breeze** causing some cooling in the surrounding areas (*Figure 18a*). In the case of moderate wind the cooling effect may be shifted corresponding to the wind direction from a few hundred meters to a few kilometres depending on the park size (*Figure 18b*).

The mentioned cooling effect extending beyond the green areas could be very important and useful for people living near the parks especially in the nocturnal hours during heat-wave periods.

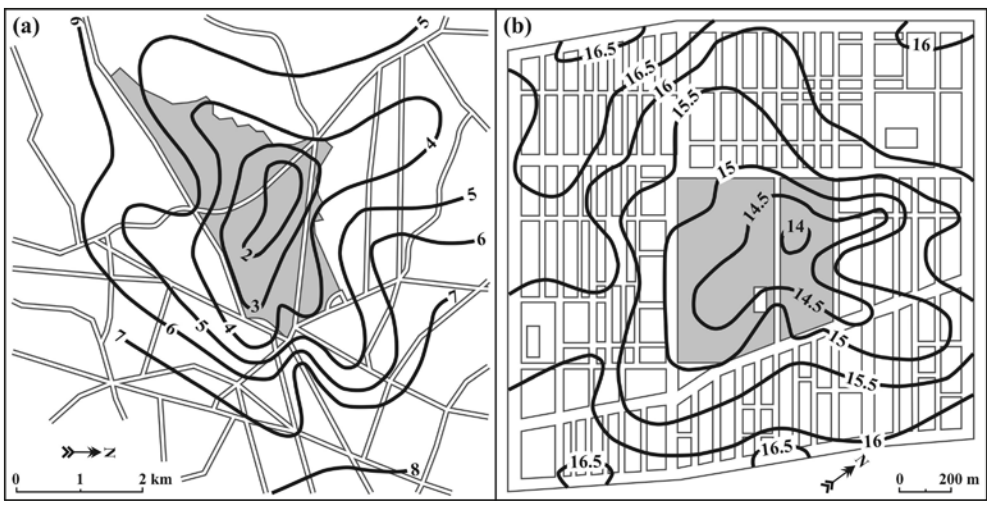

Figure 18. Isotherms (°C) (a) in Chapultepec Park (Mexico City) with clear sky and calm air (3 Dec. 1970, morning), (b) in Parc La Fontane (Montreal) with SW wind of 2 ms-1 and clear sky (28 May 1970, evening)

1.6. Direct effects of heat island

The evaluation of advantages and disadvantages of the UHI has to take into account both summer and winter aspects. The result of this will be quite different depending on a city's geographic location.

During heat-waves, the UHI puts additional heat load on human beings. In winter, the urban heat island might be beneficial by saving heating energy. In addition, a city provides a variety of microclimates that allow individuals to choose their preferred environment. The thermal differences within the various urban microclimates might be greater than the difference between the (spatial means of the) urban climate and the rural climate. The larger a city, the more pronounced the urban heat island and the higher the risk of heat stress in summer. *Table 4* summarizes some measures reflecting the urban impact. Some of them mean positive alterations for urban areas, while others mean negative ones.

1.6.1. Human comfort and health, and others

From the aspect of human comfort the extra thermal load is important. The negative impact of UHI appears mainly in summer. Heat-waves (sustained hot days) usually occur in synoptic situations with pronounced slow air mass development and movement, leading to intensive and prolonged heat stress (*Figure 19*). Global climate change is likely to be accompanied by an increase in the frequency and intensity of heat-waves.

Heat-waves present special problems in urban areas because buildings retain heat if ventilation for cooling at night is inadequate. During heat-waves, inhabitants of urban areas may experience sustained thermal stress both day and night, whereas inhabitants of rural environments often obtain some relief from thermal stress at night. In urban areas the UHI maintains higher temperatures at night, which is to

Table 4. Urban/rural numbers of different days with threshold in Gelsenkirchen (Germany) in a one-year period (Kuttler, 2006) and in Szeged (Hungary) in a three-year period (Unger and Ondok, 1995)

			Gelsenkirchen (1998-1999)		Szeged (1978-1980)	
Season	**Type**	**Threshold**	**Urban**	**Rural**	**Urban**	**Rural**
winter	frost day	$T_{min} < 0°C$	36	57	222	265
	cold day	$T_{min} < 0°C$	19	21	-	-
	winter day	$T_{max} < 0°C$	-	-	37	63
	heating day	$T_{mean} < 15°C$ (G) $T_{mean} < 12°C$ (Sz)	238	255	171	194
summer	warm day	$T_{mean} \geq 20°C$	49	25	-	-
	summer day	$T_{max} \geq 25°C$	47	39	243	208
	sultry day	$T_{max} \geq 30°C$	14	10	-	-
	'beer-garden' day	$T_{21h} > 20°C$	50	22	250	133
	'hot' night	$T_{0h} > 20°C$	21	5	-	-

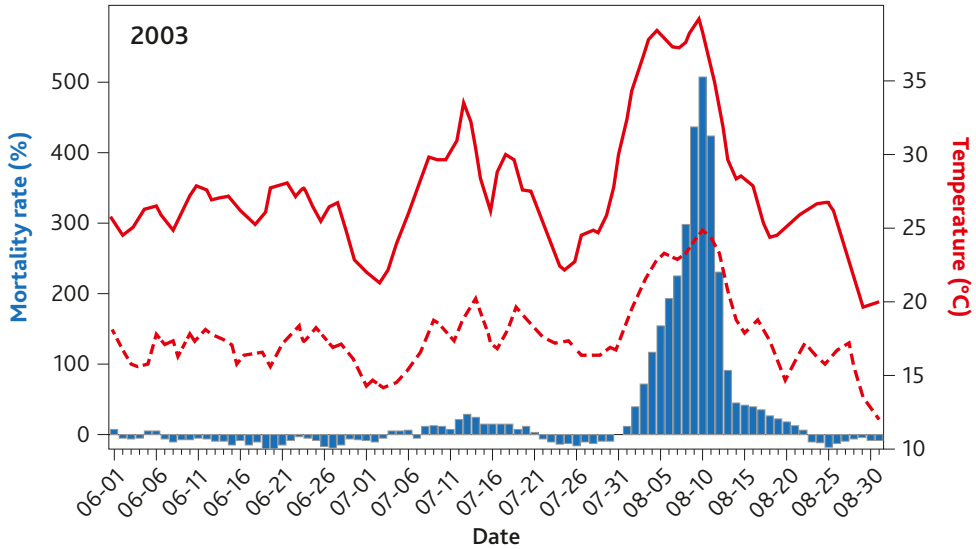

Figure 19. Variations of min., max. temperatures and excess deaths (Paris, summer 2003)

increase the impact on health of continuous hot days, as little relief is experienced at night.

As further impacts of the warmer urban areas the frost-free period becomes longer as well as the vegetation period, and the phenological phases shift (*Figures 20 and 21*). Additionally, the frost intensity and the length of the period with snow cover are reduced.

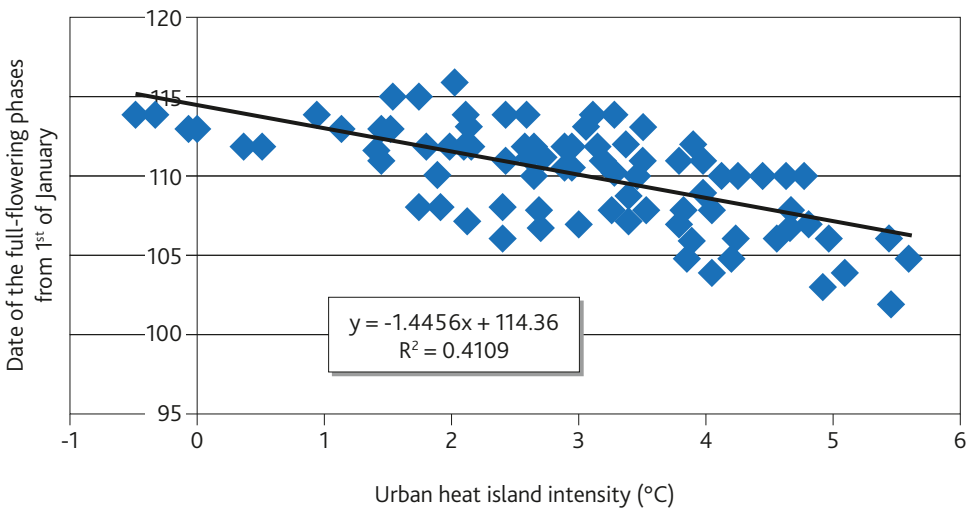

Figure 20. Correlation between the UHI intensity and the time (in Year Day) of the full-flowering in Debrecen (Hungary) in spring 2003 (Lakatos and Gulyás, 2003)

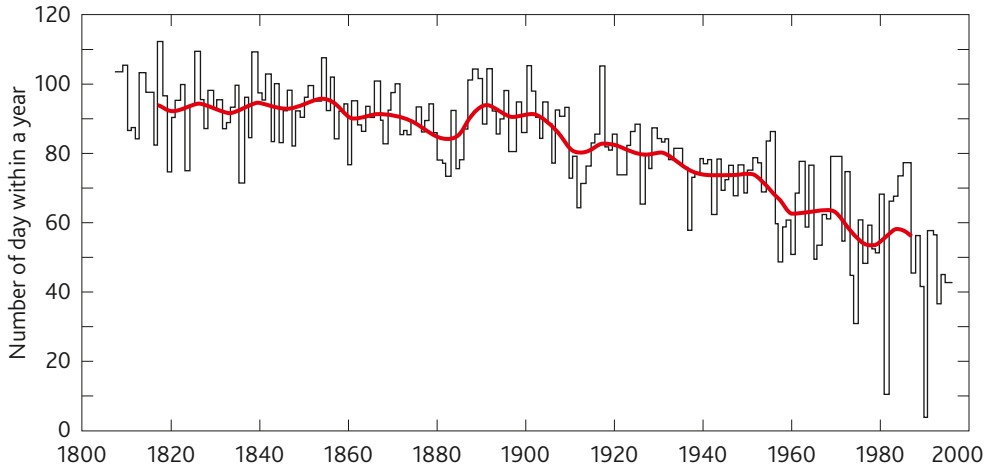

Figure 21. Variation in bud unfolding time of horse-chestnut in Geneva (1810-1995)

1.6.2. Heating/cooling energy demand

Buildings are permanent heating appliances discharging heat all year round from space heating and cooling, artificial lighting and the use of domestic and office appliances.

The need to keep warm (or cool) the buildings may use large amounts of energy. Buildings that are poorly designed can add to this burden through poor insulation, poor planning, overglazing and other aspects. They can also cause occupants to use electric lighting and other equipment more than necessary. Buildings account for about 50% of the energy used in industrialized countries, and much of this is used in building services, especially in air-conditioned buildings, where much of the energy is used as electricity.

Using air-conditioning to overcome the heat stress caused by global warming constitutes a potentially dangerous positive feedback loop. Air-conditioning leads to more energy use, which results in more carbon dioxide being emitted (unless energy that does not cause carbon dioxide emission, such as solar or wind energy, is used), which causes more warming, which requires more air-conditioning (WHO, 2004).

Anthropogenic heat production worsens the urban heat island effect: It is assumed that the increasing trend in the nocturnal urban heat island in London in spring, summer and autumn is caused in part by the greater use of air-conditioning in recent decades (Wilby, 2003). The need to use extra energy to counteract the UHI disproportionally affects resource-constrained people, who often live in urban areas and thus face the heat island phenomenon even more.

In general, the UHI would be expected to result in an increased cooling energy demand in summer and a reduced energy demand in the heating season. For the UK, measured air temperature data have been used (Kolokotroni et al., 2007) as inputs to a building energy simulation computer program to assess the heating and cooling load of a typical air-conditioned office building positioned at 24 different locations

within the London UHI. It was found that the urban cooling load is up to 25% higher than the rural load over the year, and the annual heating load is reduced by 22%. For this particular building and set of assumptions, the absolute gains due to the heating load reductions were outweighed by the increased cooling loads. For non-air-conditioned buildings, the UHI would tend to result in net energy savings, albeit coupled with higher summer temperatures.

One way of indirectly characterizing the UHI impacts is the examination of heating (HDD) and *cooling* (CDD) *degree-days* data (functions of air temperature and a given critical threshold). For example, the HDDs are calculated using the term *heating day*: in this day the daily mean temperature (t_i) is below 12°C. The heating degree-days (HDD) are then calculated by the following formula:

$$HDD = \Sigma (T - t_i)$$

where T is the required room air temperature (20°C) and the summing up refers to the heating days in a heating season. This method assumes that average space heating losses of buildings are proportional to average degree-days and it is used for estimating the energy demand of space heating in buildings (Sailor, 1998, Livada et al., 2002). Cumulative degree-days are, thus, direct indicators of the overall thermal climate for a heating season. *Table 5* gives some examples, where the heating and cooling degree-days are both calculated to a base of 18.3°C (Davies et al., 2008).

Table 5. Reduction in HDDs and increase in CDDs due to UHI effect (1941-70) (calculation base is 18.3°C) (Davies et al., 2008)

Location	Heating degree days			Cooling degree days		
	Urban	Airport	Δ	Urban	Airport	Δ
Los Angeles	384	562	–178	368	191	+177
Washington DC	1300	1370	–70	440	361	+79
St. Louis	1384	1466	–82	510	459	+51
New York	1496	1600	–104	333	268	+65
Baltimore	1266	1459	–193	464	344	+120
London	2419	2779	–360	248	207	+41
Seattle	2493	2881	–388	111	72	+39
Detroit	3460	3556	–96	416	366	+50
Chicago	3371	3609	–238	463	372	+91
Denver	3058	3342	–284	416	350	+66

1.7. Mitigation of heat island effect and related energy savings

Appropriate urban planning and building design provide measures to reduce heat stress for individuals living in cities and the urban heat island. Appropriate architecture can prevent buildings from warming up and thereby ensure comfortable indoor environments without the use of artificial air-conditioning. Architecture considers in-

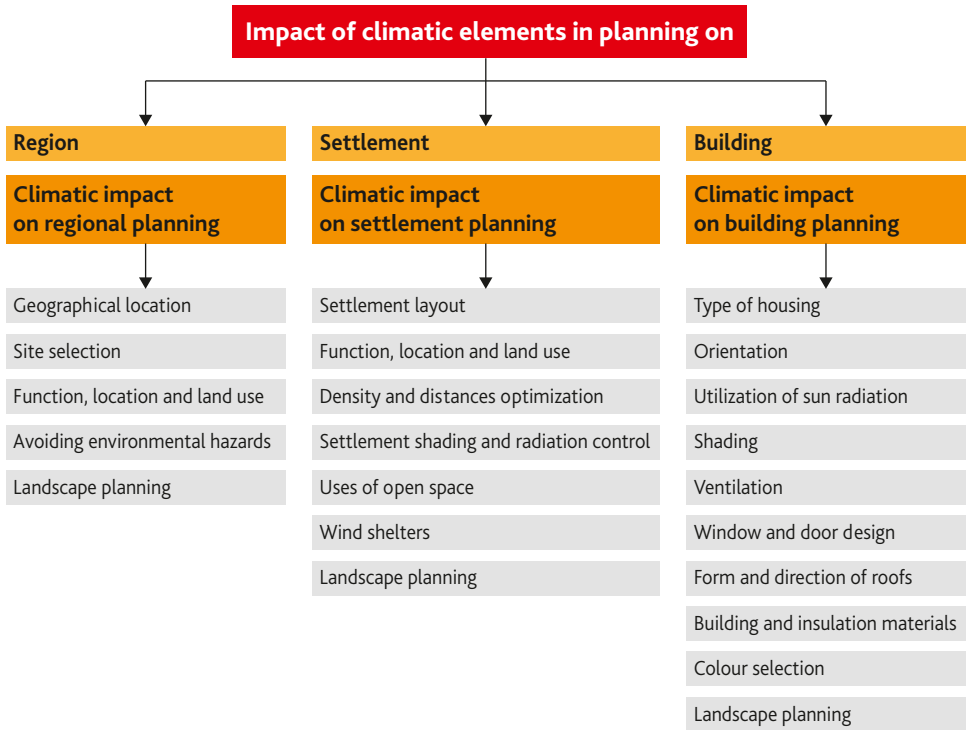

Figure 22. Impact of climatic elements on regional and settlement planning and building design (Bitan, 1988)

dividual buildings, whereas urban design deals with planning the structure of settlements. To maximize thermal comfort in urban areas, climatic aspects should be considered in all scales, from the design of the individual building to regional planning. Figure 22 summarizes the impact of climatic elements on regional settlement planning (urban design) and building design.

The most important tools reducing the UHI effect (they have different significance in different climatic zones) are (*Figure 23*):

- high reflection materials for buildings and roads
- greening the roofs and walls
- planting trees near the building reducing the solar loading and wind effects on buildings
- reducing the solar loading on buildings by artificial shading devices
- variability of building heights
- more spaces between the buildings
- porous pavement
- increase the green area fraction
- construction detention ponds to collect the precipitation (stormwater)
- developing of ventilation paths

Figures 24 and 25 illustrate some of these tools. Tools marked by italics are discussed below in details.

The effects of modifying the urban environment by planting trees and increasing albedo are best quantified in terms of '*direct*' and '*indirect*' contributions.

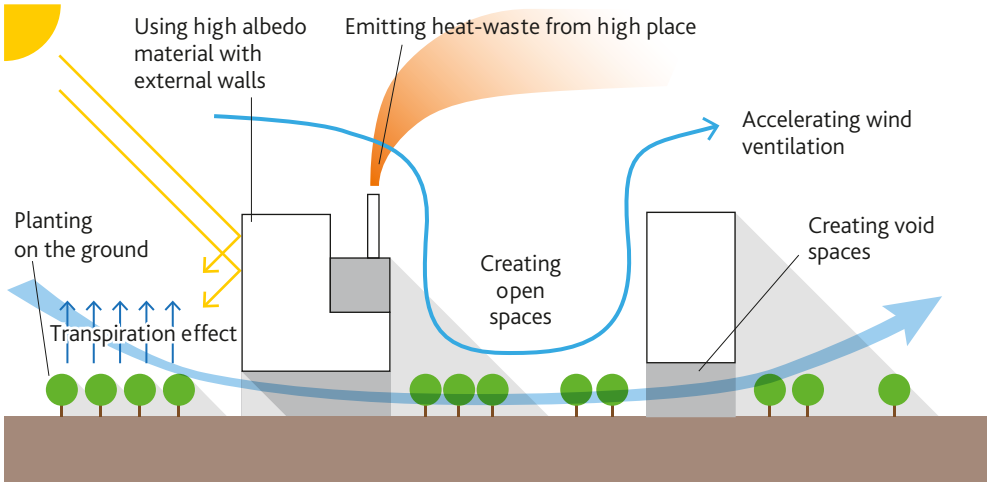

Figure 23. Tools for the mitigation of the UHI effect

The *direct effect* of planting trees around a building or using reflective materials on roofs or walls is to alter the energy balance and cooling requirements of that particular building. However, when trees are planted and albedo is modified throughout an entire city, the energy balance of the whole city is modified, producing city-wide changes in climate. Phenomena associated with city-wide changes in climate are referred to as *indirect effects*, because they indirectly affect the energy use in an individual building. Direct effects give immediate benefits to the building that applies them. Indirect effects achieve benefits only with widespread deployment.

There is an important distinction between direct and indirect effects: while direct effects are recognized and accounted for in present models of building-energy use, indirect effects are appreciated far less. Accounting for indirect effects is more difficult and the results are compar-

Figure 24. Buildings with a large roof area relative to building height make ideal candidates for cool roofing, as the roof surface area is the main source of heat gain to the building

Figure 25. Green roof (Seattle) and green wall (Auckland)

atively less certain. Understanding these effects and incorporating them into accounts of energy use and air quality is the focus of several researches. It is worth noting that the phenomenon of summer urban heat islands is itself an indirect effect of urbanization.

The issue of direct and indirect effects also enters into our discussion of atmospheric pollutants. Planting trees has the direct effect of reducing atmospheric CO_2 because each individual tree directly sequesters carbon from the atmosphere through photosynthesis. However, planting trees in cities also has an indirect effect on CO_2. By reducing the demand for cooling energy, urban trees indirectly reduce emission of CO_2 from power plants. The amount of CO_2 avoided via the indirect effect is considerably greater than the amount sequestered directly (Akbari et al., 1990). Similarly, trees directly trap ozone precursors (by dry-deposition), a direct effect, and indirectly reduce the emission of these precursors from power plants (Taha, 1996).

Figure 26 depicts the overall methodology used in analyzing the impact of heat-island mitigation measures on energy use and urban air pollution.

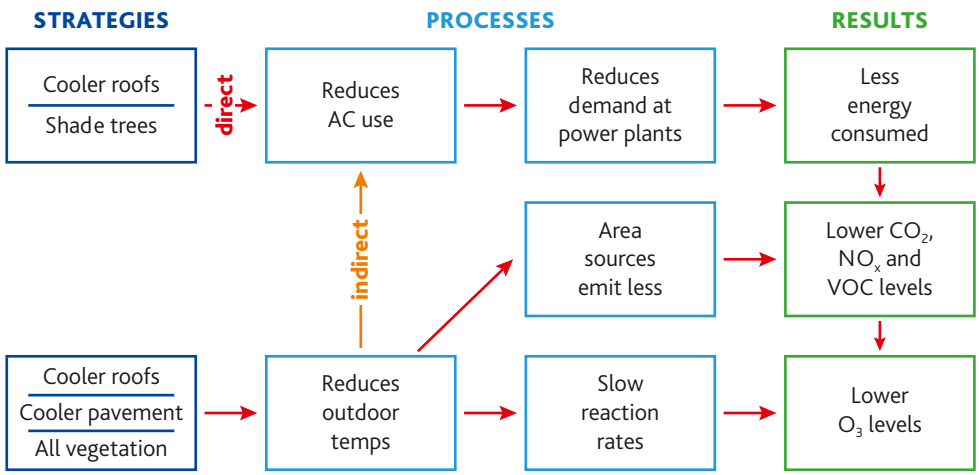

Figure 26. Methodology to analyze the impact of shade trees, cool roofs and cool pavements on energy use and air quality (smog) (Akbari et al., 2001)

Use of high-albedo urban surfaces (roofs and pavements) and the planting of urban trees are inexpensive measures that can reduce summertime temperatures.

At the building scale, a dark roof is heated by the sun and, thus, directly raises the summertime cooling demand of the building beneath it. For highly absorptive (low-albedo) roofs, the difference between the surface and ambient air temperatures may be as high as 50°C, while for less absorptive (high-albedo) surfaces with similar insulative properties, such as roofs covered with a white coating, the difference is only about 10°C (Berdahl and Bretz, 1997). For this reason, 'cool' surfaces (which absorb little 'insolation') can be effective in reducing cooling-energy use. Highly absorptive surfaces contribute to the heating of the air, and thus indirectly increase the cooling demand of (in principle) all buildings. Cool surfaces incur no additional cost if color changes are incorporated into routine re-roofing and resurfacing schedules (Bretz et al., 1998, Rosenfeld et al., 1992).

Most high-albedo surfaces are light colored, although selective surfaces that reflect a large portion of the infrared solar radiation but absorb some visible light may be dark colored and yet have relatively high albedos (Berdahl and Bretz, 1997).

The practice of widespread paving of city streets with asphalt began only within the past hundred years. The advantages of this smooth and all-weather surface for the movement of bicycles and automobiles are obvious, but some of the associated problems are perhaps not so well appreciated. One consequence of covering streets with dark asphalt surfaces is the increased heating of the city by sunlight. A dark surface absorbs light, and, therefore, it gets warmer. The pavements in turn heat the air and help create the UHI. If urban surfaces were lighter in color, more of the incoming light would be reflected back into space and the surfaces and the air would be cooler. This tends to reduce the need for air conditioning.

The benefits of trees can also be divided into direct and indirect effects: shading of buildings and ambient cooling (urban forest). Shade trees intercept sunlight before it warms a building. The urban forest cools the air by evapotranspiration. Trees also decrease the wind speed under their canopy and shield buildings from cold winter breezes. Urban shade trees offer significant benefits by both reducing building air-conditioning, lowering air temperature, and thus improving urban air quality by reducing smog. Over the life of a tree, the savings associated with these benefits vary by climate region. Tree-planting programs can be designed to be low cost, so they can offer savings to communities that plant trees.

The project is co-financed by the European Union

2. Methods of LCZ investigation and station location definition in urban areas

2.1. The Local Climate Zone classification system

In the heat island literature the term "urban" has no single, objective meaning as the areas around the measuring sites could be very different depending on the investigated cities (e.g. park, college ground, street canyon, housing estate, etc.). In addition, for landscape classification or description of the site surroundings the simple "urban" versus "rural" is not appropriate because of the abundant variety of the landscapes according to their surface properties relevant to development of near-surface micro and local climates (Stewart, 2007; 2011).

To diminish this deficiency, Stewart and Oke (2012) developed a climate-based classification system based on the earlier studies from the last decades (e.g. Auer, 1978; Ellefsen, 1991; Oke, 2004; Stewart and Oke, 2009), as well as a thorough review on the empirical heat island literature and world-wide surveys of the measurement sites with their surroundings. The elements of this system are the "local climate zones" (LCZ) and they are presented shortly in Sections 2.2 and 2.3.

The main purpose of the LCZ system is to facilitate the characterization of the local environment around a temperature measuring site with a screen-height sensor, in terms of its ability to influence the local thermal climate. To this end, the number of types is not too large and separation is based on objective, measurable parameters. LCZs are defined as "regions of uniform surface cover, structure, material, and human activity that span hundreds of meters to several kilometres in horizontal scale. Each LCZ has a characteristic screen-height temperature regime that is most apparent over dry surfaces, on calm, clear nights, and in areas of simple relief" (Stewart and Oke, 2012). Each climate zone is necessarily "local" in spatial scale because typically a 200–500 m upwind fetch is required for the air at screen-height to become fully adjusted to the underlying, relatively homogeneous surface. Among them there are ten built types (from LCZ 1 to LCZ 10) and seven land cover types (from LCZ A to LCZ G), and additionally, the types can have variable seasonal or shorter period land cover properties. The main characters of the types are reflected in their names (*Table 6*).

The LCZ types can be distinguished by the measurable physical properties (parameters) Most of them characterize

Table 6. Names and designation of the LCZ types (after Stewart and Oke, 2012)

Built types	Land cover types	Variable land cover properties
LCZ 1 – Compact high-rise LCZ 2 – Compact midrise LCZ 3 – Compact low-rise LCZ 4 – Open high-rise LCZ 5 – Open midrise LCZ 6 – Open low-rise LCZ 7 – Lightweight low-rise LCZ 8 – Large low-rise LCZ 9 – Sparsely built LCZ 10 – Heavy industry	LCZ A – Dense trees LCZ B – Scattered trees LCZ C – Bush, scrub LCZ D – Low plants LCZ E – Bare rock / paved LCZ F – Bare soil / sand LCZ G – Water	b – bare trees s – snow cover d – dry ground w – wet ground

the surface cover and geometry of a site, while others reflect the thermal, radiative and anthropogenic energy attributes of an area (*Table 7*). These parameters are partly dimensionless (e.g. sky view factor), partly given in %, m, etc. (e.g. building surface fraction) and their values have different ranges according to the different types. Stewart and Oke (2012) defined the typical range of properties for each zone.

The LCZ classification system was not designed specifically for mapping, but to standardize the classification of urban heat island observation sites, either urban or rural. Nevertheless, In case of the design of a new urban observation network, utilizing LCZ classification in the spatial mapping of a city is justifiable. The introduced classes support the categorization of the urban terrain, the identification of relatively homogeneous areas with respect to their surface properties, and the identification sites that are representative of those areas.

In the frame of this new classification system the UHI intensity is not an "urban-rural" temperature difference but an LCZ temperature difference ($\Delta T_{LCZ:X-Y}$), not an "urban-rural" difference (ΔT_{u-r}) (Stewart et al. 2013). Depending on the combination of the selected two LCZ classes, this difference can yield various outcomes. In this way, the application of the LCZ system gives an opportunity to compare the thermal reactions of different areas within a city and between cities (intra-urban and inter-urban comparisons) objectively.

It can be assumed that in many respects the interactions between the urban parameters and thermal comfort as well

Table 7. Zone properties of LCZ system (after Stewart and Oke, 2012)

	Type of properties	
	Geometric, surface cover	Thermal, radiative, metabolic
Properties	sky view factor aspect ratio building surface fraction (%) impervious surface fraction (%) pervious surface fraction (%) height of roughness elements (m) terrain roughness class	surface admittance (Jm-2s-1/2K-1) surface albedo anthropogenic heat output (Wm-2)

as some elements of the weather phenomena within the city are not yet known sufficiently. These interactions can only be analyzed properly using detailed and long-term measurements, that is the detection and analysis of the long term (several years) characteristics of these urban thermal patterns is possible only with the help of a *monitoring network* installed in appropriate density and representatively. For automatic monitoring network set up in the urban canopy layer we can find some international – mainly U.S., Japan and Taiwan – examples, while in Europe there are very few of these and none of them are aimed at the detection of patterns of human comfort conditions. In London a network began to build from 1999 on with temperature sensors located from the centre in different directions radially (Watkins et al., 2002), while in Florence there are a system with temperature-humidity sensors operating since 2004 whose elements observe the thermal features of the city's various built-up districts (Petralli et al., 2013). The most complex network (met. stations + sensors) so far started up in 2011 in Birmingham. Its development is now in progress and its elements are installed in the downtown area more densely while in the outskirts less (HiTEmp Project, 2014).

Because of the complexity of the urban terrain the monitoring of the representative intra-urban thermal features is a difficult task (Oke, 2004). The locations of the sites of an urban station network within the city and thus the question about its appropriate configuration raises an essential problem. This problem is related to the relationship between the intra-urban built and land cover LCZ types and the locations of the network sites. Two situations arise:

1. In the case of an already existing network (e.g. Schroeder et al., 2010) it may be required to characterize the relatively wider environment around the measuring sites, namely what type of urban area (LCZ) surrounds a given station and whether it can be clearly determined. In other words, how representative is the location of a station regarding a specific, clearly defined LCZ type in an urban environment?
2. In the case of a planned station network (e.g. Unger et al., 2011) the most important questions are what built and land cover LCZ types can be distinguished in a given urban area, how precisely they can be delimited, how many they are, and whether their extension is large enough to install a station somewhere in the middle of the area (representing the thermal conditions of this LCZ) while of course taking care to minimize the microclimatic effects of the immediate environment.

2.2. Sitting and configuration of a representative urban climate (human comfort) monitoring system in Szeged (Hungary)

Szeged is located in the south-eastern part of Hungary (46°N, 20°E) at 79 m above sea level on a flat terrain with a population of 160,000 within an urbanized area of about 40 km². The area is in Köppen's climatic region Cfb with an annual mean temperature of 10.4°C and an amount of precipitation of 497 mm.

The study area covers an 11.5 km × 8.5 km rectangle in and around Szeged. Within the framework of the project 23 stations was set up in Szeged. To these data the data series from the stations of the Hungarian Meteorological Service (HMS) at the road to Baja (global radiation, G and wind speed, u) and at the University of Szeged (station 5-1) (T, RH, G) are added. With the already existing station 5-1 the whole network consists of 24 measurement sites.

In order to have a representative urban human comfort monitoring network seven LCZ areas was delinated: LCZ 2 – compact mid-rise, LCZ 3 – compact low-rise, LCZ 5 – open mid-rise, LCZ 6 – open low-rise, LCZ 8 – large low-rise and LCZ 9 – sparsely built, LCZ D – low plants. Based on the LCZ map the siting and configuration of 22 stations from the above mentioned 24 ones were based on: (i) the site's distance from the border of the LCZ zone within which it was located; (ii) the ability of the selected network geometry to reproduce the spatial distribution of mean temperature surplus pattern estimated by an empirical model;

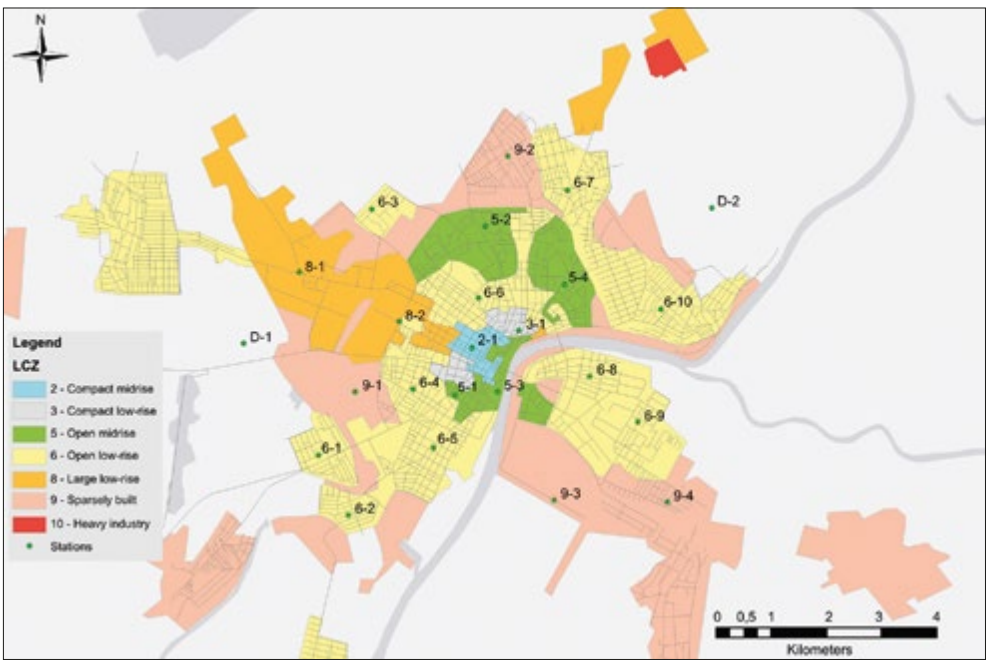

Figure 27. Urban monitoring network in Szeged and its surroundings

Table 8. Basic information about urban meteorological network in Szeged

№	Local Climate Zones	Station ID	City zone	Latitude	Longitude	Altitude (m)
1	LCZ 2	2-1	Belváros	46°15'17.70''N	20°09'39.95''E	82
2	LCZ 3	3-1	Belváros	46°15'27.74''N	20°09'19.77''E	82
3	LCZ 5	5-1	Belváros	46°15'51.42''N	20°08'24.81''E	80
4	LCZ 5	5-2	Makkosház	46°16'29.64''N	20°09'52.44''E	79
5	LCZ 5	5-3	Belváros	46°15'51.66''N	20°09'00.99''E	83
6	LCZ 5	5-4	Felsőváros	46°16'54.34''N	20°10'59.35''E	80
7	LCZ 6	6-1	Kecskés telep	46°14'15.52''N	20°06'27.71''E	80
8	LCZ 6	6-2	Klebelsberg telep	46°14'39.99''N	20°07'52.48''E	78
9	LCZ 6	6-3	Béketelep	46°17'40.58''N	20°07'16.10''E	79
10	LCZ 6	6-4	Móraváros	46°15'53.88''N	20°08'49.06''E	80
11	LCZ 6	6-5	Alsóváros	46°14'19.05''N	20°08'06.03''E	81
12	LCZ 6	6-6	Rókus	46°16'48.33''N	20°09'45.86''E	80
13	LCZ 6	6-7	Baktó	46°17'49.00''N	20°10'02.42''E	78
14	LCZ 6	6-8	Újszeged	46°15'59.88''N	20°10'19.76''E	78
15	LCZ 6	6-9	Újszeged	46°15'32.45''N	20°11'00.18''E	78
16	LCZ 6	6-10	Tápé	46°16'39.15''N	20°11'21.21''E	79
17	LCZ 8	8-1	Iparváros	46°16'04.09''N	20°06'13.63''E	80
18	LCZ 8	8-2	Móraváros	46°16'34.11''N	20°08'38.05''E	79
19	LCZ 9	9-1	Móraváros	46°15'52.71''N	20°07'59.52''E	79
20	LCZ 9	9-2	Baktói kiskertek	46°17'10.77''N	20°09'12.62''E	79
21	LCZ 9	9-3	Újszeged	46°14'40.65''N	20°10'59.58''E	78
22	LCZ 9	9-4	Marostői kiskertek	46°14'44.98''N	20°11'24.34''E	79
23	LCZ D	D-1	Rural Zone	46°15'22.19''N	20°05'25.23''E	80
24	LCZ D	D-2	Rural Zone	46°17'38.45''N	20°12'05.98''E	80

(iii) the site's representativeness of its microenvironment; and (iv) the site's suitability for instrument installation. So, in summary, two stations (D-1, D-2) represent the rural area, while the other 22 stations the different built-up areas of the city, respectively.

In the following pages will be presented basic information about each LCZ in Szeged and its surroundings. For defined LCZ's are given examples of representative meteorological stations with photos and its locations on map. This leads to the better understanding of specific urban structure and climate of Szeged area.

Compact midrise (LCZ 2) is characteristic for city downtown (Belváros). One urban monitoring station is located here (*Figure 28*).

Example of compact midrise (LCZ 2) monitoring station location (*Figure 29*).

Station ID	2-1
LCZ	compact midrise
City zone	Belváros
Address	Bartók square
Latitude	46°15'17.70''N
Longitude	20°09'39.95''E
Elevation	82 m

Figure 28. Compact midrise (LCZ 2) monitoring stations in Szeged

Figure 29. Compact midrise station location in Szeged

The project is co-financed by the European Union

Figure 30. Compact low-rise (LCZ 3) monitoring stations in Szeged

Figure 31. Compact low-rise station location in Szeged

Compact low-rise (LCZ 3) is present around the city core (N ans SW part of Belváros). One urban monitoring station is located here (*Figure 30*).

Example of compact low-rise (LCZ 3) station location (*Figure 31*).

Station ID	3-1
LCZ	compact low-rise
City zone	Belváros
Address	Dugonics Street
Latitude	46°15'27.74''N
Longitude	20°09'19.77''E
Elevation	82 m

Open midrise (LCZ 5) is characteristic for the edge of the city core and the residential part of the city (e.g. Belváros, Újrókus, Makkosháza, Északi városrész, Tarján, Felsőváros, Odessza). Four urban monitoring stations are located here (*Figure 32*).

Example of open midrise (LCZ 5) station location (*Figure 33*).

Station ID	5-2
LCZ	open midrise
City zone	Makkosház
Address	Hont Ferenc Street
Latitude	46°16'29.64''N
Longitude	20°9'52.44''E
Elevation	79 m

Figure 32. Open midrise (LCZ 5) monitoring stations in Szeged

Figure 33. Open midrise station location in Szeged

Figure 34. Open low-rise (LCZ 6) monitoring stations in Szeged

Figure 35. Open low-rise (LCZ 6) station location in Szeged

Open low-rise (LCZ 6) is present on the periphery of the city (e.g. Alsóváros, Móraváros, Felsőváros, Újszeged, Kecskés telep, Klebersberg telep, Béketelep, Tápé, Baktó, Petőfi telep) Ten urban monitoring stations are located here (*Figure 34*).

Example of open low-rise (LCZ 6) station location (*Figure 35*).

Station ID	6-8
LCZ	open low-rise
City zone	Újszeged
Address	Déryné Street
Latitude	46°15'59.88''N
Longitude	20°10'19.76''E
Elevation	78 m

Large low-rise (LCZ 8) (e.g. Iparváros, Móraváros) is located in the Western part of the city. Two urban monitoring stations are located here (*Figure 36*).

Example of large low-rise (LCZ 8) station location (*Figure 37*).

Station ID	8-1
LCZ	large low-rise
City zone	Iparváros
Address	Dorozsmai Street
Latitude	46°16'04.09''N
Longitude	20°06'13.63''E
Elevation	80 m

Figure 36. Large low-rise (LCZ 8) monitoring stations in Szeged

Figure 37. Large low-rise (LCZ 8) station location in Szeged

Figure 38. Sparsely built (LCZ 9) monitoring stations in Szeged

Figure 39. Sparsely built (LCZ 9) station location in Szeged

The city outskirts are characterized by **sparsely built (LCZ 9)** (e.g. Móraváros, Baktói kiskertek, Marostői kiskertek, Újszeged). For urban monitoring stations are located here (*Figure 38*).

Example of sparsely built (LCZ 9) station location (*Figure 39*).

Station ID	9-2
LCZ	sparsely built
City zone	Baktói kiskertek
Address	Pihenő Street
Latitude	46°17'10.77''N
Longitude	20°09'12.62''E
Elevation	79 m

Two rural stations are located west and northeast **(LCZ D – low plants)** from the city outskirts (*Figure 40*).

Example of low plants (LCZ D) station location (*Figure 41*).

Station ID	D-1
LCZ	low plants
City zone	rural area
Address	HMS station
Latitude	46°15'22.19''N
Longitude	20°05'25.23''E
Elevation	80 m

Figure 40. Low plants (LCZ D) monitoring stations in Szeged

Figure 41. Sparsely built (LCZ 9) station location in Szeged

The project is co-financed by the European Union

2.3. Sitting and configuration of a representative urban climate (human comfort) monitoring system in Novi Sad (Serbia)

Novi Sad is located in the northern part of the Republic of Serbia and in south-eastern part of Pannonian Plain. The area of the city is characterized by plain relief with elevation from 80 to 86 m and its climate is free from orographic effects. The Danube River flows by the southern and southeastern edge of the city urban area. Southern parts of the city urban area (Sremska Kamenica and Petrovaradin) are located on the northern slopes of Fruška Gora Mountain (539 m). In Novi Sad the annual mean air temperature is 11.1°C with an annual range of 22.1°C and the precipitation amount is 615 mm (based on data from 1949 to 2008). Novi Sad is the second largest city in the country with a population of about 320 000 in a built-up area of around 80 km².

On the territory of Novi Sad and its surrounding 27 stations make urban monitoring network (*Figure 42*). Stations locations were choosen based on the above mentioned parameters and rules. There are 25 urban monitoring stations in the city of Novi Sad and two rural stations (located north and northeast from the city outskirts). Seven LCZ types were defined on the territory of Novi Sad. They are as follows: compact midrise, compact low-rise, open midrise, open low-rise, large low-rise, sparsely built and heavy industry. Rural stations are located in LCZ's of low plants and dense trees.

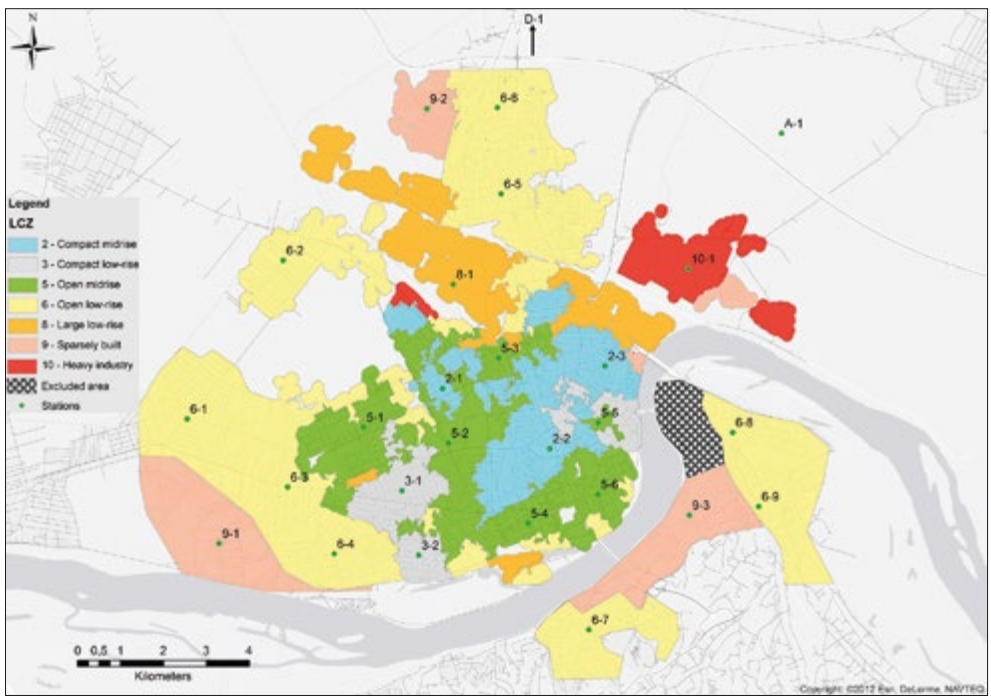

Figure 42. Urban monitoring network in Novi Sad and its surroundings

Table 9. Basic information about urban monitoring network in Novi Sad

№	Local Climate Zones	Station ID	City zone	Latitude	Longitude	Altitude (m)
1	LCZ 2	2-1	Nova Detelinara	45°15'28.79"N	19°48'53.18"E	77
2	LCZ 2	2-2	Grbavica	45°14'56.85"N	19°50'14.21"E	79
3	LCZ 2	2-3	Podbara	45°15'40.68"N	19°50'55.94"E	78
4	LCZ 3	3-1	Telep	45°14'34.53"N	19°48'22.59"E	76
5	LCZ 3	3-2	Telep	45°14'0.28"N	19°48'35.18"E	79
6	LCZ 5	5-1	Bistrica	45°15'8.16"N	19°47'53.72"E	80
7	LCZ 5	5-2	Sajmište	45°14'59.69"N	19°48'57.67"E	75
8	LCZ 5	5-3	Banatić	45°15'44.93"N	19°49'35.35"E	78
9	LCZ 5	5-4	Liman 3-4	45°14'17.21"N	19°49'57.75"E	81
10	LCZ 5	5-5	Stari Grad	45°15'10.63"N	19°50'50.61"E	80
11	LCZ 5	5-6	Liman 1-2	45°14'32.59"N	19°50'50.49"E	78
12	LCZ 6	6-1	Veternik	45°15'12.58"N	19°45'40.54"E	77
13	LCZ 6	6-2	Sajlovo	45°16'36.60"N	19°46'53.04"E	80
14	LCZ 6	6-3	Adice	45°14'36.45"N	19°46'56.38"E	77
15	LCZ 6	6-4	Adice	45°14'0.99"N	19°47'31.48"E	76
16	LCZ 6	6-5	Slana Bara	45°17'11.88"N	19°49'37.44"E	77
17	LCZ 6	6-6	Klisa	45°17'57.55"N	19°49'34.70"E	78
18	LCZ 6	6-7	Sremska Kamenica	45°13'20.74"N	19°50'43.66"E	119
19	LCZ 6	6-8	Petrovaradin	45°15'5.44"N	19°52'32.21"E	76
20	LCZ 6	6-9	Petrovaradin	45°14'26.17"N	19°52'51.77"E	92
21	LCZ 8	8-1	Industrijska zona jug	45°16'23.94"N	19°49'1.38"E	77
22	LCZ 9	9-1	Adice	45°14'6.52"N	19°46'4.68"E	75
23	LCZ 9	9-2	Gornje Livade	45°17'57.02"N	19°48'41.55"E	79
24	LCZ 9	9-3	Ribnjak	45°14'21.48"N	19°51'59.46"E	127
25	LCZ 10	10-1	Radna zona sever 4	45°16'32.20"N	19°51'58.51"E	75
26	LCZ D	D-1	Rural zone	45°23'1.62"N	19°49'55.55"E	79
27	LCZ A	A-1	Rural zone	45°17'43.98"N	19°53'9.04"E	76

In the following pages will be presented basic information about each LCZ in Novi Sad and its surroundings. For defined LCZ's are given examples of representative monitoring stations with photos and its locations on map. This leads to the better understanding of specific urban structure and climate of Novi Sad area.

Figure 43. Compact midrise (LCZ 2) monitoring stations in Novi Sad

Figure 44. Compact midrise station location in Novi Sad

Compact midrise (LCZ 2) is characteristic for city downtown (e.g. Podbara and Grbavica) and in new residential area (e.g. Nova Detelinara). Three urban monitoring stations are located here (*Figure 43*).

Example of compact midrise (LCZ 2) monitoring station location (*Figure 44*).

Station ID	2-1
LCZ	compact midrise
City zone	Nova Detelinara
Address	Cankareva Street
Latitude	45°15'28.79"N
Longitude	19°48'53.18"E
Elevation	77 m

Compact low-rise (LCZ 3) is present in the western part of the city (e.g. Telep). Two urban monitoring stations are located here (*Figure 45*).

Example of compact low-rise (LCZ 3) station location (*Figure 46*).

Station ID	3-1
LCZ	compact low-rise
City zone	Telep
Address	Ilirska Street
Latitude	45°14'34.53"N
Longitude	19°48'22.59"E
Elevation	76 m

Figure 45. Compact low-rise (LCZ 3) monitoring stations in Novi Sad

Figure 46. Compact low-rise station location in Novi Sad

Figure 47. Open midrise (LCZ 5) monitoring stations in Novi Sad

Figure 48. Open midrise station location in Novi Sad

Open midrise (LCZ 5) is characteristic for the residential part of the city (e.g. Liman 1-4, Bistrica and Banatić). Six urban monitoring stations are located here (*Figure 47*).

Example of open midrise (LCZ 5) station location (*Figure 48*).

Station ID	5-6
LCZ	open midrise
City zone	Liman 1-2
Address	Narodnog Fronta Street
Latitude	45°14'32.59"N
Longitude	19°50'50.49"E
Elevation	78 m

Open low-rise (LCZ 6) is present on the periphery of the city (e.g. Adice, Sajlovo, Slana Bara, Klisa) and in suburban settlements (e.g. Veternik, Petrovaradin and Sremska Kamenica). Nine urban monitoring stations are located here (*Figure 49*).

Example of open low-rise (LCZ 6) station location (*Figure 50*).

Station ID	6-4
LCZ	open low-rise
City zone	Adice
Address	Branka Ćopića Street
Latitude	45°14'0.99"N
Longitude	19°47'31.48"E
Elevation	76 m

Figure 49. Open low-rise (LCZ 6) monitoring stations in Novi Sad

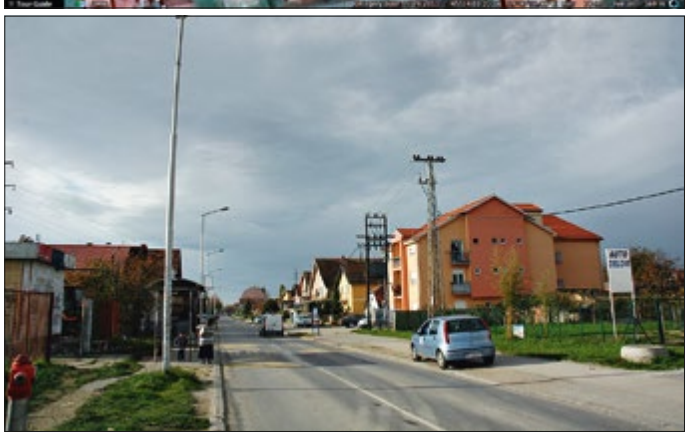

Figure 50. Open low-rise (LCZ 6) station location in Novi Sad

Figure 51. Large low-rise (LCZ 8) monitoring station in Novi Sad

Figure 52. Large low-rise (LCZ 8) monitoring station location in Novi Sad (Industrial area –south)

Large low-rise (LCZ 8) (e.g. Industrial area-south and Industrial area-north) is located in the northern part of the city. One urban monitoring station is located here (*Figure 51*).

Example of large low-rise (LCZ 8) station location (*Figure 52*).

Station ID	8-1
LCZ	large low-rise
City zone	Industrial zone south
Address	Put Partizanskog novosadskog odreda
Latitude	45°16'23.94"N
Longitude	19°49'1.38"E
Elevation	77 m

The city outskirts are characterized by **sparsely built (LCZ 9)** (e.g. Gornje Livade, Adice and Ribnjak). Three urban monitoring stations are located here (*Figure 53*).

Example of sparsely built (LCZ 9) station location (*Figure 54*).

Station ID	9-2
LCZ	sparsely built
City zone	Gornje Livade
Address	Svetlane Vranić Street
Latitude	45°17'57.02"N
Longitude	19°48'41.55"E
Elevation	79 m

Figure 53. Sparsely built (LCZ 9) monitoring stations in Novi Sad

Figure 54. Sparsely built (LCZ 9) monitoring station location in Novi Sad

Figure 55. Heavy industry (LCZ 10) monitoring station in Novi Sad

Figure 56. Heavy industry (LCZ 10) monitoring station location in Novi Sad (Oil refinery)

Heavy industry (LCZ 10) (Oil refinery) is located in the northern part of the city. One urban monitoring station is located here (*Figure 55*).

Example of large heavy industry (LCZ 10) station location (*Figure 56*).

Station ID	10-1
LCZ	heavy industry
City zone	Radna zona sever 4
Address	Put Šajkaškog odreda
Latitude	45°16'32.20"N
Longitude	19°51'58.51"E
Elevation	75 m

Two rural stations are located north **(LCZ D – low plants)** and northeast **(LCZ A – dense trees)** from the city outskirts (*Figures 57 and 58*).

Example of low plants (LCZ D) station location (*Figure 57*).

Station ID	D-1
LCZ	low plants
City zone	9 km north from the city outskirts
Address	Aeroclub "Novi Sad"
Latitude	45°23'1.62"N
Longitude	19°49'55.55"E
Elevation	79 m

Example of dense trees (LCZ A) station location (*Figure 58*).

Station ID	A-1
LCZ	dense trees
City zone	3 km northeast from the city outskirts
Address	Institute of Lowland Forestry and Environment
Latitude	45°17'43.98"N
Longitude	19°53'9.04"E
Elevation	76 m

Figure 57. Low plants (LCZ D) monitoring station north from Novi Sad

Figure 58. Dense trees (LCZ A) monitoring station northeast from Novi Sad

3. References

Akbari, H., Rosenfeld, A., Taha, H. 1990:. Summer heat islands, urban trees, and white surfaces. ASHRAE Trans. 96(1), American Society of Heating, Refrigeration, and Air Conditioning Engineers, Atlanta, Georgia.

Akbari, H., Pomerantz, M., Taha, H. 2001. Cool surfaces and shade trees to reduce energy use and improve air quality in urban areas. *Solar Energy* 70, 295-310.

Auer, A.H. 1978. Correlation of land use and cover with meteorological anomalies. *Journal of Applied Meteorology* 17, 636-643.

Balázs, B., Unger, J., Gál, T., Sümeghy, Z., Geiger, J., Szegedi, S. 2009. Simulation of the mean urban heat island using 2D surface parameters: empirical modeling, verification and extension. *Meteorological Applications* 16, 275-287.

Barry, R.G., Chorley, RJ. 1982. Atmosphere, weather and climate. Methuen, London-New York, 302-319.

Berdahl, P., Bretz, S. 1997. Preliminary survey of the solar reflectance of cool roofing materials. *Energy and Buildings* 25, 149-158.

Bitan, A. 1988. The methodology of applied climatology in planning and building. *Energy and Buildings* 11, 1-10.

Bretz, S., Akbari, H., Rosenfeld, A., 1998. Practical issues for using solar-reflective materials to mitigate urban heat islands. *Atmospheric Environment* 32, 95-101.

Davies, M., Steadman, P., Oreszczyn, T. 2008. Strategies for the modification of the urban climate and the consequent impact on building energy use. *Energy Policy* 36, 4548-4551.

Eliasson, I., Upmanis, H. 2000. Nocturnal airflow from urban parks-implications for city ventilation. *Theoretical and Applied Climatology* 66, 95-107.

Ellefsen, R. 1990. Mapping and measuring buildings in the canopy boundary layer in ten U.S. cities. *Energy and Buildings* 15-16, 1025-1049.

Hamilton, I.G., Davies, M., Steadman, P., Stone, A., Ridley, I., Evans, S. 2009. The significance of the anthropogenic heat emissions of London's buildings: A comparison against captured shortwave solar radiation. *Building and Environment* 44, 807-817.

HiTemp Project 2014. High Density Measurements within the Urban Environment. http://www.birmingham.ac.uk/schools/gees/centres/bucl/hitemp/index.aspx. Last accessed: 10 April 2014.

Klysik, K., Fortuniak, K. 1999. Temporal and spatial characteristics of the urban heat island of Lódz, Poland. *Atmospheric Environment* 33, 3885-3895.

Kolokotroni, M., Giannitsaris, I., Watkins, R. 2006. The effect of the London urban heat island on building summer cooling demand and night ventilation strategies. *Solar Energy* 80, 383-392.

Kuttler, W. 1998. Stadtklima. In Sukopp H, Wittig R (Hrsg): Stadtökologie. Gustav Fisher Verlag, Stuttgart-Jena-Lübeck-Ulm, 125-167.

Kuttler, W. 2006. Stadtklima. In Hupfer P, Kuttler W (Hrsg): Witterung und Klima. 12. Auflage. Teubner, Stuttgart-Leipzig-Wiesbaden, 371-432.

Lakatos, L., Gulyás, Á. 2003. Connection between phenological phases and urban heat island in Debrecen and Szeged, Hungary. *Acta Climatologica et Chorologica Universitatis Szegediensis* 36-37, 79-83.

Lelovics, E., Unger, J., Gál, T., Gál, C.V. 2014. Design of an urban monitoring network based on Local Climate Zone mapping and temperature pattern modeling. *Climate Research*, doi: 10.3354/cr01220 in press.

Livada, I., Santamouris, M., Niachou, K., Papanikolaou, N., Mihalakakou, G. 2002. Determination of places in the great Athens area where the heat island effect is observed. *Theoretical and Applied Climatology* 71, 219-230.

Matzarakis, A. 2001. Die termische Komponente der Stadtklimas. Berichte des Meteorologischen Institut der Universität Freiburg 6, pp 248.

Oke, T.R. 1973. City size and the urban heat island. *Atmospheric Environment* 7, 769-779.

Oke, T.R. 1974. Review of urban climatology 1968-1973. WMO Tech. Note No. 134.

Oke, T.R. 1976. The distinction between canopy and boundary-layer urban heat islands. *Atmosphere* 14, 268-277.

Oke, T.R. 1982. The energetic basis of the urban heat island. *Quarterly Journal of the Royal Meteorological Society* 108, 1-24.

Oke, T.R. 1987. Boundary layer climates. 2nd edition. Routledge, London-New York.

Oke, T.R. 1989. The micrometeorology of the urban forest. *Philosophical Transaction of the Royal Society of London* B 324, 335-349.

Oke, T.R. 1997. Urban climates and global environmental change. In: Thompson RD, Perry A (eds): Applied Climatology. Routledge, London-New York, 273-287.

Oke, T.R. 2004. Initial guidance to obtain representative meteorological observation sites. WMO/TD No. 1250, Geneva.

Oke, T.R., Hannell, F.G. 1970. The form of the urban heat island in Hamilton, Canada. In Urban climates. WMO Tech Note 108, 113-126.

Oke, T.R., Maxwell, G.B. 1975. Urban heat island dinamics in Montreal and Vancouver. *Atmospheric Environment* 9, 191-200.

Park, H-S. 1987. Variations in the urban heat island intensity affected by geographical environments. Environmental Research Center Papers 11, The University of Tsukuba, Ibaraki, Japan, pp 79.

Petralli, M., Masetti, L., Brandani, G., Orlandin, S. 2013. Urban planning indicators: useful tools to measure the effect of urbanization and vegetation on summer air temperatures. *International Journal of Climatology* 34, 1236–1244.

Robaa, S.M. 2006. A study of solar radiation climate at Cairo urban area, Egypt and is environs. *International Journal of Climatology* 26, 1913-1928.

Rosenfeld, A., Akbari, H., Taha, H., Bretz, S. 1992. Implementation of light-colored surfaces: profits for utilities and labels for paints. In Proceed. ACEEE Summer Study on Energy Efficiency in Buildings, Vol. 9, pp 141.

Sailor, D.J. 1998. Simulations of annual degree day impacts of urban vegetative augmentation. *Atmospheric Environment* 32, 43-52.

Schroeder, A.J., Basara, J.B., Illston, B.G. 2010. Challenges associated with classifying urban meteorological stations: The Oklahoma City Micronet example. *Open Atmospheric Science Journal* 4, 88-100.

Stewart, I.D., Oke, T.R., Krayenhoff, E.S. 2013. Evaluation of the 'local climate zone' scheme using temperature observations and model simulations. *International Journal of Climatology* 34,1062-1080.

Stewart, I.D., Oke, T.R. 2009. A new classification system for urban climate sites. *Bulletin of the American Meteorological Society* 90, 922-923.

Stewart, I.D., Oke, T.R. 2012. Local Climate Zones for urban temperature studies. *Bulletin of the American Meteorological Society* 93, 1879-1900.

Taha, H. 1996. Modeling the impacts of increased urban vegetation on the ozone air quality in the South Coast Air Basin. Atmospheric Environment 30, 3423–3430.

Unger, J., Ondok, J. 1995. Some features of urban influence on temperature extremities. *Acta Climatologica et Chorologica Universitatis Szegediensis* 28-29, 63-76.

Unger, J., Savić, S., Gál, T. 2011. Modelling of the annual mean urban heat island pattern for planning of representative urban climate station network. *Advances in Meteorology* 2011, ID 398613, pp 9.

Unger, J., Gál, T., Csépe, Z., Lelovics, E., Gulyás, Á. 2014. Development, data processing and preliminary results of an urban human comfort monitoring and information system. *Időjárás* (accepted).

Watkins, R., Palmer, J., Kolokotroni, M., Littlefair, P. 2002. The London heat island: Results from summertime monitoring. *Building Services Engineering Research and Technology* 23, 97–106.

Wilby, R.L. 2003. Past and projected trends in London's urban heat island. *Weather* 58, 251–260.

World Meteorological Organization 1983. Abridged final report, 8th session. Geneva, Commission for Climatology and Applications of Meteorology, World Meteorological Organization (WMO No. 600).

4. Scientific publications (related with URBAN-PATH project issues)

The project is co-financed by the European Union

Hindawi Publishing Corporation
Advances in Meteorology
Volume 2011, Article ID 398613, 9 pages
doi:10.1155/2011/398613

Research Article

Modelling of the Annual Mean Urban Heat Island Pattern for Planning of Representative Urban Climate Station Network

János Unger,[1] Stevan Savić,[2] and Tamás Gál[1]

[1] *Department of Climatology and Landscape Ecology, University of Szeged, P.O. Box 653, 6701 Szeged, Hungary*
[2] *Climatology and Hydrology Research Centre, Faculty of Science, University of Novi Sad, Trg Dositeja Obradovića 3, 21000 Novi Sad, Serbia*

Correspondence should be addressed to János Unger, unger@geo.u-szeged.hu

Received 22 December 2010; Revised 26 April 2011; Accepted 10 August 2011

Academic Editor: C. S. B. Grimmond

The spatial distribution of the annual mean urban heat island (UHI) intensity pattern was analysed for the medium-sized city Novi Sad, Serbia, located on the low and flat Great Hungarian Plain. The UHI pattern was determined by an empirical modelling method developed by (Balázs et al. 2009). This method was based on datasets from urban areas of Szeged and Debrecen (Hungary). The urban study area in Novi Sad (60 km^2) was established as a grid network of 240 cells (0.5 km $\times$ 0.5 km). A Landsat satellite image (from June 2006) was used in order to evaluate normalized difference vegetation index and built-up ratio by cells. The pattern of the obtained UHI intensity values show concentric-like shapes when drawn as isotherms, mostly increase from the suburbs towards the inner urban areas. Results of this thermal pattern and determination of one of the local climate classification systems were used for recommending 10 locations for representative stations of an urban climate network in Novi Sad.

1. Introduction

In the second part of the 20th century, urbanization accelerated and reached enormous magnitude. The growth rate of the Earth's urban population is greater than that of the total population; therefore, more and more people live in urbanized regions. Nowadays, about half of the human population is affected by the burdens of urban environments: environmental pollution, noise, stress of the accelerated life-style, and last but not least the modified parameters of the urban atmosphere compared to the natural environment. This makes studies dealing with the urban impact on climate particularly important.

Not only the large cities but also the smaller ones modify materials, structure, and energy balance of the surface and almost all properties of the urban atmospheric environment compared to the natural surroundings. Thus, owing to the artificial factors, a local climate (urban climate) develops which means a modification to the preurban situation. This climate is a result of the construction of buildings as well as by the emission of heat, moisture, and pollution related to human activities.

According to Oke [1], two layers can be distinguished in the urban atmosphere. The first one is the urban canopy layer (UCL) containing air between the urban roughness elements (mainly buildings). It is a microscale concept, and its climate is dominated geographical factors and modified by the nature of the immediate surroundings. The upper boundary of the UCL is at about roof level. The second layer is the urban boundary layer (UBL) which is situated directly above the first layer. This is a local or mesoscale concept whose characteristics are governed by the nature of the whole urban area.

In the course of urban climate development, the near-surface air or (UCL) temperature shows the most obvious modification compared to the rural area [2]. This urban warming is commonly referred to as the urban heat island (UHI), and it is a good example of inadvertent climatic change. We note that all temperatures referred to this study are in the UCL at 1.5–2 metres above ground level.

It is anticipated that continuous, quality-assured observations provide new research opportunities focused on the spatial and temporal variability in UHI patterns. In order to acquire long-term data as a basis for studies, measurements

in a network established in the city are needed. Selecting the exact sites of the individual stations to ensure the representativeness of the thermal conditions across a wider area in the complex urban environment is a difficult problem [3]. Theoretically, this representativeness can only be assessed in the context of its micro-, and local-scale properties of surface geometry (sky view factor, height-to-width ratios, and aerodynamical roughness length), cover (percentage of built material, albedo, and thermal admittance), and artificial heat (space heating/cooling and traffic density) [4]. If the aim is to monitor local climate attributable to an urban area, it makes sense to avoid locations with extreme microclimatic influences or nonurban local climatic phenomena that may complicate the urban record.

Methodologically, determination of the temperature increasing effect of an urban area means the calculation of difference between the temperature values measured at representative "rural" and "urban" sites. In order to classify these sites, several classification systems exists [3, 5–7], and these classify the terrain into different areas called for example, Urban Climate Zones [3] or Local Climate Zones (LCZ) [5]. LCZs are defined by Stewart [6] as regions of relatively uniform surface-air temperature distribution across horizontal scales of 10^2 to 10^4 metres. The LCZ system is currently under development by Stewart and Oke, and thus, the version used in this paper is a prototype, as given in [7], and consists of 16 zones in urban, rural, and transitional areas.

Given the above-mentioned requirements for siting an urban climate network, two initial steps can be regarded as highly useful:

(1) (a) conducting some preliminary mobile spatial surveys traversed through areas of interest to see where are the areas of thermal anomaly of interest or (b) modelling the general thermal patterns by applying the obtained results from other cities with similar environmental conditions and built-up structures,

(2) mapping of some type of climate zone classifications (e.g., LCZ system in [7]) within the urban area of the city. The importance of this kind of classification lays not in the absolute accuracy of a given type to describe the site but in its ability to classify areas of a settlement with similar capacities of modifying the local climate [2]. Such classification is crucial when setting up an urban station to ensure that spatial homogeneity criteria are met for a station in the UCL.

The climate zone classification systems were not originally designed for mapping, it was designed to classify and standardize urban heat island observation sites, whether urban or rural, fixed or mobile. If the aim is to establish a new urban station network, the mapping seems to be a good application of the system for delineating the approximate sites of the stations representing a wider urban area.

The main objectives of this study are:

(a) to determine the built-up density distribution and the mean pattern of nocturnal urban canopy layer UHI intensity in the city of Novi Sad, Serbia using a model developed by [8],

(b) to map the climate zones using the LCZ system in [7] in the studied urban area,

(c) to determine the possible sites of the stations of a planned urban climate network in Novi Sad based on the obtained UHI pattern in (a) and the map of the climate zone classification in (b). The three existing stations (one in urban and two in rural zones) would be expanded with the recommended urban station network providing high-time frequency data of main climate parameters (air temperature and humidity, global radiation, and precipitation). The main purposes of this combined network are (i) to monitor the seasonal and diurnal patterns of the urban heat island in the UCL of Novi Sad and (ii) to determine areas inside the city being less stressful for the citizens during the more and more frequent heat waves using thermal comfort indices.

2. Study Area

Novi Sad is located in the northern part of Serbia (Vojvodina Province), that is, on the southern part of the Great Hungarian Plain (45°15′ N, 19°50′ E) (Figure 1). The investigated area is plain (mostly from 80 to 86 m a.s.l.) on Holocene sediments with a gentle relief, so generally, the climate is free from orographic effects. The river Danube passes on the southern and eastern edge of the urban area, and its width varies from 260 to 680 meters. The relatively narrow DTD channel (Danube-Tisza-Danube) passes through the northern part of the city and its climatic influence is probably negligible. South of the Novi Sad urban area, the northern slopes of Fruška Gora Mountains are located (the highest peak is 538 m a.s.l.) which descend steeply towards the Danube.

According to Köppen-Geiger climate classification, the region around Novi Sad is categorised as Cf climate (temperate warm climate with a rather uniform annual distribution of precipitation) [10, 11]. In Novi Sad, the annual mean air temperature is 11.1°C with an annual range of 22.1°C. The mean annual precipitation amount is 615 mm (based on data from 1949 to 2008). Szeged and Debrecen in Hungary, whose UHI and surface cover data were used for the development of the applied statistical method [8], are also in climate region Cf [11].

Novi Sad is the second largest city in Serbia (and in the mentioned geographical region) and has a population of 285,756 inhabitants (data from 2009) in a built-up area of approximately 60 km^2.

The recent city structure and the main buildings in the inner parts of these cities (Novi Sad, Szeged, and Debrecen) were developed at around the turn of the 20th century, and until the end of the World War 1, these cities belonged to the same country (Hungary). After this time, the development of the settlements in this region was almost parallel. After the Second World War, in both countries there were social regimes with similar urbanization policy and architecture (from 1945 until nineties). Therefore, these cities in Hungary and Serbia have very similar urban structure.

The project is co-financed by the European Union

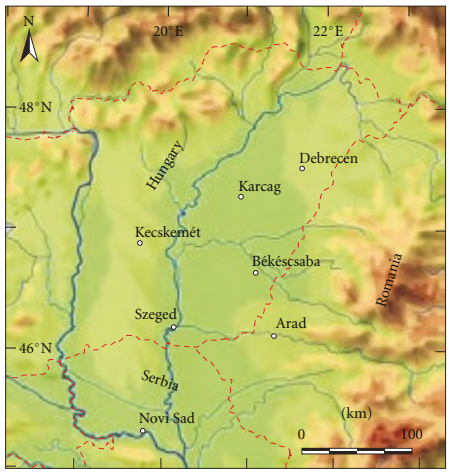

Figure 1: Locations of Novi Sad and the investigated cities in [8] with the relief map [9] of the Great Hungarian Plain and country borders (dashed lines).

Novi Sad has a densely built central area with medium-wide streets and avenue-boulevard roads network connecting different areas of the city. Around the city's central part, there are areas occupied by tall apartment buildings (mostly from 4 to 8 stories and with few examples with more than 10 stories) set in wide green space and detached houses (in most cases with 1 story). In the northern part, Novi Sad also contains zones used for industry and warehousing (flat and horizontal buildings, not higher than 10 m, i.e., 3 stories), and open space along the banks of the Danube, in parks, and around the city's outskirts.

In and around Novi Sad, four meteorological stations have been established in the last 60 years. The main meteorological station Rimski Šančevi (network of Republic Hydrometeorological Sevice) is situated in rural area (45°19′ N, 19°49′ E, 84 m a.s.l.), 1.9 km from the northern outskirts of the city and in 7.5 km distance from downtown (E1 in Figure 7(a)). The meteorological station was established in 1949, and up to now, it provides an undisturbed time series longer than 60 years. The Petrovaradin meteorological station was established in the middle of 20th century, and observations were taken in the period between 1956 and 1992. The station was situated in the southeastern part of the urban area at the Petrovaradin fortress (45°15′ N, 19°52′ E, 132 m a.s.l.) between compact lowrise apartment buildings and green space outskirts. Two automatic weather stations (AWS) were set up in 2009. The first AWS is situated at the Petrovaradin fortress (E2 in Figure 7(a)) and replaces of the closed Petrovaradin meteorological station, and the second one is situated in the rural zone (village Kać) approximately 9 km from Novi Sad downtown (E3 in Figure 7(a)). All mentioned stations measure or measured parameters like air temperature, precipitation, air humidity, winds, air pressure and various indices.

3. Previous UHI Investigations in Novi Sad

So far, a small number of papers have been published considering UHI investigations in Novi Sad. The first publication is theoretically based that is, it presents all parameters, methods and measurements which have to be used in order to work on UHI research of Novi Sad [12]. The next studies analyzed temperature values based on 30–40 year long time series (until 1990) [13, 14]. These studies used one rural (Rimski Šančevi) and one urban (Petrovaradin fortress) stations (see Figure 7). As the results showed, there are increasing trends of mean, maximum, and minimum temperatures at Petrovaradin, and in most cases, these trends are higher than trends at Rimski Šančevi. Based on meteorological parameters and the structure of urban area, Popov and Savić [15] showed the necessity of defining locations of an urban climate network in order to advance further UHI research in Novi Sad.

4. Method for Modelling the Mean UHI Pattern in Novi Sad

The applied method for the determination of the suspected spatial structure of the mean annual UHI intensity in Novi Sad is based on the study of Balázs et al. [8]. The main advantage of this regression method was to predict the spatial distribution of the annual mean UHI using just a few input parameters which can be determined in a simple way (remote sensing) without having detailed local information about the city. In this section, a short description is given on the UHI modelling in general and also on the used method (for more details, see Balázs et al. [8]).

4.1. Modelling the UHI Patterns. According to Oke [16] and Svensson et al. [17], three types of models can be applied for climate related research in urban environments: numerical, physical, and empirically based models. The advantage of the empirical models is that they are based on observed statistical properties, but their disadvantage is that they are often restricted to a specific location. Among the empirical models, statistical approaches are the most common methods to reveal relationships between the canopy layer UHI intensity and the meteorological as well as other physical parameters (including variables describing surface properties) which influence its formation. Thus, these models may provide useful quantitative information on the roles of the above-mentioned parameters in the development and spatial distribution of the UHI (e.g., [18–21]).

The spatial distribution of ΔT (UHI intensity) exhibits seasonal and diurnal variations as a result of meteorological and urban characteristics and location [2]. Simplifying the factors of a location (topography, water bodies) to a flat area and considering the annual mean UHI, its form and size are mainly a result of the urban factors [22, 23]. There are several studies which simulate ΔT using partly or entirely urban surface features as independent variables (e.g., [24–28]).

It has to be mentioned that the weakness of most of these studies is the lack of validation.

As detailed collection of urban data is complicated and requires significant technical investment, satellite images of settlements situated on a plain (no orographical influence) can serve as a tool to estimate the mean UHI intensity, because some parameters (e.g., covered or built-up surfaces) of the artificial urban environment can be easily determined through the evaluation of these images.

Experiments to model the spatial distribution of canopy layer ΔT for relatively large (several dozens of km^2 or more) urban areas are rather scarce. Some of them are listed in chronological order as follows: a numerical model for a 140 km^2 area of Christchurch, New Zealand [29], empirical models for a ~120 km^2 area of Łódź, Poland [30], for a ~700 km^2 area of Göteborg and its wide surroundings [17], for a ~30 km^2 area of Szeged, Hungary [31], and for a ~30 km^2 area of Debrecen, Hungary [32], and a numerical model for a ~400 km^2 area of Rome, Italy [33].

The empirical modelling study of Balázs et al. [8] dealt with UHI patterns of cities located in a rather homogeneous region therefore, it is more region than site specific. As we used their method, we give a short description of it. Datasets from Szeged (population 165 000) and Debrecen (population 204 000) situated on the Great Hungarian Plain in Hungary (Figure 1) were used to construct their empirical model. The measurements and modelling focused on the urbanized areas, about 30 km^2 for both cities. According to the original project plan, the annual mean UHI patterns of fifteen cities with different sizes and population, situated on the Great Hungarian Plain, were to be modelled using the obtained empirical model regardless of the existing country borders. As examples, Balázs et al. [8] presented modelled UHI patterns of only four of these cities.

4.2. Dependent Variable: UHI Intensity. For the information on the UHI intensity and its pattern (as dependent variable), temperature data were collected by mobile measurements in the urban areas of Szeged and Debrecen, which were divided into 0.5 km × 0.5 km grid cells. The study areas consisted of 107 cells (25.75 km^2) in Szeged and 105 cells (26 km^2) in Debrecen and covered the inner and suburban parts of the cities. One rural cell in both cities was used as a reference area for the comparison of temperature data. These cells are located outside of the cities, and their areas are agricultural fields with cereals and corn, that is, both cells belong to the LCZ "Low plant cover" [7], so they can be characterized as rural.

The required data were collected by cars on assigned routes, in a one-year period between April, 2002 and March, 2003. The survey routes passed through all cells but not always through the centre of them, since they were constricted by the road network. As the temperature does not vary abruptly within short distances, the obtained values can be regarded as repsentative ones for the cells. This type of mobile measurement is widespread in observing urban climate parameters (e.g., [34, 35]). The measurements took place at a frequency of about 10 days simultaneously, altogether 35 times in both cities. They were carried out under all kinds of weather conditions except rain. Based on experiences from previous studies, data collection took place at around the expected time of the daily maximum development of the UHI, which is 4 hours after sunset (e.g., [36, 37]). The UHI intensity (ΔT) by cells is defined as follows [19]:

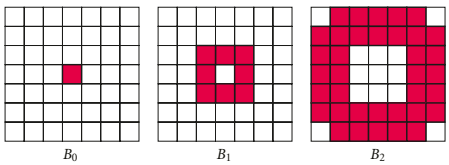

Figure 2: Cells which take part in the calculation of B_0, B_1, and B_2 surface parameters.

$$\Delta T = T_{\text{cell}} - T_{\text{cell(R)}}, \tag{1}$$

where T_{cell}= temperature of an urban cell and $T_{\text{cell(R)}}$ = temperature of the rural cell. Annual mean ΔTs were determined by averaging the ΔT values of the 35 measurements by cells.

4.3. Independent Variables. As independent variables for estimating the UHI field, 2D urban surface cover data and the distance from the city boundary were determined for each element of the 0.5 km × 0.5 km mesh in the study areas in Szeged and Debrecen.

The artificially covered surface ratio (streets, pavements, parking lots, roofs, etc.), or built-up ratio (B_0), horizontally characterizes the surface of a settlement. This parameter was determined for each cell using GIS (geographical information system) methods combined with the remote sensing analysis of Landsat satellite images [19]. The satellite images were taken in 2000, so they provide accurate data on the built-up conditions in the time of temperature measurements (2002-2003). Normalised difference vegetation index (NDVI) was calculated from the pixel values [38, 39], then the ratio of water, built-up, and vegetation surfaces in each cell were determined with this index by cells.

It is also important to consider the surface conditions around the cells, because the wider surroundings can influence the temperature of a given cell. In order to take the effect of the surroundings into account, a set of derived variables (average built-up ratio of concentric areal extensions around the cells, B_1, B_2) were constructed (Figure 2). The distinction of urban and rural cells based on an arbitrary but low value of B_0. If $B_0 < 5\%$, then the cell is considered rural, otherwise urban. This threshold ensures that cells defined as rural correspond with landscapes of cropped fields and few roads or buildings. The obtained zones of surface variables cover the entire study areas and their 1.5 km wide extensions in the investigated settlements. These extensions are needed in the calculations of B_1 and B_2 parameters for cells near the edges of study areas.

The distance (from the city centre or from the boundary) can be regarded as a parameter that characterizes the location of a place inside the city. That is, considering the areas with

The project is co-financed by the European Union

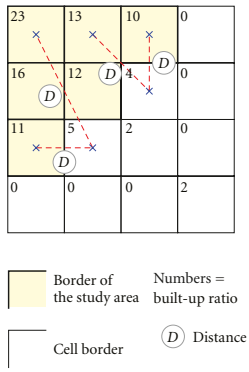

Figure 3: Examples for the determination of the distance (D) (built-up ratios are in %).

the same building structure and design in the suburbs and in the centre, a reduced ΔT can be experienced in the suburbs compared to that in the centre. Now, the distance from the city boundary (D in m) is considered. This D is defined as the distance between a given cell inside the study area and the nearest cell with a built-up ratio of less than 5% outside the study area (Figure 3).

In order to take into account the integrated affects of distance (D) and the above-mentioned surface parameters (B_0, B_1, and B_2) in the formation of UHI, some new combined urban parameters were constructed (marked by apostrophes: B_0', B_1', and B_2'). Based on the work of Fortuniak [20], distance is considered as $\ln D$. So, the combined parameters are generated by multiplying (or weighing) the surface parameters by the logarithmic distance by cells:

(i) parameter $B_0' = B_0 \cdot \ln D$,

(ii) parameter $B_1' = B_1 \cdot \ln D$,

(iii) parameter $B_2' = B_2 \cdot \ln D$.

4.4. Construction of the Multiple-Parameter Models. The relationship between the obtained combined urban surface parameters and the annual mean UHI intensity were determined to construct a general multiple-parameter model based on data from Szeged and Debrecen which can be used for the estimation of mean ΔT patterns in other settlements situated on a plain. The elements of the model are the following:

(i) ΔT, as variable parameter (°C),

(ii) B_0', B_1', B_2', as invariable parameters.

A stepwise multiple regression analysis was done with SPSS 11 software in order to compute the model equation [40]. The equation takes the following form:

$$\Delta T = 0.001032 \cdot B_0' + 0.002455 \cdot B_1' + 0.002629 \cdot B_2'. \quad (2)$$

Table 1: Validity intervals of the basic parameters for the obtained model based on the datasets of Balázs et al. [8].

Parameter	Min	Max
B_0 (%)	0	85.5
B_1 (%)	0.1	63.1
B_2 (%)	8.1	49.7
D (m)	0<	3162

Based on the ranges of the applied datasets from Szeged and Debrecen, the obtained model equation can be regarded as strictly valid in the parameter intervals presented in (Table 1). The equation has no constant; therefore, if the invariable parameters are equal to zero, the equation gives an UHI intensity of zero. It is in line with the experience that the unbuilt or barely built areas do not generate any temperature excess.

In order to properly test the obtained model equation, temperature datasets from three settlements having similar environmental conditions but being independent from those of Szeged and Debrecen were used. As a result, there was good correspondence between the measured values and the estimated ones by the model [8].

This general model was extended to other, different-sized settlements (Karcag, Kecskemét, Békéscsaba, and Arad), where the environment, like topography and climate, is similar to that of Szeged and Debrecen without taking country borders into account. As mentioned earlier, only certain Landsat satellite images of the settlements are necessary, from which the built-up ratio and its areal extensions (weighing with the log-distance from the city border) can be determined as independent variables for this purpose. The standard Kriging method and linear variogram model of Surfer 8 software were used to interpolate the temperature values by cells and for the spatial tracing of the isotherms [41, 42]). For the obtained UHI pattern, Balázs et al. [8], see Figures 8–11.

The obtained model equation can be considered applicable and appropriate for other cities of different size if the invariable parameter values of the study areas are within the intervals given in Table 1. Now, we apply the model to the city of Novi Sad (Serbia) situated at the edge of the Great Hungarian Plain not far (115 km) from Szeged (Figure 1).

5. Results and Discussion

5.1. Patterns of Built-Up Ratio and Modelled Mean UHI Intensity in the Study Area. According to the methods described in Section 4, first, a grid network (500 × 500 m) was established which contains the study area (240 cells) and its 1.5 km wide extension in and around Novi Sad. It covers the main urban areas of the city without the satellite settlements around it (Figure 4). The UTM coordinates of the NW and SE corners of the rectangle containing the grid network are 34T 400500 5019000 and 34T 415000 5000500, respectively.

A Landsat satellite image taken at June 26, 2006 [43] was used for the evaluation of NDVI and then of built-up ratio (B_0) by cells. The built-up ratio inside the study area ranges from values near 0% to values over 90% because of the River

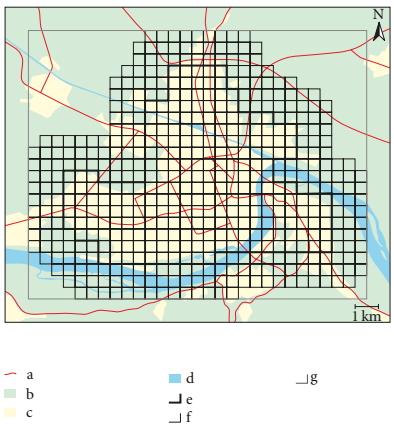

Figure 4: Grid network of the study area with its 1.5 km wide extension in Novi Sad: (a) main roads, (b) rural areas, (c) urban areas, (d) water bodies, (e) border of the study area, (f) cell border in the study area and in its extension, and (g) border of the rectangle containing the grid network.

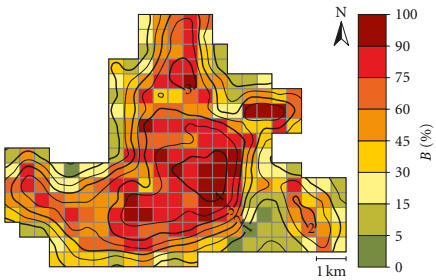

Figure 5: Spatial distribution of the built-up ratio (%) and the modelled annual mean UHI intensity (°C) in the study area of Novi Sad.

Danube and the densely built-up city centre (Figure 5). Large density can be found in the central part of the study area (about 30 cells) with the highest B values in its eastern areas near the Danube (in 10 neighbouring cells). More local built-up maxima are located in the western, northern, north-eastern and eastern, parts of the study area.

Based on the B_0 values, the other two built-up parameters B_1 and B_2, as well as the distance parameter D, were determined for each of the 240 cells of the study area. In order to model the annual mean UHI intensity values by cells, the combinations of these parameters (B_0', B_1', B_2') were calculated and then substituted into (2). As mentioned in Section 4, the development of the empirical model was based on the dataset of Szeged and Debrecen, so the largest B_0 values in Novi Sad slightly exceed the base data (see Table 1). This means a slight extrapolation of the model for certain cells (less than 10% of the cells) therefore, the obtained ΔT values in these cases should be treated cautiously. However, we are sure that the structure of the obtained ΔT field certainly reflects the main characteristic of the pattern of the UHI in Novi Sad (Figure 5).

As the predictors (B_0', B_1', B_2') of the model based primarily on the built-up ratio of the cells (B_0), already this measure itself has a significant influence on the spatial pattern of the mean UHI intensity (Figure 5): the ΔT values follow the change in the built-up values. In detail, the main feature of this pattern in the central study area is that the isotherms show concentric-like shapes with values increasing from the suburbs towards the inner urban areas with a highest ΔT(>4°C) in the densely built-up centre. Deviations from this concentric-like shape occur in the western, northern and north-eastern parts where the isotherm of 2°C stretches towards the outskirts. In addition, three island-like local maxima appear in the northern, north-eastern and eastern parts of the study area with values over 3°C, 2.5°C and 2°C, respectively. The largest area with very low ΔT values, owing to the influence of the River Danube, can be found in the south-eastern part of the study area.

For the evaluation of the model estimation a comparison have been made using the dataset of Rimski Šančevi (rural) and Petrovaradin (urban) stations (1956–1992) (Figure 7). In this period, the observations were taken three times a day (07, 14 and 21 according to Central European Time), and the dataset contains the observed temperatures and daily maximum, minimum, average temperatures. Since there were not night time measurements, the daily minimum temperature data was used for the comparison. The difference of the two measured daily minimum temperature were calculated for each day of the mentioned 37 years. The average of these differences (ΔT_{min}) can be considered as an approximate value of the annual mean urban heat island intensity (ΔT) [44]. The ΔT value for Petrovaradin calculated by the statistical model is 1.66°C and the measured (ΔT_{min}) is 1.8°C. This insignificant difference proves that the accuracy of the model estimation meets the requirements of the aim of this study.

5.2. Mapping of LCZs in the Study Area. The identification of climate zones in Novi Sad was based on information extracted from Google Maps [44], on guidance given by [7], and on the personal experiences of the second author (Figure 6). Since in Central-European urban areas the LCZ classes of *compact highrise*, *open-set highrise* and *lightweight lowrise* are missing, only the pattern of the remaining classes typical for this region were taken into account.

5.3. Recommendation for Station Sites of an Urban Climate Network. The planning of the possible sites of the stations of an urban climate network in Novi Sad is based on the structural features of the obtained UHI intensity pattern (Figure 5) and on the LCZ map (Figure 6). While searching

The project is co-financed by the European Union

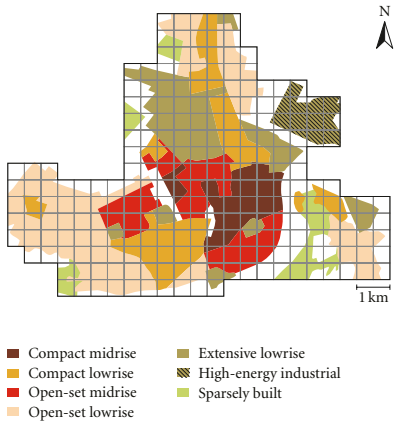

Figure 6: Spatial distribution of urban Local Climate Zones (based on [7]) occurring in the study area of Novi Sad.

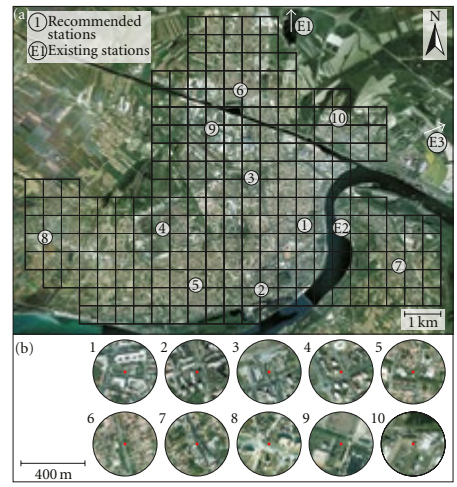

Figure 7: Satellite image of the study area in Novi Sad [45] with the existing stations and the recommended sites of a 10-station urban climate network (a) and the immediate surroundings (diameter—400 m) of these sites (b) (E1—Rimski Šančevi, E2—Petrovaradin, E3—Kać).

for the appropriate (representative) locations, two criteria were considered:

(1) the stations should be located at around the high and low ΔT areas, as well as at around the areas of the local maxima and stretches assumed by the modelled UHI pattern,

(2) homogeneous LCZ areas a few hundred metres wide should be around the sites.

According to previous criteria, ten representative station locations in the urban area of Novi Sad have been detected (Figure 7(a)). The locations represent the different neighbourhoods of the city, from the densely built-up area with medium narrow streets to the almost natural outskirts. The location numbered 1 is placed into the city's downtown with *compact midrise* landscape. The next three locations are situated in *open-set midrise* zones, with open natural surroundings among >3 stories tall buildings. Locations 5 and 6 characterise *compact lowrise* areas with tall buildings <3 stories and separeted by narrow streets, whereas locations 7 and 8 are in *open-set lowrise* zones, mostly with detached buildings separated by natural surfaces. The last two stations (9 and 10) are situated in industrial and warehouses zones (*high-energy industrial* and *extensive lowrise*). Also, it is important to mention that the two existing stations in the rural and in the urban (*open-set midrise*) area respectively (see Section 2), can be utilized to be a part of recommended urban climate network (Figure 7(a)). Furthermore, all stations would be set up at representative urban sites, according to scientific guidance [3, 45] (Figure 7(b)).

6. Conclusions

According to the analysis of the urban heat island pattern in Novi Sad (Serbia), the main conclusions of this study are as follows.

(1) Urban area of Novi Sad with its more than 280,000 inhabitants is located in a rather homogeneously relieved region in the Great Hungarian Plain. Therefore, research of UHI pattern can be based on empirical modelling study of Balázs et al. [8], where datasets from Szeged and Debrecen (Hungary) were used to construct an empirical model. The study area has been divided into a 0.5 km × 0.5 km mesh (240 cells) and has an extension of 1.5 km in and around Novi Sad.

(2) Evaluation of NDVI and built-up ratio values by cells varies from 0% in and around the Danube to over 90% in densely built-up downtown. Also, western, northern, north-eastern and eastern parts of Novi Sad's urban area are characterised as maximally built-up. These densely built-up area has a significant influence on the spatial pattern of the mean UHI intensity. The isotherms show concentric-like shapes with highest ΔT (>4°C) in the densely built-up centre and decrease towards the outskirts. A few local temperature islands (from 2°C to 3°C) occurred in the suburbs with intensive built-up areas.

(3) Analysis of UHI intensity and some type of climate zone classifications (e.g., LCZs in [7]) is very important in order to detect sites which can be suggested for the stations of an urban climate network in Novi Sad. According to defined criteria, a representative 10-station network in the urban area has been determined in order to prepare further UHI

research, that is, to monitor and provide measurement data of the urban heat island in the UCL of Novi Sad city, and to determine areas inside the city being less stressful for the citizens during heat waves using thermal comfort indices. The locations represent the complete range of the city's neighbourhoods, reaching from the densely built-up area with medium narrow streets to the almost natural outskirts. The result of this study is point out that the estimated mean UHI pattern and the distribution of some type of climate zone classifications in a city provide useful information in order to give recommendation on the possible sites of an urban UHI measurement network.

(4) The presented empirical model can be regarded as a useful tool for estimating the mean heat island patterns for small, Central European cities (typically of little vertical development) situated on a plain cities in the humid-continental climate type.

Acknowledgments

This research was supported by the Hungarian Scientific Research Fund (OTKA K-67626) and Serbian Ministry of Education and Science (Project no. 176020). The authors' special thanks are due to the anonymous reviewers for their several suggestions which improved the paper and to Mr. M. Hämmerle (University of Freiburg, Germany) for the language revision of the paper.

References

[1] T. R. Oke, "The distinction between canopy and boundary-layer urban heat islands," *Atmosphere*, vol. 14, no. 4, pp. 269–727, 1976.

[2] T. R. Oke, *Boundary Layer Climates*, Routledge, London ,UK, 2nd edition, 1987.

[3] T. R. Oke, "Initial guidance to obtain representative meteorological observation sites," WMO/TD 1250, 2004.

[4] I. D. Stewart, "Landscape representation and urban-rural dichotomy in empirical urban heat island literature, 1950–2006," *Acta Climatologica et Chorologica Universitatis Szegediensis*, vol. 40-41, pp. 111–121, 2007.

[5] I. D. Stewart and T. R. Oke, "Conference notebook—a new classification system for urban climate sites," *Bulletin of the American Meteorological Society*, vol. 90, pp. 922–923, 2009.

[6] I. D. Stewart, "Classifying urban climate field sites by "Local Climate Zones"," *Urban Climate News*, vol. 34, no. 4, pp. 8–11, 2009.

[7] I. D. Stewart and T. R. Oke, "Thermal differentiation of Local Climate Zones using temperature observations from urban and rural field sites," in *Proceedings of the 9th Symposium, on the Urban Environment*, Keystone, Colo, USA, August 2010.

[8] B. Balázs, J. Unger, T. Gál, Z. Sümeghy, J. Geiger, and S. Szegedi, "Simulation of the mean urban heat island using 2D surface parameters: empirical modelling, verification and extension," *Meteorological Applications*, vol. 16, no. 3, pp. 275–287, 2009.

[9] L. Zentai, "Relief of central Europe," in *Atlas of Central Europe*, A. Rónai, Ed., p. 411, Szent István Társulat—Püski Kiadó, Budapest, Hungary, 1993.

[10] L. Lazić and D. Pavić, *Climate of Banat*, University of Novi Sad, Faculty of Science, Department of Geography, Tourism and Hotel Management, Novi Sad, Vojvodina, 2003.

[11] M. Kottek, J. Grieser, C. Beck, B. Rudolf, and F. Rubel, "World map of the Köppen-Geiger climate classification updated," *Meteorologische Zeitschrift*, vol. 15, no. 3, pp. 259–263, 2006.

[12] Z. Popov, *Urban Climate, Methods, Measurements and Research*, Republic Hydrometeorological Service, Belgrade, Serbia, 1994.

[13] Z. Popov, *The Proposal for Setting Station Network to Monitor Urban Climate of in Novi Sad*, Republic Hydrometeorological Service, Belgrade, Serbia, 1995.

[14] L. Lazić, S. Savić, and Ż. Tomić, "Analysis of the temperature characteristics and trends in Novi Sad area (Vojvodina, Serbia)," *Geographica Pannonica*, vol. 10, pp. 14–21, 2006.

[15] Z. Popov and S. Savić, "The urban climate of Novi Sad," in *Proceedings of the 2nd Serbian Geographers' Congress—Towards Europe*, p. 62, Book of Abstract, Novi Sad, Vojvodina, 2010.

[16] T. R. Oke, "Towards a prescription for the greater use of climatic principles in settlement planning," *Energy and Buildings*, vol. 7, no. 1, pp. 1–10, 1984.

[17] M. Svensson, I. Eliasson, and B. Holmer, "A GIS based empirical model to simulate air temperature variations in the Göteborg urban area during the night," *Climate Research*, vol. 22, no. 3, pp. 215–226, 2002.

[18] H.-S. Park, "Features of the heat island in Seoul and its surrounding cities," *Atmospheric Environment*, vol. 20, no. 10, pp. 1859–1866, 1986.

[19] J. Unger, Z. Sümeghy, Á. Gulyás, Z. Bottyán, and L. Mucsi, "Land-use and meteorological aspects of the urban heat island," *Meteorological Applications*, vol. 8, no. 2, pp. 189–194, 2001.

[20] K. Fortuniak, "An application of the urban energy balance scheme for a statistical modeling of the UHI intensity," in *Proceedings of the 5th International Conference on Urban Climate*, K. Klysik, T. R. Oke, K. Fortuniak et al., Eds., vol. 1, pp. 59–62, University of Lodz, Lodz, Poland, 2003.

[21] M.-J. Alcoforado and H. Andrade, "Nocturnal urban heat island in Lisbon (Portugal): main features and modelling attempts," *Theoretical and Applied Climatology*, vol. 84, no. 1–3, pp. 151–159, 2006.

[22] W. P. Lowry, "Empirical estimation of urban effects on climate: a problem analysis," *Journal of Applied Meteorology*, vol. 16, no. 2, pp. 129–135, 1977.

[23] J. Unger, Z. Sümeghy, and J. Zoboki, "Temperature cross-section features in an urban area," *Atmospheric Research*, vol. 58, no. 2, pp. 117–127, 2001.

[24] Y. Goldreich, "Computation of the magnitude of Johannesburg's heat island," *Notos*, vol. 19, pp. 95–106, 1970.

[25] W. Kuttler, A.-B. Barlag, and F. Roßmann, "Study of the thermal structure of a town in a narrow valley," *Atmospheric Environment*, vol. 30, no. 3, pp. 365–378, 1996.

[26] J. Unger, Z. Bottyán, Z. Sümeghy, and Á. Gulyás, "Urban heat island development affected by urban surface factors," *Időjárás—The Quaterly Journal of the Hungarian Meteorological Service*, vol. 104, pp. 253–268, 2000.

[27] M. Szymanowski, "Spatial structure of the urban heat island in Wroclaw, Poland," in *Proceedings of the 5th International Conference on Urban Climate*, K. Klysik, T. R. Oke, K. Fortuniak, C. S. B. Grimmond, and J. Wibig, Eds., vol. 1, pp. 151–154, University of Łódź, Łódź, Poland, 2003.

[28] R. Giridharan, S. S. Y. Lau, S. Ganesan, and B. Givoni, "Urban design factors influencing heat island intensity in high-rise

high-density environments of Hong Kong," *Building and Environment*, vol. 42, no. 10, pp. 3669–3684, 2007.

[29] N. J. Tapper, P. D. Tyson, I. F. Owens, and W. J. Hastie, "Modeling the winter urban heat island over Christchurch," *Journal of Applied Meteorology*, vol. 20, no. 4, pp. 365–376, 1981.

[30] K. Fortuniak and K. Klysik, "Intensity of the urban heat island in Lodz under winter conditions and its simple model," *Acta Universitatis Lodziensis, Folia Geographica Physica*, vol. 3, pp. 83–90, 1998.

[31] Z. Bottyán and J. Unger, "A multiple linear statistical model for estimating the mean maximum urban heat island," *Theoretical and Applied Climatology*, vol. 75, no. 3-4, pp. 233–243, 2003.

[32] Z. Bottyán, A. Kircsi, S. Szegedi, and J. Unger, "The relationship between built-up areas and the spatial development of the mean maximum urban heat island in Debrecen, Hungary," *International Journal of Climatology*, vol. 25, no. 3, pp. 405–418, 2005.

[33] V. Bonacquisti, G. R. Casale, S. Palmieri, and A. M. Siani, "A canopy layer model and its application to Rome," *Science of the Total Environment*, vol. 364, no. 1–3, pp. 1–13, 2006.

[34] T. R. Oke and R. F. Fuggle, "Comparison of urban/rural counter and net radiation at night," *Boundary-Layer Meteorology*, vol. 2, no. 3, pp. 290–308, 1972.

[35] M. C. Moreno-Garcia, "Intensity and form of the urban heat island in Barcelona," *International Journal of Climatology*, vol. 14, no. 6, pp. 705–710, 1994.

[36] T. R. Oke, "Canyon geometry and the nocturnal urban heat island: comparison of scale model and field observations," *Journal of Climatology*, vol. 1, no. 3, pp. 237–254, 1981.

[37] J. Unger, "Intra-urban relationship between surface geometry and urban heat island: review and new approach," *Climate Research*, vol. 27, no. 3, pp. 253–264, 2004.

[38] K. P. Gallo and T. W. Owen, "Satellite-based adjustments for the urban heat island temperature bias," *Journal of Applied Meteorology*, vol. 38, no. 6, pp. 806–813, 1999.

[39] T. M. Lillesand and R. W. Kiefer, *Remote Sensing and Image Interpretation*, John Wiley & Sons, New York, NY, USA, 1987.

[40] J. Cohen, P. Cohen, S. G. West, and L. S. Aiken, *Applied Multiple Regression/Correlation Analysis for the Behavioral Sciences*, Lawrence Erlbaum Associates, Hillsdale, NJ, USA, 2nd edition, 2003.

[41] J.-P. Chiles and P. Delfiner, *Geostatistics, Modeling Spatial Uncertainty*, Wiley Series in Probability and Statistics, New York, NY, USA, 1999.

[42] X. Emery, "Multigaussian kriging for point-support estimation: incorporating constraints on the sum of the kriging weights," *Stochastic Environmental Research and Risk Assessment*, vol. 20, no. 1-2, pp. 53–65, 2006.

[43] NASA Landsat Program, Landsat ETM+ scene L5187028_02820060626, Orthorectified, USGS, Sioux Falls 26/06/2006, http://glcfapp.glcf.umd.edu:8080/esdi/index.jsp, 2008.

[44] Google maps, http://maps.google.com/, 2010.

[45] I. D. Stewart, "A systematic review and scientific critique of methodology in modern urban heat island literature," *International Journal of Climatology*, vol. 31, no. 2, pp. 200–217, 2011.

A VECTOR-BASED GIS METHOD FOR MAPPING OF LOCAL CLIMATE ZONES AND ITS APPLICATION IN A CENTRAL-EUROPEAN CITY

Unger J., Lelovics E., Gál T.

Department of Climatology and Landscape Ecology, University of Szeged

unger@geo.u-szeged.hu

Summary

A new vector-based method was developed to determine geometrical and land cover parameters of different urban neighborhoods. The database for this method contains 3D building database and remotely sensed information from Landsat satellite images. The obtained parameters are the sky view factor, aspect ratio, mean building height, terrain roughness, building surface fraction and impervious/pervious surface fractions. The aim of this automatic procedure is the delineation of thermally different Local Climate Zones (LCZs) based the value ranges of the mentioned parameters.

The mapping of LCZs was performed in a South-Hungarian city of Szeged where the urban climate investigations have already a long history. These studies have provided a thorough knowledge about the thermal peculiarities of the city, namely about the intra-urban temperature distribution on average and in different synoptic situations. These earlier obtained temperature data across the city provided an opportunity for us to verify whether the delineated zones with different physical properties have indeed different thermal reactions. According to our preliminary results the mean seasonal temperature by zones meet the expectations, ie, the more urbanized the warmer is an area within the city.

As a second step of our study we will (i) involve satellite and aerial images in order to determine other physical properties (e.g. albedo) of the urban surfaces and (ii) gather information about the distribution of transport density, domestic and industrial energy usage in order to assess the anthropogenic heat flux. With this additional information the mapping of the LCZs may be more accurate. The final version of the standalone GIS method will be appropriate for use in any other urban areas if the necessary input data are available.

Keywords: Local Climate Zones, GIS methods, temperature patterns, Szeged, Hungary

INTRODUCTION

Nowadays about half of the human population is affected by the burdens of urban environments: pollution, noise and the modified characteristics of the urban atmosphere compared to the natural environment. This makes studies dealing with the urban impact on climate particularly important. Owing to the anthropogenic activity, a local climate develops in the built-up areas. This urban climate is different from the pre-urban (natural) one and is a result of the construction of buildings, roads, etc., as well as of the emission of heat, moisture and pollution related to human activities.

ISBN 9788895597188

Among the parameters of the urban atmosphere the near-surface (1.5-2 metres above ground level or screen-height) air temperature shows the most obvious modification compared to the rural area (Oke, 1987). This urban warming is commonly referred to as the urban heat island (UHI) and its magnitude is the UHI intensity (ΔT_{u-r}). Nevertheless, in the heat island literature the term "urban" has no single, objective meaning as the areas around the measuring sites could be very different depending on the investigated cities (e.g. park, college ground, street canyon, housing estate, etc.). In addition, for landscape classification or description of the site surroundings the simple "urban" versus "rural" is not appropriate because of the abundant variety of the landscapes according to their surface properties relevant to development of near-surface micro and local climates (Stewart 2007, 2011).

To diminish this deficiency, Stewart and Oke (2012) developed a climate-based classification system for describing the local physical conditions around the temperature measuring field sites universally and relative easily based on the earlier studies from the last decades (e.g. Auer, 1978; Ellefsen, 1991; Oke, 2004; Stewart and Oke, 2009), as well as a thorough review on the empirical heat island literature and world-wide surveys of the measurement sites with their surroundings. The elements of this system are the "local climate zones" (LCZ) and they are presented shortly in Section 2.2.

Because of the complexity of the urban terrain the monitoring of the representative intra-urban thermal features is a difficult task (Oke, 2004). The locations of the sites of an urban station network within the city and thus the question about its appropriate configuration raises an essential problem. This problem is related to the relationship between the intra-urban built and land cover LCZ types and the locations of the network sites. Two situations arise:

(1) In the case of an already existing network (e.g. Schroeder et al. 2010) it may be required to characterize the relatively wider environment around the measuring sites, namely what type of urban area (LCZ) surrounds a given station and whether it can be clearly determined. In other words, how representative is the location of a station regarding a specific, clearly defined LCZ type in an urban environment?

(2) In the case of a planned station network (e.g. Unger et al. 2011) the most important questions are what built and land cover LCZ types can be distinguished in a given urban area, how precisely they can be delimited, how many they are, and whether their extension is large enough to install a station somewhere in the middle of the area (representing the thermal conditions of this LCZ) while of course taking care to minimize the microclimatic effects of the immediate environment.

The aims of this study are: (i) to determine the LCZ types in Szeged which are representative for the urbanized area of the city using seven geometric, surface cover and radiative properties from the ten ones listed by Stewart and Oke (2012), (ii) to develop GIS methods in order to calculate these seven property values for any part of the study area and (iii) to compare the thermal reactions of the selected LCZ areas based on the earlier temperature measurement campaigns carried out in this city.

STUDY AREA AND METHODS

Temperature measurements in Szeged

Szeged is located in the south-eastern part of Hungary (46°N, 20°E) at 79 m above sea level on a flat terrain (Figures 1a and 1b) with a population of 160,000 within an administration district of 281 km^2. The area is in Köppen's climatic region Cf (temperate warm climate with a rather uniform annual distribution of precipitation). The annual mean temperature is 10.4ºC and the amount of precipitation is 497 mm (Unger et al., 2001).

ISBN 9788895597188

The study area consists of 103 cells (500 × 500 m) covering the urban and suburban parts of Szeged (25.75 km^2). Additionally, in order to represent non built-up areas four cells (1 km^2) were added to the network at the western side of the area (Figure 1c).

Figure 1: (a) Location of the Szeged in Europe, (b) in Hungary and (c) the grid network of the study area (gray – urbanized area).

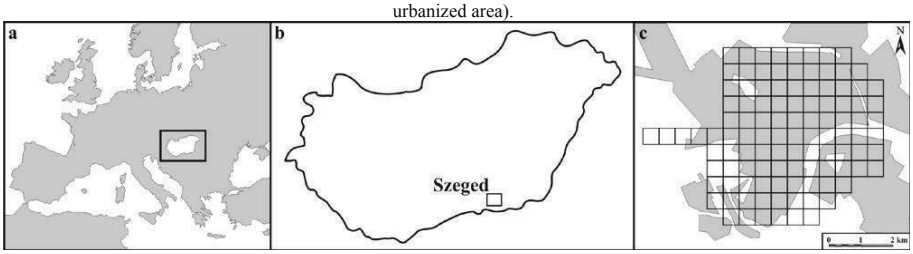

Mobile measurements were taken by cars at the same time on fixed return routes during a one-year period (April 2002 – March 2003) by several times. Return routes were taken to make time-based corrections to a reference time (4 hours after sunset). Readings were obtained using radiation-shielded resistance sensors mounted at 1.45 m above ground and connected to data loggers. Data were collected every 10 s, so at a car speed of 20-30 kmh^{-1} the distance between measuring points was 55-83 m. The logged values at forced stops were omitted. After averaging the usually 15-20 measurement values by cells in every measurement nights, the obtained values referred to the cell centres (for more details see Unger, 2004, 2006; Balázs et al., 2009).

That is, as a result of mobile measurements, our "measuring sites" are in the centres of the cells so the obtained average values by cells are regarded as "measured" temperature values in these "measuring sites" in a given night. As the most ideal conditions for UHI developments prevail in summer and early autumn in this region (WMO, 1996), two nights were selected in summer (15 July 2002, 21 August 2002), one in autumn (18 September 2002), and additionally one in spring (25 March 2003). At these times the weather was clear and calm in the preceding days too, thus during these nights the weather conditions promoted the surface influence on the thermal conditions in the near-surface air layer. Additionally, the ground was relatively dry and the trees had foliage.

Key features of the lcz classification system

The necessity and ideas of the development of "local climate zone" classification system and its structure are presented and discussed in details by Stewart and Oke (2012). Therefore here we highlight only the key features of the system. LCZs are defined as "regions of uniform surface cover, structure, material, and human activity that span hundreds of meters to several kilometres in horizontal scale. Each LCZ has a characteristic screen-height temperature regime that is most apparent over dry surfaces, on calm, clear nights, and in areas of simple relief." (Stewart and Oke, 2012). Among them there are ten built types (from LCZ 1 to LCZ 10) and seven land cover types (from LCZ A to LCZ G), and additionally, the types can have variable seasonal or shorter period land cover properties. The main characters of the types are reflected in their names (Table 1).

ISBN 9788895597188

Table 1. Names and designation of the LCZ types (after Stewart and Oke, 2012)

Built types	Land cover types	Variable land cover properties
LCZ 1 – Compact high-rise	LCZ A – Dense trees	b – bare trees
LCZ 2 – Compact midrise	LCZ B – Scattered trees	s – snow cover
LCZ 3 – Compact low-rise	LCZ C – Bush, scrub	d – dry ground
LCZ 4 – Open high-rise	LCZ D – Low plants	w – wet ground
LCZ 5 – Open midrise	LCZ E – Bare rock / paved	
LCZ 6 – Open low-rise	LCZ F – Bare soil / sand	
LCZ 7 – Lightweight low-rise	LCZ G – Water	
LCZ 8 – Large low-rise		
LCZ 9 – Sparsely built		
LCZ 10 – Heavy industry		

The LCZ types can be distinguished by the measurable physical properties (parameters) (Table 2). These parameters are partly dimensionless (e.g. sky view factor), partly given in %, m, etc. (e.g. building surface fraction) and their values have different ranges according to the different types. Stewart and Oke (2012) give the typical values of them (see Table 3 too).

Table 2. Zone properties of LCZ system (after Stewart and Oke, 2012)

	Type of properties	
	Geometric, surface cover	Thermal, radiative, metabolic
Properties	sky view factor	surface admittance ($Jm^{-2}s^{-1/2}K^{-1}$)
	aspect ratio	surface albedo
	building surface fraction (%)	anthropogenic heat output (Wm^{-2})
	impervious surface fraction (%)	
	pervious surface fraction (%)	
	height of roughness elements (m)	
	terrain roughness class	

In the frame of this new classification system the intra-urban UHI intensity is an LCZ temperature difference ($\Delta T_{LCZ:X–Y}$), not an "urban-rural" difference ($\Delta T_{u–r}$) (Stewart and Oke, 2012).

Vector based GIS method

From the ten geometric, surface cover and radiative properties listed by Stewart and Oke (2012) we can determine seven of them with our methods for any given area inside the study area. These are the sky view factor (SVF), building surface fraction (BSF), impervious surface fraction (ISF), pervious surface fraction (PSF), height of roughness elements (HRE), terrain roughness class (TRC) and albedo (A). Our calculations were carried out in circle areas with 250 m radius centered in the middle of the grid network cells. This size is necessary as the upwind fetch of typically 200-500 m is required for air at screen-height to become fully adjusted to the underlying, relatively homogeneous surface (Stewart and Oke, 2012).

The applied methods by parameters:

- SVF: The input was a SVF database with 5 m horizontal resolution originated from our earlier studies. It was calculated using the 3D building database of Szeged with a vector based method. The building database contains building footprint areas as polygons, and the height value for each building measured with photogrammetric methods. During the SVF calculation all of the buildings were regarded with flat roof and the effect of the vegetation was neglected (Gál et al., 2009; Unger, 2006). Now the SVF values of grid points inside the examined circle area were averaged.

- BSF: The input was the 3D building database of Szeged where all of the footprints of the buildings are available from the study area. BSF is the fraction of summarized area of buildings inside the circle. The buildings on the border of the circle were divided into two parts, and the area of intersecting part had been taken into account for the summarized building area.

- PSF: The input for the PSF was a built-up dataset calculated from RapidEye satellite image using NDVI index, a 1:25000 topographic map, a road database and the Corine Land Cover (CLC) (Bossard et al., 2000) database. The

ISBN 9788895597188

RapidEye image is atmospherically corrected (resolution of 5.16 m) and the NDVI was calculated using bands 3 and 5. Basically the point where the NDVI is above 0.3 was regarded as built-up area. The CLC dataset was used to locate the agricultural areas as these areas have small NDVI because after harvest the amount of plants on them is almost zero. As a second correction the shape of water bodies were digitized in the topographic map because water has NDVI values very similar to the values of some building materials. As a last correction the road database was used to locate the asphalt roads in the area because in the urban canyons these roads are usually under tree cover and roads (ISF) which slice agricultural areas do not appear in CLC dataset.

- ISF: The value of the ISF were calculated using this formula: ISF = 1 – (BSF + PSF).

- HRE: The input for the HRE was also the 3D building database of Szeged. For each examined circle area height of the buildings (and building parts) weighting with their footprint areas were averaged.

- TRC: For describing the roughness the Davenport roughness classification method was used (Davenport et al., 2000). All of the circle areas were classified into roughness classes with visual interpretation of aerial photographs, the topographical map and the building database.

- A: As an input we used the atmospherically corrected reflectance values of the 5 band RapidEye satellite image. Broadband albedo was calculated as an average of reflectance values weighted with the integral of the radiation within the spectral range of a given band (Starks et al. 1991).

Results

As a first step we determined the possible LCZ types occurring in the study area of Szeged and we selected areas with 250 m radius for each type which represent them. Secondly, the temperature differences between these areas were compared on the above mentioned measurements nights separately and on average, too.

LCZ types in Szeged and their representative areas

With the help of the obtained parameter values supplemented by viewing aerial photographs and authors' local knowledge of the study area, theoretically every areas in the 103 cells can be classified. In Szeged the high-rise type areas (LCZs 1 and 4), the lightweight low-rise shanty districts (LCZ 7) and the heavy type industry (LCZ 10) are not present among the built type LCZs, thus we searched for representative areas of the remaining six types (LCZs 2, 3, 5, 6, 8 and 9). As the study area of temperature measurements concentrated on the urbanized parts of the city (Fig. 1c), only the westernmost cell can be regarded as a non built-up cell, because it consists of agricultural fields with low plants without trees and a few small houses. So, according to the land cover type classification, the circle area in this cell can be regarded as a representative area of LCZ D type (low plants). As a result, Figures 2 and 3 show the locations and aerial photographs of the selected circle areas.

ISBN 9788895597188

Figure 2: Locations of the selected circle areas representing the LCZ types occurring in Szeged with their names and designations.

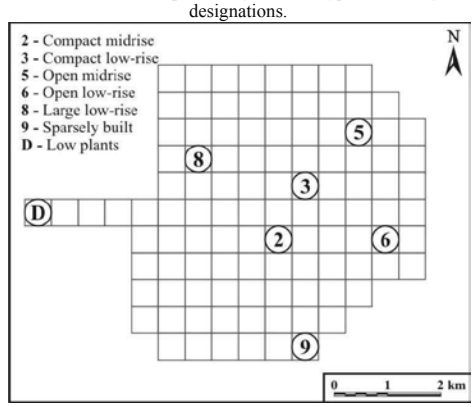

The values of the areas characterized as LCZs 2 and 6 fit into the formally defined parameter ranges given in Table 3. Nevertheless, in some cases there are smaller deviations in the obtained parameter values from the defined ranges (these values are marked with underlines). The aerial pictures in Figure 3 give us much help in the final decision regarded the classification. Although we are convinced that the selected areas represent the LCZ types as we specified, these deviations require some explanation:

- LCZ 3 "Compact low-rise" – It has extended covered areas, the ISF barely exceeds the upper limit (50.4%), thus it has a slightly higher SVF (0.68). The BSF is a bit under the lower limit of this parameter (31.4%) so it could be even LCZ 6 (open low-rise), but the PSF is under 20% which is typical of LCZ 3.

- LCZ 5 "Open midrise" – As this area is well vegetated the PSF is slightly higher (41.5%) than the upper limit with the result of a bit lower BSF value (16.2%). This could us lead to classify this area even as LCZ 6 (open low-rise), but the HRE value (15.4 m) justifies the selection of LCZ 5.

- LCZ 8 "Large low-rise" – The PSF is larger (24.9%) as this area has a sport field, as well as the ISF is also higher (59.6%) thus the BSF is a bit smaller (15.5%). However, as the picture in Figure 3 shows, it is a typical warehouse area with factory buildings, so it is classified as LCZ 8.

- LCZ 9 "Sparsely built" – This area is characterized with low BSF (2.5%) and TRC (4) so it could be even LCZ D (low plants), but because of its high ISF (22.5%) it is better classified as LCZ 9.

ISBN 9788895597188

Figure 3: Aerial photographs of the circle areas with their designations representing the LCZ types occurring in Szeged.

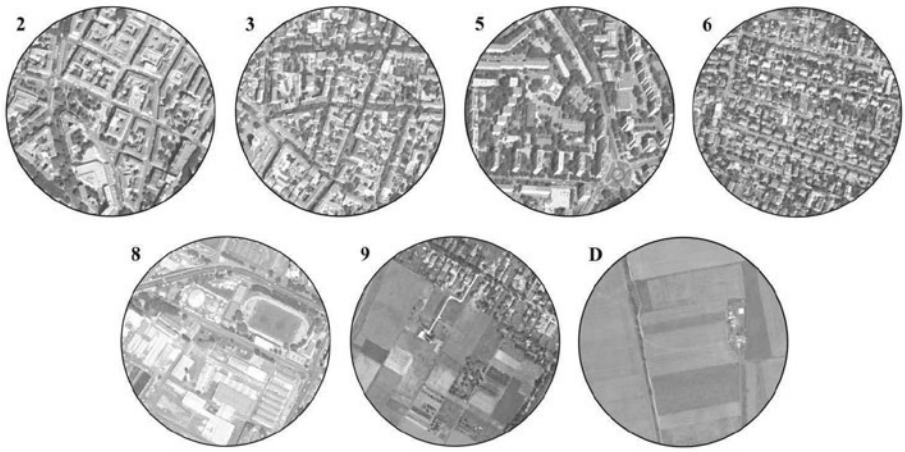

Table 3. Formally defined ranges of the properties for LCZ types (Stewart and Oke, 2012) compared to the values (*italics*) of the representative areas in Szeged (underlined values deviate from the defined ranges).

LCZ name and designation	Properties						
	SVF sky view factor	BSF building surface fraction (%)	ISF impervious surface fraction (%)	PSF pervious surface fraction (%)	HRE height of roughness elements (m)	TRC terrain roughness class	A albedo
LCZ 2	0.3–0.6	40–70	30–50	< 20	10–25	6–7	0.10–0.20
Compact midrise	*0.59*	*45.4*	*44.0*	*10.5*	*13.6*	*7*	*0.15*
LCZ 3	0.2–0.6	40–70	20–50	< 30	3–10	6	0.10–0.20
Compact low-rise	*0.68*	*31.4*	*50.4*	*18.2*	*7.9*	*6*	*0.14*
LCZ 5	0.5–0.8	20–40	30–50	20–40	10–25	5–6	0.12–0.25
Open midrise	*0.74*	*16.2*	*42.3*	*41.5*	*15.4*	*6*	*0.12*
LCZ 6	0.6–0.9	20–40	20–50	30–60	3–10	5–6	0.12–0.25
Open low-rise	*0.83*	*20.3*	*45.3*	*34.4*	*5.4*	*6*	*0.16*
LCZ 8	> 0.7	30–50	40–50	< 20	3–10	5	0.15–0.25
Large low-rise	*0.92*	*15.5*	*59.6*	*24.9*	*6.6*	*5*	*0.16*
LCZ 9	> 0.8	10–20	< 20	60–80	3–10	5–6	0.12–0.20
Sparsely built	*0.99*	*2.5*	*22.5*	*75.0*	*5.0*	*4*	*0.17*
LCZ D	> 0.9	< 10	< 10	> 90	< 1	3–4	0.15–0.25
Low plants	*0.999*	*0.2*	0.0	99.8	*0.0*	*3*	*0.15*

Thermal differentiation: comparison of LCZ temperatures

Figure 4 shows the temperature differences of the built LCZ types from the land cover D type ($\Delta T_{LCZ:X-D}$) at the selected nights and on average, too. The average and individual values follow the expected sequence: compact built and midrise types have larger temperatures than open and low-rise ones, respectively. That is, the differences decrease from compact midrise (LCZ 2) to open low-rise (LCZ 6) areas, then there is an increment at the large low-rise (LCZ 8) area and finally, the difference is around 0ºC at the sparsely built (LCZ 9) area.

The largest average difference, $\Delta T_{LCZ:2-D}$ is more than 4ºC which means a very significant temperature deviation between the two areas. Even the smallest differences (at LCZs 6 and 8) are about 1ºC, only the LCZ 9 located at the city edge has similar value as the westernmost (agricultural) LCZ D.

ISBN 9788895597188

At the individual nights deviation can be even larger: as an example, in March the $\Delta T_{LCZ:2-D}$ reaches almost 6ºC, but the $\Delta T_{LCZ:3-D}$ were over 4.5ºC, as well as even $\Delta T_{LCZ:5-D}$ and $\Delta T_{LCZ:8-D}$ exceeded 3ºC (Figure 4). These findings are similar to those obtained by Stewart and Oke (2010) in Uppsala (compact midrise and low plants difference can exceed 5ºC).

Figure 4: Temperature differentiation of built LCZ types from the LCZ D type at the selected nights and on average in Szeged.

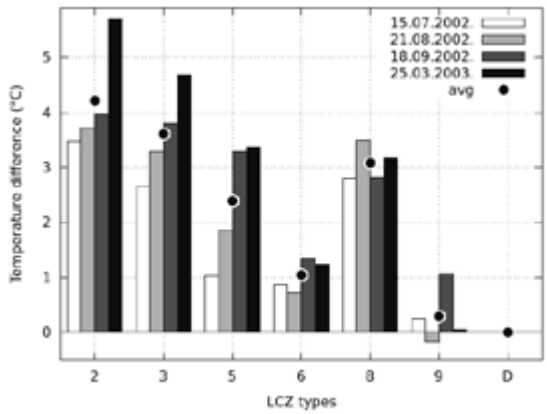

Table 4. Pairwise average temperature differences (ºC) of LCZ types in Szeged (line 1 minus column 1)

LCZ code	2	3	5	6	8	9	D
2	0.00	-0.61	-1.83	-3.17	-1.14	-3.92	-4.22
3	0.61	0.00	-1.21	-2.56	-0.53	-3.31	-3.60
5	1.83	1.21	0.00	-1.35	0.69	-2.10	-2.39
6	3.17	2.56	1.35	0.00	2.04	-0.75	-1.04
8	1.14	0.53	-0.69	-2.04	0.00	-2.78	-3.08
9	3.92	3.31	2.10	0.75	2.78	0.00	-0.29
D	4.22	3.60	2.39	1.04	3.08	0.29	0.00

As already mentioned above, in this new system the UHI intensity not an "urban-rural" difference but a temperature difference between the LCZ areas. This is reflected in the values of Table 4 which contains the pairwise average temperature differences (ºC) of LCZs representative for Szeged. The largest average difference is 4.22ºC ($\Delta T_{LCZ:2-D}$), but $\Delta T_{LCZ:2-9}$, $\Delta T_{LCZ:2-6}$, $\Delta T_{LCZ:3-D}$, $\Delta T_{LCZ:3-9}$, $\Delta T_{LCZ:8-D}$ mean also significant differences, as they all are above 3ºC.

Conclusions

In this study we determined the LCZ types in Szeged which are representative for the urbanized area of the city using seven geometric, surface cover and radiative properties from the ten ones listed by Stewart and Oke (2012) and compared their thermal reactions based on the earlier temperature measurement campaigns carried out in this city.

The values of the seven properties were calculated by GIS methods developed for this purpose and for the appropriate classification of the selected areas we used also our local knowledge about the districts of Szeged. As a result, six built and one land cover LCZ types were distinguished in the studied urban area.

The temperature comparisons of LCZs at selected times which were characterized with calm and clear weather conditions, relatively dry ground surfaces and leafy trees confirmed the findings of Stewart and Oke (2012): the thermal influence of any change or difference in landscapes (thus the different levels of urbanization too) are better expressed

ISBN 9788895597188

using LCZ difference concept than a simple but generally not clear urban-rural approach, and additionally, it provides an opportunity for intra- and inter-urban comparisons.

ACKNOWLEDGMENTS

The study was supported by the Hungarian Scientific Research Fund (OTKA PD-100352). The authors' thanks are due to László Mucsi (University of Szeged) for providing RapidEye satellite image.

REFERENCES

Auer, A. H. (1978) Correlation of land use and cover with meteorological anomalies. *Journal of Applied Meteorology* 17: 636-643.

ASTM (2012) American Society for Testing and Materials Reference Solar Spectral Irradiance: Air Mass 1.5 http://rredc.nrel.gov/solar/spectra/am1.5 (accessed on January, 25, 2013)

Balázs, B., Unger, J., Gál, T., Sümeghy, Z., Geiger, J. and Szegedi, S. (2009) Simulation of the mean urban heat island using 2D surface parameters: empirical modeling, verification and extension. *Meteorological Application* 16: 275-287.

Bossard, M., Feranec, J., Otahel, J. (2000) CORINE land cover technical guide – Addendum 2000. Technical report No 40. European Environment Agency, Copenhagen, Denmark.

Davenport, A. G., Grimmond, C. S. B., Oke, T. R. and Wieringa, J. (2000) Estimating the roughness of cities and sheltered country. Proceed. 12th Conference on Applied Climatology, Asheville, NC, 96-99.

Ellefsen, R. (1990) Mapping and measuring buildings in the canopy boundary layer in ten U.S. cities. *Energy and Buildings* 15-16: 1025-1049.

Gál, T. and Unger, J. (2009) Detection of ventilation paths using high-resolution roughness parameter mapping in a large urban area. *Building and Environment* 44: 198-206.

Oke T. R. (1987) *Boundary Layer Climates. (2nd ed.)* Routledge, London-New York.

Oke T. R. (2004) *Initial guidance to obtain representative meteorological observation sites*. WMO/TD No. 1250, Switzerland: Geneva.

Schroeder, A. J., Basara, J. B. and Illston, B. G. (2010) Challenges associated with classifying urban meteorological stations: The Oklahoma City Micronet example. *Open Atmospheric Science Journal* 4: 88-100.

Starks, P. J., Norman, J. M., Blad, B. L., Walter-Shea, E. A., Walthall, C. L. (1991) Estimation of shortwave hemispherical reflectance (albedo) from bidirectionally reflected radiance data. *Remote Sensing of Environment* 38: 123–134.

Stewart, I. D. (2007) Landscape representation and urban-rural dichotomy in empirical urban heat island literature, 1950-2006. *Acta Climatologica et Chorologica Universitatis Szegediensis* 40-41: 111-121.

Stewart, I. D. (2011) A systematic review and scientific critique of methodology in modern urban heat island literature. *International Journal of Climatology* 31: 200-217.

Stewart, I. D. and Oke, T. R. (2009) A new classification system for urban climate sites. *Bulletin of the American Meteorologial Society* 90: 922-923.

Stewart, I. D. and Oke, T. R. (2010) Thermal differentiation of local climate zones using temperature observations from urban and rural field sites. Extended Abstracts, Ninth Symposium on Urban Environment, Keystone, CO, Amer. Meteorol. Soc.

ISBN 9788895597188

Stewart, I. D. and Oke, T. R. (2012) Local Climate Zones for urban temperature studies. *Bulletin of the American Meteorological Society* 93: 1879-1900.

Unger, J. (2004) Intra-urban relationship between surface geometry and urban heat island: review and new approach. *Climate Research* 27: 253-264.

Unger, J. (2006) Modelling of the annual mean maximum urban heat island using 2D and 3D surface parameters. *Climate Research* 30: 215-226.

Unger, J., Sümeghy, Z., Gulyás, Á., Bottyán, Z. and Mucsi, L. (2001) Land-use and meteorological aspects of the urban heat island. *Meteorological Applications* 8: 189-194.

Unger, J., Savic, S. and Gál, T. (2011) Modelling of the annual mean urban heat island pattern for planning of representative urban climate station network. *Advances in Meteorology* 2011: ID 398613, 9p.

WMO, (1996) *Climatological Normals (CLINO) for the period 1961–1990*. WMO/OMM-No. 847. Secretariat of the World Meteorological Organization, Geneva, Switzerland.

ISBN 9788895597188

TWO HUNDRED YEARS OF URBAN METEOROLOGY IN THE HEART OF FLORENCE

Proceedings of the International Conference On Urban Climate And History Of Meteorology

Firenze, Italy, 25th /26th February 2013

Edited by
T. GEORGIADIS, M. A. LOKOSHCHENKO , C. SCRETI, C. VAGNOLI

Firenze, Italy, June 2013
ISBN 9788895597188

Hungarian Geographical Bulletin 63 (1) (2014) 29–41.
DOI: 10.15201/hungeobull.63.1.3

Local Climate Zone mapping using GIS methods in Szeged

János UNGER[1], Enikő LELOVICS[1] and Tamás GÁL[1]

Abstract

Owing to anthropogenic activity, local climate develops in the area of built-up zones. The characteristics of built-up zones can be quantified by different methods. One of the methods is the Local Climate Zones (LCZ) classification system which describes the physical conditions of a local-scale environment of a measuring site from the viewpoint of the generated local climate. It is applicable worldwide universally and relatively easily based on objective geometric, radiative and thermal properties of the surface. The objectives of this study are to develop GIS methods in order to calculate several parameters describing the LCZs for any part of the study area using different databases and to identify and delineate the LCZ types which occur in and around the city of Szeged (Hungary) using the developed methods. As a result, six built LCZ types were distinguished and mapped in the studied urban area: "compact mid-rise", "compact low-rise", "open mid-rise", "open low-rise", "large low-rise" and "sparsely built". The developed method can be used in any urban area if the necessary input databases are available.

Keywords: climate mapping, Local Climate Zones, surface parameters, lot area polygons, GIS, Szeged

Introduction

Nowadays about half of the human population is affected by the burdens of urban environments, therefore studies dealing with the urban impact on climate are particularly important. By definition, the urban climate is a local climate which is modified by the interactions between the built-up area and the regional climate (WMO, 1983). Among the parameters of the urban atmosphere, the near-surface (screen-height) air temperature shows the most obvious modification compared to the rural area. Urban warming is commonly referred to as the urban heat island (UHI) and its magnitude is the UHI inten-

[1] Department of Climatology and Landscape Ecology, University of Szeged, H-6720 Szeged, Aradi vértanúk tere 1. E-mails: unger@geo.u-szeged.hu, lelovics@geo.u-szeged.hu, tgal@geo.u-szeged.hu

sity (Oke, T.R. 1987). Traditionally, UHI intensity is interpreted and calculated as the difference between the temperature values of a central urban site and those of a nearby rural site.

In the literature of heat island, the terms "urban" and "rural" have no single, objective meaning as the areas around the measuring sites can be very different. For example, an "urban" site can be in a park, college ground, street canyon, housing estate, etc., while "rural" sites are placed e.g. at airports, farmlands, fields or in the suburb areas depending on the investigated cities. It makes difficult to compare the results obtained in the different settlements of the world (Stewart, I.D. 2011).

To improve the characterization of the surrounding environment of the measurement sites based on their ability to influence the local thermal and dynamic conditions of the near-surface atmosphere, Stewart, I.D. and Oke, T.R. (2012) developed a classification system. Their Local Climate Zones (LCZ) system is based on the earlier works of Auer, A.H. (1978), Ellefsen, R. (1991), Oke, T.R. (2004), and Stewart, I.D. and Oke, T.R. (2009) as well as a personal worldwide survey of heat island measurement sites and their local environments (Stewart, I.D. 2011).

The objectives of this paper are

– to develop GIS methods in order to calculate some geometric, surface cover and radiative parameters describing the LCZs for any part of the study area using different databases which are available or created for that purpose,
– to identify and delineate the LCZ types which occur in and around the city of Szeged using the calculated surface parameters by the developed methods.

Short introduction of the LCZ system and the study area

The main purpose of the LCZ system is to facilitate the characterization of the local environment around a temperature measuring site with a screen-height sensor in terms of its ability to influence the local thermal climate. To this end, the number of types is not too large and the separation is based on objective, measurable parameters. LCZs are defined as "regions of uniform surface cover, structure, material, and human activity that span hundreds of metres to several kilometres on horizontal scale" (Stewart, I.D. and Oke, T.R. 2012). The spatial extension of the zones is local because an upwind fetch of typically 200–500 metres is required for the air at screen-height to become fully adjusted to the underlying, relatively homogeneous surface (Oke, T.R. 2004). The main characteristics of the LCZ types are reflected in their names (*Table 1*).

LCZ types can be distinguished by typical value ranges of measurable physical properties which characterize the surface geometry and cover, the thermal, radiative and anthropogenic energy features of the surface (*Table 2*).

Table 1. Names and codes of the LCZ types

Built types		Land cover types	
LCZ 1	compact high-rise	LCZ A	dense trees
LCZ 2	compact mid-rise	LCZ B	scattered trees
LCZ 3	compact low-rise	LCZ C	bush, scrub
LCZ 4	open high-rise	LCZ D	low plants
LCZ 5	open mid-rise	LCZ E	bare rock / paved
LCZ 6	open low-rise	LCZ F	bare soil / sand
LCZ 7	lightweight low-rise	LCZ G	water
LCZ 8	large low-rise		
LCZ 9	sparsely built		
LCZ 10	heavy industry		

Source: Stewart, I.D. and Oke, T.R. 2012.

Table 2. Physical properties characterizing the elements of the LCZ system

Types of properties	
Geometric, surface cover	Thermal, radiative, metabolic
sky view factor	surface admittance
aspect ratio	surface albedo
building surface fraction	anthropogenic heat output
pervious surface fraction	
impervious surface fraction	
height of roughness elements	
terrain roughness class	

Source: Stewart, I.D. and Oke, T.R. 2012.

The LCZ classification system was not designed specifically for mapping but to standardize the classification of urban heat island observation sites, either urban or rural. Nevertheless, the spatial mapping of the urban terrain is a justifiable use of the system to determine the areas which are relatively homogeneous in surface properties and human activities.

In the context of the new LCZ classification system, the inter-urban UHI intensity is not an "urban-rural" temperature difference, but a temperature difference between the pairs of LCZ types (Stewart, I.D. *et al.* 2013). In this way, the application of the LCZ system gives an opportunity to compare the thermal reactions of different areas within a city and between cities (intra-urban and inter-urban comparisons) objectively.

Szeged as a study area is located in the South-Eastern part of Hungary (46°N, 20°E) at 79 metres above sea level on a flat terrain with a population of 160,000 within an urbanized area of about 40 km^2. The area is in Köppen's climatic region Cfb with an annual mean temperature of 10.4 °C and an amount of yearly precipitation of 497 mm. The study area covers a 10 km × 8 km rectangle in and around Szeged (*Figure 1*).

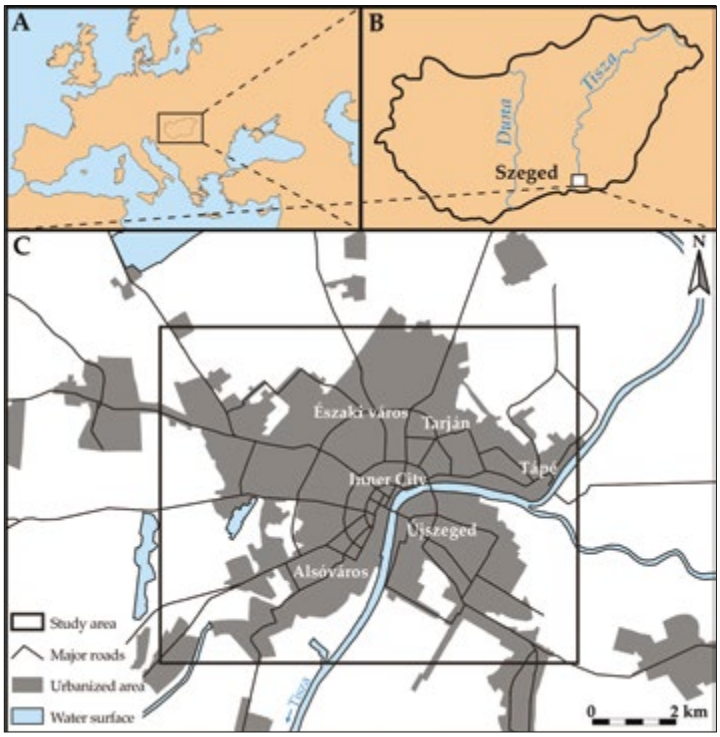

Fig. 1. Location of Szeged in Europe (A) and in Hungary(B) as well as the study area in and around Szeged (C)

GIS methods developed for LCZ mapping

Parameter calculations for lot area polygons

Using our method we can determine seven properties out of ten listed by Stewart, I.D. and Oke, T.R. (2012) for any given area inside the study area based on the available databases. From the initial parameters, we omitted the *aspect ratio* since it can be clearly calculated only in the case of the regular street network. The patterns of the *surface admittance* and the *anthropogenic heat output* were not available in the study area, either.

During the determination process of the other seven parameters the basic area of the calculation was the building block and the area belonging to it (called lot area polygon, *Figure 2*).

Fig. 2. Examples of lot area polygons in the study area. – a = building block; b = lot area polygon; c = open area without buildings

The determination of the building block footprints and lot area polygons is based on the 3D building database of Szeged which contains more than 22,000 individual buildings with building height information in ESRI shape-file format (Gál, T. and Unger, J. 2009). The calculation processes, the necessary databases and the outputs are shown in *Figure 3*.

All of the calculations were carried out with self-developed Fortran algorithms and for the visualization of the outputs, Quantum GIS was used. The calculation methods and the applied databases by parameters were as follows:

– *Sky view factor* (SVF): The input was a SVF database originated from our earlier studies (e.g. Gál, T. *et al.* 2009). During the SVF calculation, each building was considered with flat roofs and the effect of the vegetation was neglected. SVF values refer to the street level and they are averaged inside the polygons.

Fig. 3. Flow chart of the automated classification and aggregation of the lot area polygons to determine the appropriate size of LCZ areas

– *Building surface fraction* (BSF): The input was also the 3D building database. BSF is the ratio of the summarized footprint areas and the polygon area.

– *Pervious surface fraction* (PSF): The input was a built-up dataset calculated from RapidEye (2012) satellite image using NDVI index, a 1:25,000 topographic map, a road database and the Corine Land Cover (CLC) database (Bossard, M. *et al.* 2000). The RapidEye image (resolution of 5.16 m) was atmospherically corrected and the NDVI was calculated using bands 3 and 5 (Tucker, C.J. 1979), and the points where the NDVI was below 0.3 were regarded as a covered area. The CLC dataset was used to locate the agricultural areas as these areas have small NDVI (like the covered areas) because the amount of plants is negligible after harvest. As a second correction, the shapes of water bodies were digitized from the topographic map because in several cases the water had NDVI values very similar to the values of some building materials. As a last correction, the road database was used to locate the asphalt roads in the area because in the urban canyons asphalt roads are usually under tree cover and the roads which dissect agricultural areas do not appear in CLC dataset.

– *Impervious surface fraction* (ISF): It is the paved area outside the buildings and it can be calculated as the remnant from the total area, ISF = 1 – (BSF + PSF).

– *Height of roughness elements* (HRE): Using the 3D building database for each area, the building heights were averaged weighted with their footprint areas.

– *Terrain roughness class* (TRC): For describing the roughness, the Davenport roughness classification method was used (Davenport, A.G. *et al.* 2000). The widespread method comprises eight classes of roughness. Larger areas were classified into different roughness classes using CLC dataset with the visual interpretation of aerial photographs, the topographical map and the building database.

– *Surface albedo* (SA): As an input, the atmospherically corrected reflectance values of the 5 band RapidEye satellite image were used. Broadband albedo was calculated as an average of the reflectance values weighted with the integral of the radiation within the spectral range of a given band (Starks, P.J. *et al.* 1991; Tasumi, M. *et al.* 2008).

In order to illustrate the obtained patterns of the calculated parameters with some examples, *Figure 4.* shows the spatial patterns of two parameters in the study area. Regarding the PSF, the pattern is generally higher on the edge of the city and near the city centre.

The largest parks and green areas of the city (e.g. banks of the Tisza, the forested areas along the circle dam) also appear on the map. In the case of HRE, most of the values are between 10 and 20 metres in the inner part of the city and only a few of them (e.g. church, clinical block, educational centre, theatre) are higher than 30 metres in the Western side of the Tisza. Some blocks of flats exceed this height on its Eastern side. Family houses are generally below 5 m.

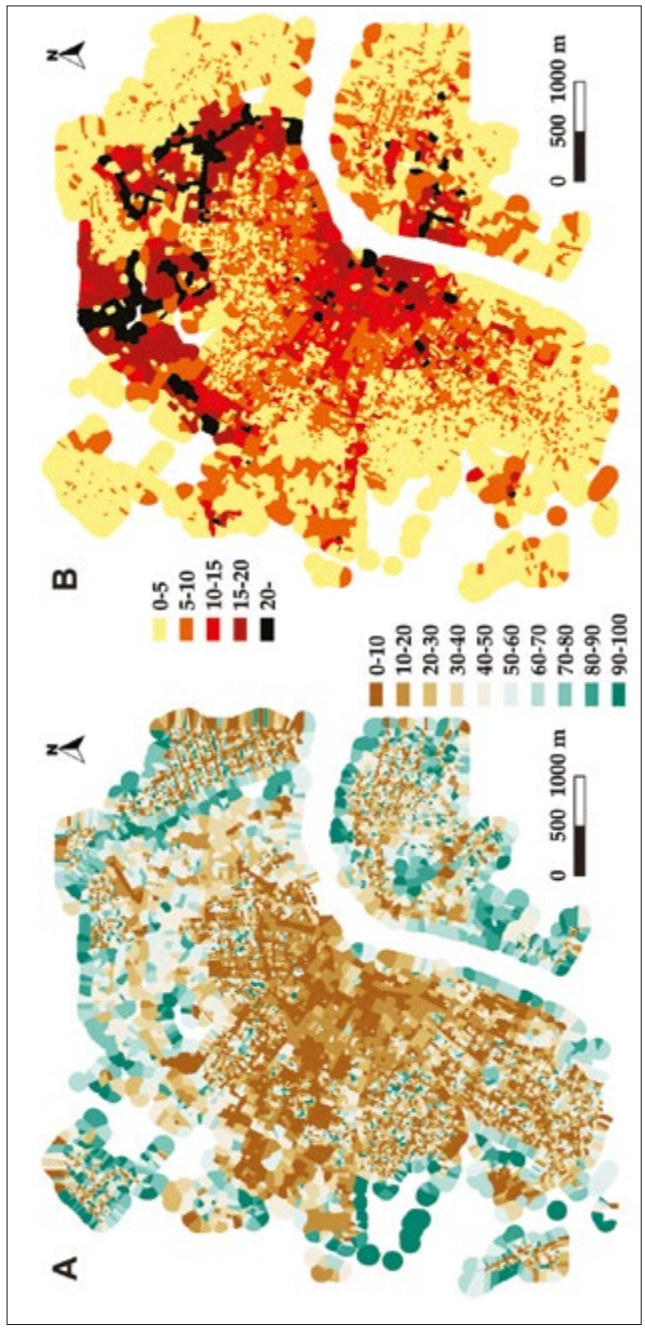

Fig. 4. Patterns of pervious surface fraction in % (A) and the height of roughness elements in m (B) based on their values in lot area polygons

To get some verification, the PSF field was compared to the European soil sealing database published by EEA (2009) which is available with a spatial resolution of 20 metres. The patterns of the two PSF databases are very similar to each other, both represent the structure of the city well. The main difference between them is that the EEA database is less detailed.

Aggregation and generalization of lot area polygons

In line with the definition of LCZs, the lot area polygons classified into the same or similar LCZ classes (*Figure 5.* A) were merged into zones of hundreds of metres to several kilometres (*Figure 5.* B). In that case, we meet the minimum condition that the central point of an LCZ is at least 250 metres from the boundaries of the zone, such the relatively homogeneous area constitutes an area with a radius of 250 metres or greater. In order to get LCZ areas with appropriate size, the lot area polygons were aggregated into groups according to the following procedure.

First, the polygons were classified separately.

(1) From the obtained surface parameters, areal mean or percentage values were calculated to represent the polygons. Seven scores were assigned to each LCZ categories by polygons according to its fit (*Figure 6*) into the typical ranges given by Stewart, I.D. and Oke, T.R. (2012) and then they were summarized.

Two of the best fitting LCZ categories were assigned to every polygon (for each polygon the best was LCZ_1 and the second best was LCZ_2) if their scores were high enough. In the case of too low scores to fit to any LCZ categories, the polygon was considered unclassified.

Secondly, the lot area polygons were merged according to their LCZ categories and their locations related to each other.

(2) If a small polygon was located inside another polygon, the first LCZ class of the small polygon was set to the same as the outer polygon.

(3) If all of the neighbours of a polygon (except perhaps one of them) belonged to the same LCZ class, the class of the polygon was modified to the same as its neighbours.

(4) If a polygon did not have any neighbours in the same class, there were two cases: if there was a neighbour with the same LCZ_1 like the polygon's LCZ_2 or same LCZ_2 like the polygon's LCZ_1, the LCZ_1 of the polygon was set to the same like its neighbour; if there was a neighbour with LCZ_1 category similar to the polygon's LCZ_1 category, the LCZ_1 of the polygon was modified to the LCZ_1 of the neighbour.

In this context, 'similarity' refers to the condition when categories share certain properties. For example, the "compact mid-rise" or LCZ 2 class

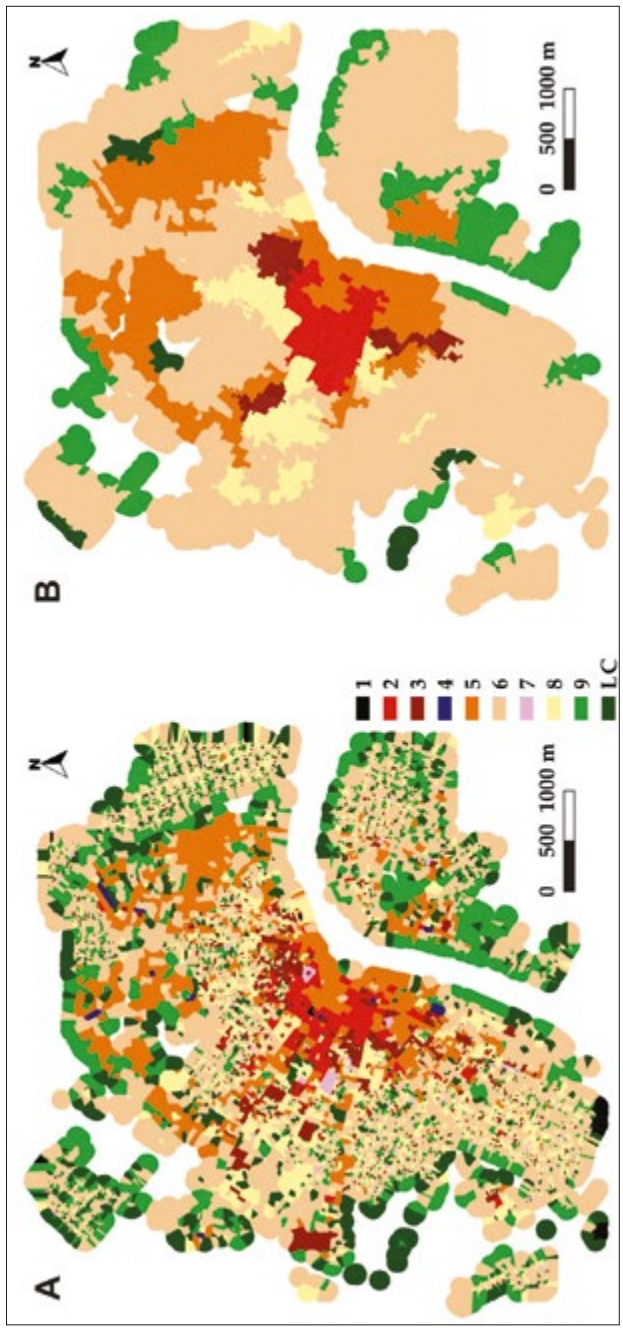

Fig. 5. Originally classified lot area polygons (A) polygons aggregated into groups and (B). – LC = land cover LCZ types. 1–9 = For explanation see the text.

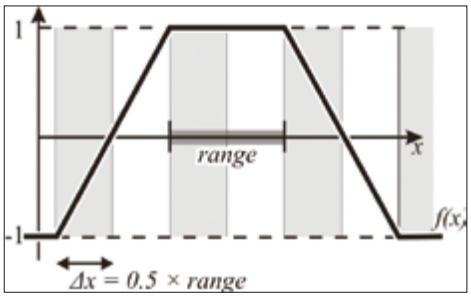

Fig. 6. Function of score assignment to a polygon according to its surface parameter values

is similar to the "compact high-rise" (LCZ 1) and "compact low-rise" (LCZ 3) classes as they belong to the same density category. Likewise, the "open mid-rise" (LCZ 5) class can also be regarded as similar to LCZ 2 as they share the same height category.

(5) The LCZ categories of the remaining unclassified and non-aggregated polygons were defined as the most frequent classes of their neighbours.

Thirdly, the groups of adjacent polygons with a given LCZ category were investigated according to their spatial extension.

(6) If the area of a group covered at least one circle with a radius of 250 m, it was regarded as an independent LCZ area.

(7) The polygons of groups which did not satisfy the criterion of the size were merged without considering their properties if they were adjacent. If the obtained group was large enough, the category of the group was set to the most frequent category of its parts; otherwise it was joined to one of the adjoining LCZ areas which had the largest number of contacting lot area polygons with it.

Finally, some manual corrections were made according to aerial photographs and our local knowledge of the area because of inadequate detachment of the zones. The most difficult task is the recognition of LCZ 8 (large low-rise) from the surface parameters. As a final result, we obtained several LCZ polygons in ESRI shape-file format suitable to produce maps or to extract spatial information as well.

LCZ map of Szeged

As the study area covered mostly the urbanized parts of Szeged, we focused on the "built" LCZ types. Due to the peculiarities of the city, it was to be expected prior to calculations that some "built" types did not occur there, namely the high-rise, lightweight low-rise and heavy industrialized zones (LCZ 1, 4, 7 and 10).

Aggregating the similar lot areas using the methods described above (the result is shown in *Figure 5.* B) and supplemented by the authors' local knowledge on the study area, a generalized LCZ map was obtained (*Figure 7*).

Fig. 7. The obtained LCZ map of Szeged. – LCZ 2 = compact mid-rise; LCZ 3 = compact low-rise; LCZ 5 = open mid-rise; LCZ 6 = open low-rise; LCZ 8 = large low-rise; LCZ 9 = sparsely built

During the generalization, the outlines of the polygons were simplified, some corrections and supplements were made according to aerial photographs and our local knowledge. For example, for our method the most challenging task was to separate LCZ 6 (open low-rise) and LCZ 8 (large low-rise) because of their similar properties. Water surfaces were not handled by our algorithms because they were located outside the lot area polygons for which the calculations were applied. These surfaces were digitized from the topographic map and the areas on the edges of the city without building database (and so without lot area polygons) were also digitized.

As the map shows, the remaining six "built" types cover the urbanized parts of Szeged (LCZ 2, 3, 5, 6, 8 and 9). Their extent and the number of constituent lot area polygons are different (*Table 3*) and altogether they cover an urban area of 46.50 km^2 in Szeged.

Table 3. Areal extensions of the delineated LCZ zones

LCZ zones	Number of polygons	Summarized	Mean	Largest
		area, km^2		
LCZ 2	176	0.63	0.63	0.63
LCZ 3	248	0.67	0.33	0.35
LCZ 5	796	4.35	1.18	1.98
LCZ 6	9,303	19.63	2.80	5.22
LCZ 8	798	5.91	2.96	5.87
LCZ 9	566	15.32	1.93	5.71

Conclusions

In this study we determined the LCZ types in Szeged which are representative for the urbanized area of the city using seven geometric, surface cover and radiative properties from the ten listed by Stewart, I.D. and Oke, T.R. (2012). The values of the properties were calculated by GIS methods developed for that purpose and for the appropriate classification of the selected areas, we used also our local knowledge about the districts of Szeged. As a result, six built LCZ types were distinguished and mapped in the studied urban area.

The developed method could be used in any urban area if the necessary input databases are available. The further steps in our investigation will be the application of the developed method in the LCZ mapping of Novi Sad (Serbia) and the discussion about the relation of the findings of this paper to the existing knowledge on an international level. Furthermore, we are going to acquire and utilize more GIS databases (e.g. EEA Urban Atlas) to have an even more detailed description of the urban surface.

Acknowledgement: The study was supported by the Hungary-Serbia IPA Cross-border Co-operation Programme (HUSRB/1203/122/166 – URBAN-PATH) and in the case of the second author by the TÁMOP 4.2.4.A/2-11/1-2012-0001 „National Excellence Program – Elaborating and operating an inland student and researcher personal support system convergence program" which project was subsidized by the European Union and co-financed by the European Social Fund. In the case of the third author this research was realized in the frames of the Hungarian Scientific Research Fund (OTKA PD-100352) and the János Bolyai Research Scholarship of the Hungarian Academy of Sciences.

REFERENCES

Auer, A.H. 1978. Correlation of land use and cover with meteorological anomalies. *Journal of Applied Meteorology* 17. 636–643.

Bossard, M., Feranec, J. and Otahel, J. 2000. *CORINE land cover technical guide – Addendum 2000. Technical report No 40.* Copenhagen, European Environment Agency, 105 p.

Davenport, A.G., Grimmond, C.S.B., Oke, T.R. and Wieringa, J. 2000. *Estimating the roughness of cities and sheltered country.* Asheville, NC, Proceedings on 12th Conference on Applied Climatology, 96–99.

EEA, 2009. *FTSP Degree of soil sealing – Updated Delivery Report, European Mosaic, Issue 1.0.* European Environmental Agency, 13 p.

Ellefsen, R. 1991. Mapping and measuring buildings in the canopy boundary layer in ten U.S. cities. *Energy and Buildings* 15–16. 1025–1049.

Gál, T. and Unger, J. 2009: Detection of ventilation paths using high-resolution roughness parameter mapping in a large urban area. *Building and Environment* 44. 198–206.

Gál, T., Lindberg, F. and Unger, J. 2009. Computing continuous sky view factor using 3D urban raster and vector data bases: comparison and application to urban climate. *Theoretical and Applied Climatology* 95. 111–123.

Oke, T.R. 1987. *Boundary Layer Climates. 2nd edition.* London–New York, Routledge, 435 p.

Oke, T.R. 2004. *Initial guidance to obtain representative meteorological observation sites*. Geneva, WMO/TD No. 1250, 47 p.

RapidEye, 2012. *Satellite Imagery Product Specifications, Version 4.1.* 46 p.

Starks, P.J., Norman, J.M., Blad, B.L., Walter-Shea, E.A. and Walthall, C.L. 1991. Estimation of shortwave hemispherical reflectance (albedo) from bi-directionally reflected radiance data. *Remote Sensing of Environment* 38. 123–134.

Stewart, I.D. 2011. A systematic review and scientific critique of methodology in modern urban heat island literature. *International Journal of Climatology* 31. 200–217.

Stewart, I.D. and Oke, T.R. 2012. Local Climate Zones for urban temperature studies. *Bulletin of the American Meteorological Society* 93. 1879–1900.

Stewart, I.D. and Oke, T.R. 2009. A new classification system for urban climate sites. *Bulletin of the American Meteorologial Society* 90. 922–923.

Stewart, I.D., Oke, T.R. and Krayenhoff, E.S. 2013. Evaluation of the 'local climate zone' scheme using temperature observations and model simulations. *International Journal of Climatology*. DOI: 10.1002/joc.3746, 19 p.

Tasumi, M., Allen, R.G. and Trezza, R. 2008. At-Surface Reflectance and Albedo from Satellite for Operational Calculation of Land Surface Energy Balance. *Journal of Hydrologic Engineering* 13 (2): 51–63.

Tucker, C.J. 1979. Red and Photographic Infrared Linear Combinations for Monitoring Vegetation. *Remote Sensing of Environment* 8. 127–150.

WMO, 1983. *Abridged final report, 8th session*. Geneva, Commission for Climatology and Applications of Meteorology,WMO, No. 600, 72 p.

2014-CR-60-Lelovics-et-al

Password protected

2014-CR-60-Lelovics-et-al

Password protected

2014-CR-60-Lelovics-et-al

Password protected

The project is co-financed by the European Union

2014-CR-60-Lelovics-et-al

Password protected

2014-CR-60-Lelovics-et-al

Password protected

The project is co-financed by the European Union

2014-CR-60-Lelovics-et-al

Password protected

2014-CR-60-Lelovics-et-al

Password protected

2014-CR-60-Lelovics-et-al

Password protected

2014-CR-60-Lelovics-et-al

Password protected

2014-CR-60-Lelovics-et-al

Password protected

2014-CR-60-Lelovics-et-al

Password protected

The project is co-financed by the European Union

2014-CR-60-Lelovics-et-al

Password protected

Időjárás, 2014 (in press)

Development, data processing and preliminary results of an urban human comfort monitoring and information system

Unger J, Gál T, Csépe Z, Lelovics E, Gulyás Á
Department of Climatology and Landscape Ecology, University of Szeged
P. O. Box 653, 6701 Szeged, Hungary

Corresponding author's E-mail: unger@geo.u-szeged.hu

Abstract In this study the infrastructure development and operation of an urban human comfort monitoring network and information system in Szeged and the related preliminary research results are discussed. The selection of the representative sites of the network is based primarily on the pattern of the Local Climate Zones in and around the city. After the processing of the incoming data (air temperature and relative humidity, as well as global radiation and wind speed) a human comfort index (PET) is calculated from the four meteorological parameters with a neural network method (MLP), then the measured and calculated parameters interpolated linearly into a regular grid with 500 m resolution. As public information maps and graphs about the thermal and human comfort conditions appear in 10-minute time steps as a real-time visualisation on the internet. As the preliminary case studies show the largest intra-urban thermal differences between the LCZ areas in a two-day period occurred in the nocturnal hours reaching even 5ºC in early spring. In the spatial distribution of human comfort conditions there are distinct differences in the strength of the loading or favourable environmental conditions between the neighbourhoods during the daytime. Finally, the utilization possibilities of the results in the future are detailed.

Key words: Local Climate Zones (LCZ), representative measurement sites, monitoring network, Psychologically Equivalent Temperature (PET), Multilayer Perceptron, thermal and human comfort maps, real-time visualisation, Szeged, Hungary

1. Introduction

Examination taking place in the field of urban environmental changes due to the large number of people affected is considered as an important task. The urban environments are specific – compared to the natural ones – because of the alteration in land cover and surface geometry characteristics as well as the human activity, which may significantly affect the energy and water balance of the area leading to local-scale climate modifications in the atmosphere of cities. As a result, the so called *urban climate* develops (e.g. *Oke*, 1987). The residents are affected directly to the alterations taking place in the *urban canopy layer* (a layer of air between the average height of the buildings and the street level). The most significant modification is the change in the thermal environment (the *urban heat island* phenomenon, UHI), as well as in the human bioclimatic (thermal comfort) conditions influenced by the thermal environment and other weather parameters.

The importance of the investigation of these issues is supported that in cases of some of the already loading or unfavourable weather situations, the city still adheres to these effects. For example, at heat wave situations in cities the nocturnal cooling weakens, thus the periods characterized by significant physiological load are extended.

Within larger settlements due to the intra-urban heterogeneity of the physical attributes of the surface the thermal modifying effect is also different. It can be assumed that in many

respects the interactions between the urban parameters and thermal comfort as well as some elements of the weather phenomena within the city are not yet known sufficiently. These interactions can only be analyzed properly using detailed and long-term (several years) measurements, like detection and analysis of the characteristics of these urban thermal patterns. This analysis can be performed with the help of a *monitoring network* installed representatively and in appropriate density. For automatic monitoring network set up in the urban canopy layer there can be found some international – mainly U.S., Japan and Taiwan – examples, while in Europe there are very few of these and none of them are aimed at the detection of patterns of human comfort conditions. A network began to be build from 1999 on with temperature sensors located from the centre in different directions radially in London (*Watkins et al.*, 2002), while in Florence there is a system with temperature-humidity sensors operating since 2004 whose elements observe the thermal features of the city's various built-up districts (*Petralli et al.*, 2013). The most complex network (utilizing meteorological stations and sensors) so far was started up in 2011 in Birmingham. Its development is now in progress and its elements are installed at higher density in the downtown area while less densely in the outskirts of the city (HiTEmp Project, 2014).

However obviously it is not a realistic option to establish monitoring stations network to all major urban areas, therefore, in the long run the presentation and prediction of the prevailing thermal comfort conditions in urban areas only through the proper downscaling of weather forecasting models is possible. Development of such a method, however, is only possible using representative and high resolution measurement data in space and time, as well as parameters characterize the urban surface and geometry in an appropriate manner. The forecasting of weather processes in urban areas – at least in the structure and functioning of the models used – is similar to the issue of climate change prediction. Because urban areas significantly influence the local climate, so in order to estimate the possible outcomes of climate change, these areas should be taken into account. At the same time – as the majority of the world's population already lives in cities – if the urban areas are implemented to climate models in appropriate manner and they are transposed to the climate models, it will be possible to have correct forecasts for these areas in the future.

In the present paper we aim to show the principle and the practice of the siting and configuration of a representative urban human comfort monitoring system and its data processing. Furthermore to present the preliminary results related to the spatial distribution of the intra-urban human comfort conditions and their real-time visualisation as a public information and finally, the utilization possibilities of the results in the future.

2. Local Climate Zones (LCZ), station place selection, monitoring network

2.1 The LCZ concept

The main purpose of the LCZ system is the characterization of the local environment around a temperature measurement site in terms of its ability to influence the local thermal climate. Therefore, the number of types is not too large and their separation is based on objective, measurable parameters. LCZs are defined as "regions of uniform surface cover, structure, material, and human activity that span hundreds of meters to several kilometres in horizontal scale" (*Stewart* and *Oke*, 2012). Their names reflect the main characteristics of the types (*Table 1*).

Table 1. Names and codes of the LCZ types (after *Stewart* and *Oke*, 2012)

Built types		Land cover types	
LCZ 1	compact high-rise	LCZ A	dense trees
LCZ 2	compact mid-rise	LCZ B	scattered trees
LCZ 3	compact low-rise	LCZ C	bush, scrub
LCZ 4	open high-rise	LCZ D	low plants
LCZ 5	open mid-rise	LCZ E	bare rock / paved
LCZ 6	open low-rise	LCZ F	bare soil / sand
LCZ 7	lightweight low-rise	LCZ G	water
LCZ 8	large low-rise		
LCZ 9	sparsely built		
LCZ 10	heavy industry		

The LCZ types can be distinguished by typical value ranges of measurable physical properties. These properties describe the surface geometry and cover (sky view factor, aspect ratio, fractions of building, pervious and impervious surfaces, height of roughness elements, terrain roughness class) as well as the thermal, radiative and anthropogenic energy (surface admittance and albedo, anthropogenic heat output) features of the surface. As a result, the LCZ system consists of ten 'built' and seven 'land cover' LCZ types (*Table 1*). Although, originally it was not designed for mapping, but mapping of the urban terrain can be proved an efficient use of the system to determine areas which are relatively homogeneous in surface properties and human activities.

In the context of the LCZ classification system, the UHI intensity is not an "urban-rural" temperature difference (ΔT_{u-r}), but a temperature difference between pairs of LCZ types ($\Delta T_{LCZ\ X-Y}$), that is an inter-zone temperature difference (*Stewart et al.*, 2013). Consequently, the usage of the system allows the objective comparison of the thermal reactions in different areas within a city and between cities (intra-urban and inter-urban comparisons).

2.2 LCZs in Szeged

Szeged is located in the south-eastern part of Hungary (46°N, 20°E) at 79 m above sea level on a flat terrain with a population of 160,000 within an urbanized area of about 40 km^2. The area is in Köppen's climatic region Cfb with an annual mean temperature of 10.4°C and an amount of precipitation of 497 mm (*Unger et al.*, 2001). The study area covers an 11.5 km × 8.5 km rectangle in and around Szeged (*Fig. 1*).

In order to apply the LCZ system in the study area, that is to delineate the types occurring therein, a recently developed automated method was used (*Lelovics et al.*, 2014). *Fig. 1.* shows the obtained seven 'built' and four 'land cover' LCZ types and their pattern in and around Szeged.

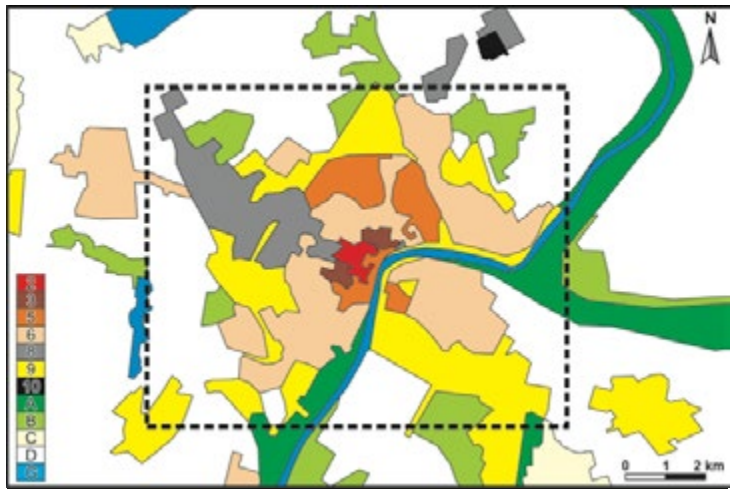

Fig. 1. The obtained LCZ map in Szeged (LCZ 2 – compact mid-rise, LCZ 3 – compact low-rise, LCZ 5 – open mid-rise, LCZ 6 – open low-rise, LCZ 8 – large low-rise and LCZ 9 – sparsely built, LCZ A – dense trees, LCZ B – scattered trees, LCZ C – bush, scrub, LCZ D – low plants, LCZ G – water) and the study area (broken line)

2.3. Installed and already existing stations

Within the framework of an EU project (URBAN-PATH Project, 2014) a monitoring network with 23 stations (air temperature, *T* and relative humidity, *RH*) was set up in Szeged (*Fig. 3*). Additionally, a data series from the stations of the Hungarian Meteorological Service (HMS) are added. One of them is at the same place where the station D-1 is located (global radiation, *G* and wind speed, *u*) and the other is at the University of Szeged (station 5-1) (*T*, *RH*, *G*) (*Fig. 2*). Altogether, the whole network consists of 24 measurement sites.

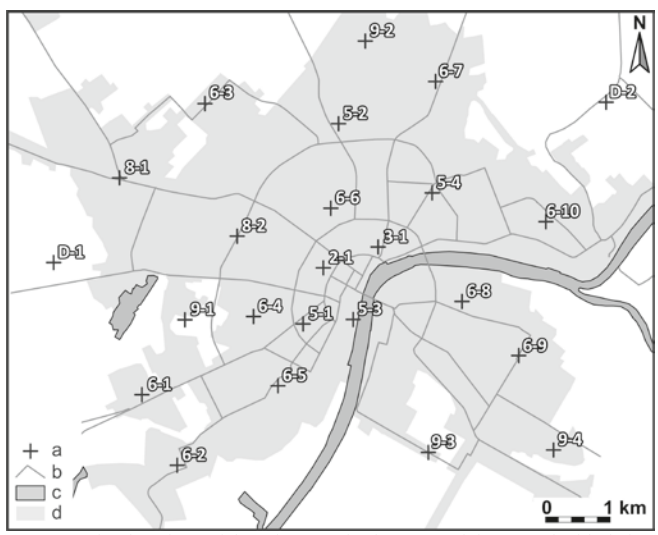

Fig. 2. Station locations of the urban monitoring network in Szeged with their notations (first number indicates the LCZ type, second one indicates the station number in a given LCZ type) (a – station, b – main road, c – water, d – urbanized area) (after Lelovics et al. 2014)

In order to have a representative urban human comfort monitoring network within the seven delineated 'built' LCZ areas the siting and configuration of 22 stations from the above mentioned 24 ones were based on: (i) the distance of the site from the border of the LCZ zone within it was located; (ii) the ability of the selected network geometry to reproduce the spatial distribution of mean temperature surplus pattern estimated by an empirical model (*Balázs et al.*, 2009); (iii) the site's representativeness of its microenvironment; and (iv) the site's suitability for instrument installation. Thus in summary, two stations (D-1, D-2) represent the rural area, while the other 22 stations the different built-up areas of the city (*Lelovics et al.*, 2014) (*Fig. 2*).

2.4. Measuring equipments

In each monitoring station the measurement is provided by a Sensirion SHT25 sensor in a radiation protection screen (220 x 310 mm) at the end of a 60 cm console. The accuracy of the sensor is 0.4°C and 3% for the temperature and relative humidity, respectively. The radiation protection shield is the same as the model used by the HMS. The consoles are mounted on lamp posts at a height of 4 m above the ground for security reasons. As the air in the urban canyon is well mixed the temperature measured at this height is representative for the lower air layers too (but not for the air near the wall or ground) (*Nakamura* and *Oke,* 1988). At the beginning of the console there are two boxes (*Fig. 3*). The upper one contains the central processor, data storage (microSD) card, GPRS/EDGE/3G modem, battery and charger. The lower box is utilised in the case of 20 stations where the local electricity provider has made it possible to use the power for the station, and it contains only a separate power switch. At the remaining 4 stations there is direct access to the power so they do not need any additional box.

Fig. 3. One of the stations of the monitoring network on a lamp post (temperature and relative humidity sensors are inside of the radiation shield cylinder)

The system time of the stations (and the whole monitoring system) is in UTC and this time is regularly synchronized by the main server. Most of the stations (17 items) have continuous power supply but seven stations have power supply only when the city lights are on. These seven stations use the power of built in batteries during daytime or at power failure. These stations can operate up to 10 days using only battery power. The stations measure the parameters every minute and they send the readings with some technical information (battery

voltage, temperature inside the box, sensor status) into the main server (Dell PowerEdge T420 tower server) every 10 minute. If there is no mobile internet connection or the main server does not receive the data the station tries to send it repeatedly until it succeeded. If the station's battery level is low, the station increases the time between two data transfer to decrease the power consumption. One station (D-1) is located in the garden of the HMS station in order to provide calibration information for the network.

3. Data processing

3.1. Calculation of the human bioclimatological index (PET)

The human (bioclimatological) comfort sensation is formed as the complex effect of air temperature, air humidity, radiation and wind conditions. In order to characterize this comfort sensation, one of the rational indices, the Physiologically Equivalent Temperature (*PET*) is used, which is defined as 'the temperature (in ºC) of a standardized fictitious environment (where the mean radiation temperature = air temperature, vapour pressure = 12 hPa, wind speed = 0.1 ms^{-1}), in which the body, in order to maintain its energy balance, gives the same physiological responses like in the complex real-world conditions' (*Mayer* and *Höppe*, 1987).

The PET value categories were initially defined according to thermal sensations and physiological stress levels of Central European people where the comfortable thermal heat sensation (no stress level) are indicated by a range of 18–23°C (*Matzarakis* and *Mayer,* 1996). Furthermore, ranges of 13-18°C and 23-29°C mean slightly cool and slightly warm sensations, that is slightly cool stress and slightly heat stress levels, respectively, etc.

For the calculation of the PET index an algorithm, the Multilayer Perceptron (MLP) network structure (*Haykin*, 1999) was developed (*Fig. 4*). It consists of neurons organized in layers. The neuron's differentiable outputs have non-linearity, which ensure that the output of the network is a continuous differentiable function of the weights. The output layer can be linear or non-linear. Even in the simplest case when an MLP contains only one hidden layer, it implements nonlinear mapping in his parameters. MLP use the error backpropagation learning algorithm which is an iterative learning process based on an instantaneous gradient.

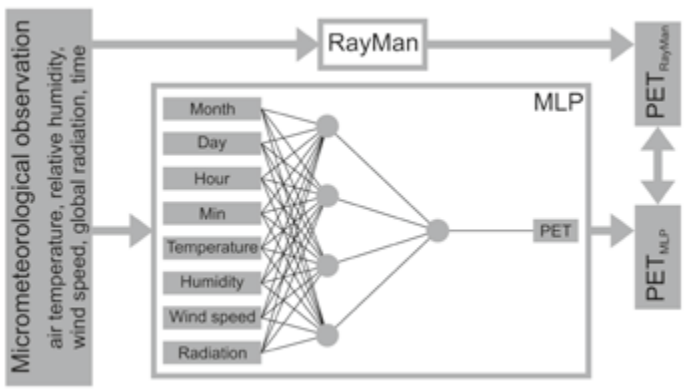

Fig. 4. Flow chart of the development of the MLP

In our case the input data (air temperature, relative humidity, wind speed, global radiation, time) are derived from the results of the field measurements carried out in different urban microenvironments in Szeged between 2009 and 2013 (e.g. *Kántor* and *Unger,* 2010;

Égerházi et al., 2012a, 2012b) (*Fig. 4*). The target output data for the learning was a PET dataset calculated from the same input by the widely used RayMan software (*Matzarakis et al.,* 2007). The MLP model always has one hidden layer and MLP has several parameters that need to be set. They are training time, learning rate, hidden layers and neurons in the layers. The training time was 1500 epoch, the learning rate started from 0.3 and it was reduced in each step. This helps to stop the network from diverging from the target output as well as improve the general performance. The number of hidden layers and the nodes in each layer were generated automatically by the WEKA data mining software (*Hall et al.*, 2009). The MLP with these options was applied for predicting the PET index.

3.2. Estimation of the wind and global radiation

For PET calculation in one site in the urban area the wind speed and radiation data measured there would be ideal. In contrary if the aim is the monitoring of the thermal comfort conditions in a local scale the direct measurement is not appropriate as the wind speed and radiation measured on site are highly affected by several micro scale phenomena like the arrangement of the nearby obstacles and their effect for the shading and wind flow. Moreover, the deployment of expensive wind and radiation sensors in every urban monitoring site is also not practical because of the safety and financial reasons. By virtue of these reasons we used mean wind speed (u_{UCL}) in the Urban Canopy Layer and the undisturbed global radiation (G). The height of the UCL is Szeged is assumed about 30 metres based on the available building database.

As we mentioned, in the study area the global radiation data are available from the two HMS stations (sites D-1 and 5-1, see Section 2.3). For every monitoring sites we used the nearest measured global radiation data.

Application of the different forms of logarithmic wind profile (*Oke*, 1987; *Foken*, 2008) for the reduction of the wind speed is prevalent in several thermal comfort studies (*Spagnolo* and *de Dear*, 2003; *Bröde et al.*, 2012). However, this method is questionable if the sum of the roughness length (z_0) and the displacement height (z_d) are higher than the height where we want to calculate the wind speed, because the logarithmic approximation gives 0 ms^{-1} in these cases (*Oke*, 1987; *Foken*, 2008). Therefore, in our study we had to find another solution, because the values of the roughness parameters in urban area (*Gál* and *Unger*, 2009) exceed this limitation. For the estimation of the mean wind speed in UCL we applied a new method developed for this purpose, however it is mainly based on the power law equation (*Counihan*, 1975):

$$u_1 = u_2 \cdot \left(\frac{z_1}{z_2} \right)^{\alpha} \tag{1}$$

where u_1 and u_2 is the wind speed at z_1 and z_2 heights, respectively, and α is estimated as a function of z_0:

$$\alpha \approx \frac{1}{\ln\left(\frac{\sqrt{z_1 \cdot z_2}}{z_0} \right)}. \tag{2}$$

Firstly, we used the Roughness Mapping Tool developed by *Gál* and *Unger* (2013) and its basics are presented there. This is a standalone software for calculation the roughness parameters (z_0, z_d) using building and tree crown database. With this software we calculated the z_0 and z_d at the monitoring sites and 8 additional areas. These additional areas are the sites of the earlier thermal comfort studies in Szeged between 2009 and 2012 (*Égerházi et al.,* 2012a, 2012b; *Kántor et al.*, 2011, 2012), and for these areas 59 523 individual wind speed readings are available. We calculated the 10 minute average wind speeds (u_{UCL}) from the 1

minute data of these field measurements and compared them to the 10 minute average wind speed data (u_{10}) from the HMS station. We assumed that u_{UCL} is a constant inside the UCL and is equal to u_{10}. Finally, we got 1615 data pair after filtering out the no and very weak wind situations ($u < 1$ ms^{-1}).

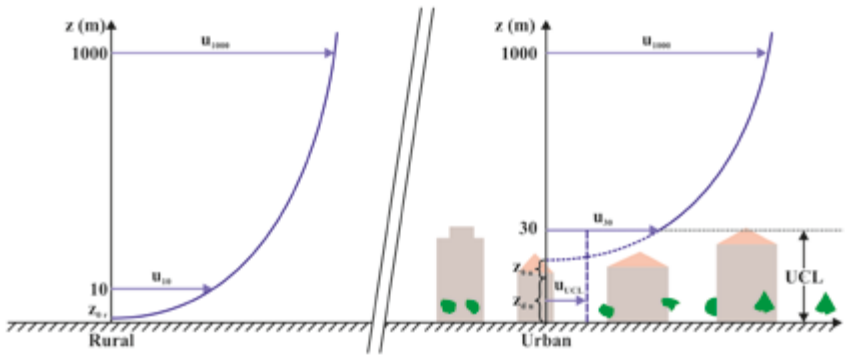

Fig. 5. Concept of the wind speed reduction (for explanation of symbols see the text)

Secondly, the wind speed at a height 1000 m (u_{1000}) was calculated from u_{10} using the logarithmic formula assuming that this u_{1000} value is the regional wind speed unaffected by the drag of the surface (*Fig. 4*). As a next step we determined the wind speed at the top of the UCL (u_{30}) and we calculated a constant (k) with the minimization of the mean square error (MSE) (*Scharf*, 1991) which describes the difference between u_{30} and the measured u_{UCL} (*Fig. 4*). This constant is 0.3331 (MSE=0.3284).

Finally, we obtained the Equation 1 as a formula for the wind reduction.

$$u_{UCL} = u_{10} \cdot \left(\frac{1000}{10}\right)^{\alpha_1} \cdot \left(\frac{30 - z_{du}}{1000 - z_{du}}\right)^{\alpha_2} \cdot k \qquad (1)$$

where

$$\alpha_1 \approx \frac{1}{\ln\left(\frac{\sqrt{10 \cdot 1000}}{z_{0r}}\right)} \qquad \alpha_2 \approx \frac{1}{\ln\left(\frac{\sqrt{(1000 - z_{du}) \cdot (30 - z_{du})}}{z_{0u}}\right)}$$

and subscripts r and u mark the rural and urban sites.

From Equation 1 the complex wind reduction constant (r) was calculated for each monitoring site (*Table 2*). We used this value to calculate the wind speed for the stations from the wind speed measured at D-1 the HMS station at the same time as the time of the PET calculation.

Table 2. Displacement height (z_d), roughness length (z_0), and complex wind reduction constant (r) at urban stations

Station ID	z_d (m)	z_0 (m)	r
2-1	8.7183	1.7455	0.2932
3-1	6.3586	1.4968	0.3116
5-1	6.0872	1.6751	0.3065
5-2	4.6924	2.2986	0.2937
5-3	7.6809	2.0346	0.2887
5-4	5.7750	2.8261	0.2765

6-1	1.7582	0.6740	0.3663
6-2	1.4402	0.4290	0.3856
6-3	1.0717	0.3134	0.3982
6-4	2.6706	0.8682	0.3521
6-5	3.4694	1.0783	0.3392
6-6	3.1466	0.9509	0.3463
6-7	1.5964	0.4782	0.3809
6-8	3.1734	1.1458	0.3372
6-9	1.5275	0.4108	0.3870
6-10	1.2339	0.5226	0.3784
8-1	1.8155	0.2798	0.4001
8-2	2.1910	0.2509	0.4028
9-1	0.1703	0.2000	0.4157
9-2	0.7589	0.2199	0.4111
9-3	0.2805	0.2000	0.4154
9-4	0.7641	0.2177	0.4115

3.3. Operational data processing and display

After the transmission of the station data into the main server every 10 minutes the automatic data procession system creates the final two (site and spatial) database (*Fig. 6*) in order to make it possible to present these data as charts and maps on the public homepage of the project (urban-path.hu). Using this public display system all of the measured and calculated parameters can be accessed a way that the time of the maps and charts can be freely modified by the visitors.

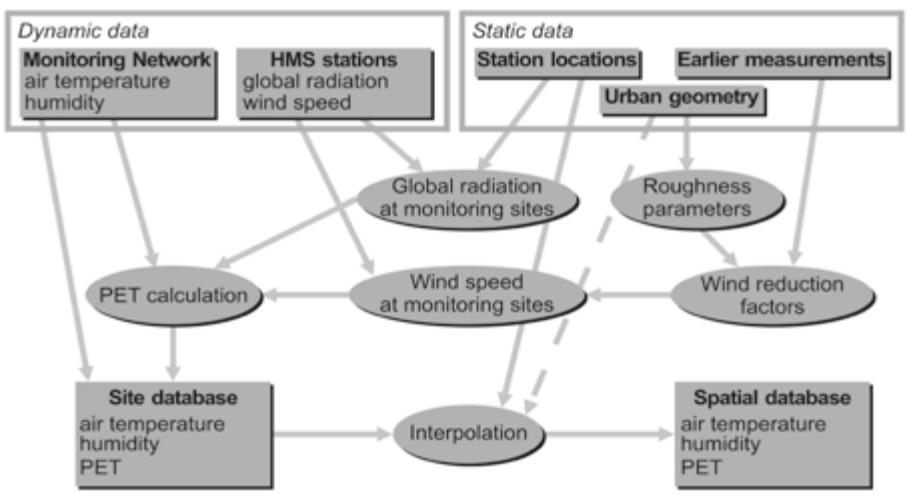

Fig. 6. Flow chart of the automatic data processing of the monitoring system

The received data from the monitoring network are stored in one text file per day on the server, and also stored in a MySQL database. Every 10 minutes a Java software calculates the PET value describing the human comfort conditions (see Section 3.1.) for each station using

the temperature and relative humidity values measured there, as well as global radiation and wind speed data measured at the HMS stations (*Fig. 6*). The results of this calculation are also stored in the MySQL database (*Fig. 6*). On the homepage the data stored in the MySQL database are displayed by charts using PHP scripts.

For the automatic interpolation of the spatial patterns of the measured and calculated data a Java software was developed. This program applies simple linear interpolation for a 500 m resolution grid of the study area using the data of the three nearest station of each grid point. In order to avoid the incorrect interpolation in the edge of the study area, the two rural stations considered as the background station, thus at the bordering (non-urban) grid points we used the data of the nearest rural station, and all of these points were added to the original measurement points for the interpolation (*Fig. 6*). The coordinates of the grid points and the stations are in the Unified Hungarian Projection, but at the end of the interpolation they were converted to WGS84 latitude and longitude coordinates because it is more appropriate for the further processing (drawing maps with GrADS, comparing the measurements with weather prediction models). At the first hand we applied a weighting constant (currently it is 1) in the interpolation and after further investigations we will alter this constant using the statistical connection between the surface parameters (e.g. built up ratio, SVF, green area, water surface) and the measured temperature, relative humidity or the PET in order to increase the precision of the interpolation (*Fig. 6*). The final patterns are stored in another, the spatial database, which is technically a NetCDF file. The public project homepage presents these patterns as maps created by GrADS and PHP scripts.

4. Intra-urban variation of the measured and calculated parameters

In this section the intra-urban differences in the thermal and human comfort conditions are illustrated in selecting time periods when the weather conditions promoted the microclimatic effects of the spatially varied surface features.

4.1. Temperature data series – comparison of LCZs' thermal reactions

The distinct thermal behaviour of the different LCZ areas is shown during a 48 h cloudless period between 29 and 31 March 2014 (from morning to morning) as an example. This period is characterized as a pleasant spring weather. According to the data of the rural HMS station, the insolation was undisturbed during the daylight hours with maximum values of 750-780 Wm^{-2}. The air movement was moderate (0-3 ms^{-1}) except of the first few (daytime) hours (~4-5 ms^{-1}). The days were rather warm with maximum values of 18-20ºC, but the mornings were a bit chilly with the minimum values of 2-4ºC because of the intense nocturnal cooling provided by the cloudless sky.

In order to compare the temperature variations of LCZs during the 48 h period the areal averages were calculated for every LCZ area. As the number of stations located at these areas are different because of their different areal extent (from one in LCZ 2 to ten in LCZ 6, see *Fig. 2* too) the *T*-averages based on original data with different number of sites. As a result seven temperature series are compared ($\Delta T_{LCZ\ X–Y}$), in accordance with the number of LCZs occur in the study area (except 'heavy industry' (*Fig. 7*).

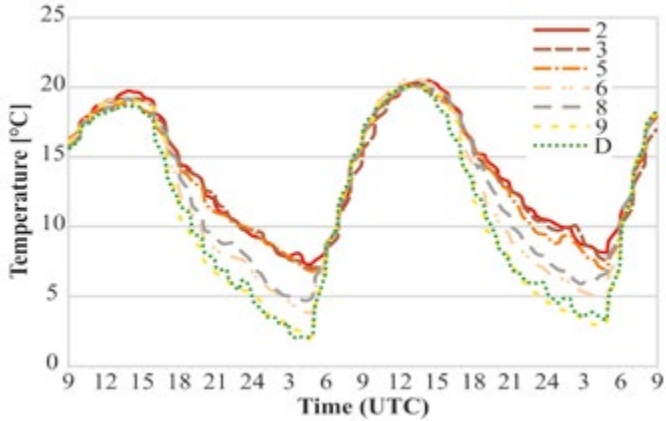

Fig. 7. Temporal variation of the mean LCZ temperatures during a 48 h period (29 – 31 March 2014)

As *Fig. 7.* shows the *T*-curves follow the regular shape of the daily temperature cycle in spring, that is warming in the daytime until early afternoon (~8-10 hours) then cooling until dawn (14-16 hours). As expected, the LCZ 2 area is the warmest and the LCZ 9 and LCZ D types are the coolest but this is really prevalent at night as in the daytime the curves almost move together. The largest temperature differences occur in the nocturnal hours: for example at 4.30 UTC $\Delta T_{LCZ\ 2–D} \sim 5$ºC, $\Delta T_{LCZ\ 5–D} \sim 4.5$ºC, but $\Delta T_{LCZ\ 8–D} \sim 2{,}5$ºC only, while $\Delta T_{LCZ\ 9–D} \sim 0$ºC at both night. This can be explained by the slower cooling of the built-up areas compared to the open and more vegetated rural areas because of the radiation processes at the mentioned weather conditions.

4.2. Maps on temperature, relative humidity and human comfort

During the processing of incoming data (see Section 3) high resolution maps are produced automatically showing the spatial structures of the thermal, humidity and human comfort conditions, which appear on the project website continuously updated in 10-minute interval (online) from June 2014.

As an example, in the case of air temperature and relative humidity we present the situations in the evening hours (2000 UTC, 7 April 2014). That day was also a typical nice spring one with some cloud drift so the global radiation was a bit disturbed, therefore in the most intensive period it varied between 550 and 780 Wm^{-2}. The temperature reached 19ºC at the rural HMS station and it was about 10 ºC at 2000 UTC. The daytime wind speed was 2-3 ms^{-1} then it decreased to about 1 ms^{-1} in the evening.

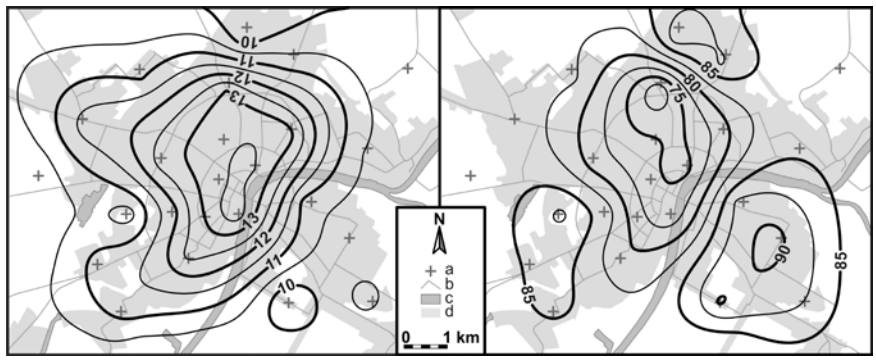

Fig. 8. Intra-urban patterns of temperature (ºC) and relative humidity (%) at 2000 UTC, 7 April 2014 (a – station, b – main road, c – water, d – urbanized area)

The *T*-pattern shows a typical 'island-like' shape with a maximum of over 13.5ºC in the inner city. The values decrease toward the outskirts until about 10ºC (as mentioned above in the case of rural HMS station). A small deviation from the quasi-concentric shape can be found in the western parts of the city, where small lakes and large green areas are predominant. An opposite case can be experienced for the RH: the largest values (85-90%) occur in the periphery and the smallest ones (under 75%) in the inner parts stretching a bit toward the hosing estates in the north-eastern parts of the city. The shape of the temperature pattern is mostly similar to the results of the previous UHI measurement campaign in Szeged (*Unger et al.*, 2001; *Balázs et al.*, 2009) thus the selection of the sites was really representative.

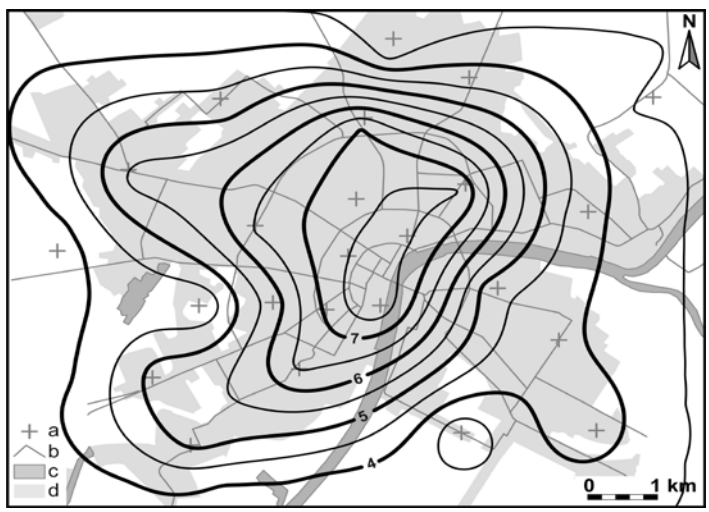

Fig. 9. Intra-urban pattern of human comfort conditions (PET ºC) at 1200 UTC, 7 April 2014 (a – station, b – main road, c – water, d – urbanized area)

In the case of human comfort conditions the *PET*-pattern for the daytime (1200 UTC) is presented. At that time the distribution of temperature (not shown) is almost homogeneous in the study area (with a variation of less than 0.5ºC around 17ºC) but in the *PET* values a

range of 20.5-25.5ºC occurs. Accordingly, there is comfortable thermal heat sensation (no stress level) in outer parts of the city (below 23ºC *PET*) and much of the city has been experiencing a very slightly warm sensation (slight heat stress level) (from 23 to 25.5ºC *PET* in the inner parts). Consequently, already in this nice and not too warm early spring day the environmental conditions in the inner urban parts can be a bit loading for the people. This can be explained by the altered wind conditions (lower wind speeds in the inner urban parts) with rather uniform insolation. This (thermal) load could be strengthened by the fact that after the colder winter days the thermal contrast (e.g. stronger sunshine) is rather large suddenly for the unprepared (not accustomed) people staying outdoors.

5. Conclusions and outlook

Based on this study the following conclusions can be drawn in accordance with the aims set in the Introduction:

Besides the two already existing measurement points 22 additional sites were selected within the seven delineated Local Climate Zones in Szeged in order to develop a representative urban human comfort monitoring network and information system.

The incoming data (*T*, *RH* from 24 stations, *G*, *T* and *RH* from the urban HMS station, as well as *G* and *v* from the two HMS stations) were processed by the following steps: firstly, G estimation for each station where it is not measured, then wind reduction for each station using roughness parameters, logarithmic wind profile and final adjustment using previous street level wind measurements. Secondly, PET calculation from the four meteorological parameters with a neural network method (MLP), then finally, linear interpolation of the measured and calculated parameters into a regular grid with 500 m resolution.

As public information, the maps about the thermal and human comfort conditions and additionally different graphs about the temporal variations of T, RH and PET appear in 10-minute time steps as a real-time visualisation on the project homepage (URBAN-PATH Project, 2014).

According to the preliminary outcomes as case studies, the largest intra-urban thermal differences between the LCZ areas in a two-day period occurred in the nocturnal hours reaching even 5ºC in early spring. These results confirm the findings of *Stewart* and *Oke* (2012), that is the thermal influence of any change or difference in landscapes (e.g. the different levels of urbanization) are better demonstrated using LCZ difference concept than a simple but generally not clear urban-rural approach, and additionally, it provides an opportunity for intra- and inter-urban comparisons. In the spatial distribution of human comfort conditions there are distinct differences in the strength of the loading or favourable environmental conditions between the neighbourhoods during the daytime. As the inhabitants can meet large differences even within relatively short distances, the urban areas can not be considered at all homogeneous from this respect.

In summary, as a result of the infrastructure development and related research in the frame of the URBAN-PATH project an operating urban human comfort monitoring network and information system was established in Szeged.

The utilization possibilities of the results in the future related to the high-resolution weather prediction models which can be applied in the urban environments – these are real alternatives of urban climate measurement networks – but their results are not yet adequate enough (*Case et al.,* 2008; *Chen et al.,* 2011; *Salamanca et al*., 2011). The real time predictions of urban meteorological environment are not only based on the attributes of static urban parameters (built-up ratio, sky-view factor, building heights etc.) because these data are basically constant in the prognostic time-scales. On the other hand the actual weather of a given urban region strongly depends on physical processes being worked in macro- and meso-

scales. The mentioned processes can be taken into account only using a well-defined, telescopic downscaling method with the help of a high resolution numerical weather prediction model (such as WRF). Today these high resolution models are directly able to predict the urban meteorological effects and give adequate data for a complex urban weather prediction system. Nevertheless the basic urban surface data sets and their attributes which are needed to make a successful forecast will have to be specified. Since the urban weather factors mainly work on meso-γ and micro-α scales the applied numerical model will be able to run with 300 m horizontal resolution and dense vertical layering. Based on the mentioned challenges it is important to implement a high-resolution urban static database into the WRF system as well as the global and local (urban) meteorological data assimilation are also required. An WRF-based urban meteorological prediction system can be able to give fundamental data for some new research aspects such as military, urban planning, public health etc. applications.

Acknowledgements
The study was supported by the Hungary-Serbia IPA Cross-border Co-operation Programme (HUSRB/1203/122/166 – URBAN-PATH), in case of the second author by the Hungarian Scientific Research Fund (OTKA PD-100352) and by the János Bolyai Research Scholarship of the Hungarian Academy of Sciences, and in case of the fourth author by the TÁMOP 4.2.4. A/2-11-1-2012-0001 „National Excellence Program – Elaborating and operating an inland student and researcher personal support system convergence program", which project was subsidized by the EU and co-financed by the European Social Fund.

References

Balázs, B., Unger, J., Gál, T., Sümeghy, Z., Geiger, J. and *Szegedi, S.*, 2009: Simulation of the mean urban heat island using 2D surface parameters: empirical modeling, verification and extension. *Meteorol. Appl. 16,* 275–287.

Bröde, P., Fiala, D., Błażejczyk, K., Holmér, I., Jendritzky, G., Kampmann, B., Tinz, B. and *Havenith, G.,* 2012: Deriving the operational procedure for the Universal Thermal Climate Index (UTCI). *Int. J. Biometeorol. 56*, 481–494.

Case, J., Crosson, W., Kumar, S.V., Lapenta, W.M. and *Peters-Lidard, C.D.*, 2008: Impacts of high-resolution land surface initialization on regional sensible weather forecasts from the WRF model. *J. Hydromet. 9*, 1249–1266.

Chen, F., Kusaka, H., Bornstein, R., Ching, J., Grimmond, C.S.B., Grossman-Clarke, S., Loridan, T., Manning, K.W., Martilli, A., Miao, S., Sailor, D., Salamanca, F.P., Taha, H., Tewari, M., Wang, X., Wyszogrodzki, A.A. and *Zhang, C.,* 2011: The integrated WRF/urban modelling system: development, evaluation, and applications to urban environmental problems. *Int. J. Climatol. 31*, 273–288.

Counihan, J., 1975: Adiabatic atmospheric boundary layers: A review and analysis of data from the period 1880-1972. *Atmos. Environ. 9*, 871–905.

Égerházi, L., Kántor, N., Takács, Á. and *Unger, J.*, 2012a: Patterns of attendance and thermal conditions on a pedestrian street. *Proceed of the 8th Int. Conf. on Urban Climate.* Dublin, Ireland, Paper no. 170.

Égerházi, L., Kántor, N., Takács, Á., Gál, T. and *Unger, J.*, 2012b: Thermal stress maps validation with on-site measurements in a playground. *Proceed of the 8th Int. Conf. on Urban Climate.* Dublin, Ireland, Paper no. 169.

Foken, T., 2008: Angewandte Meteorologie. Springer, Berlin–Heidelberg, 306 p.

Gál, T. and *Unger, J.*, 2009: Detection of ventilation paths using high-resolution roughness parameter mapping in a large urban area. *Build. Environ. 44*, 198–206.

Gál, T. and *Unger, J.,* 2013: Calculation of the aerodynamical roughness parameters using building and tree-crown database. In: *Pajtókné Tari I, Tóth A* (eds): *Changing Earth, Changing Society, Changing Learning – The role of renewable energy in regional development Int. Conf.* Eger, Hungary, 43–48.

Hall, M., Frank, E., Holmes, G., Pfahringer, B., Reutemann, P. and *Witten, I.H.*, 2009: The WEKA data mining software: an update. *ACM SIGKDD Explorations Newsletter 11*, 10–18.

Haykin, S., 1999: Neural Networks: a comprehensive foundation (2nd ed.). Prentice Hall, Upper Saddle River, NJ.

HiTemp Project, 2014: High Density Measurements within the Urban Environment. http://www.birmingham.ac.uk/schools/gees/centres/bucl/hitemp/index.aspx. Last accessed: 10 April 2014.

Kántor, N. and *Unger, J.,* 2010: Benefits and opportunities of adapting GIS in thermal comfort studies in resting places: An urban park as an example. *Landsc. Urban Plan. 98,* 36–46.
Kántor, N., Gulyás, Á., Égerházi, L. and *Unger, J.,* 2011: Assessments of the outdoor thermal conditions in Szeged, Hungary: thermal sensation ranges for local residents. In *Gerdes, A., Kottmeier, C.* and *Wagner, A.* (eds): *Climate and Construction Int. Conf*. Karlsruhe, Germany, 181–190.
Kántor, N., Égerházi, L. and *Unger, J.*, 2012: Subjective estimation of thermal environment in recreational urban spaces—Part 1: investigations in Szeged, Hungary. *Int. J. Biometeorol. 56,* 1075–1088.
Lelovics, E., Unger, J., Gál, T. and *Gál, C.V.,* 2014: Design of an urban monitoring network based on Local Climate Zone mapping and temperature pattern modeling. *Climate Res.* (doi: 10.3354/cr01220)
Matzarakis, A. and *Mayer, H.,* 1996: Another kind of environmental stress: thermal stress. *WHO Newsletter 18,* 7–10.
Matzarakis, A., Rutz, F. and *Mayer, H.,* 2007: Modelling radiation fluxes in simple and complex environments—application of the RayMan model. *Int. J. Biometeorol. 51,* 323–334.
Mayer, H. and *Höppe, P.,* 1987: Thermal comfort of man in different urban environments. *Theor. Appl. Climatol. 38*, 43–49.
Nakamura, Y. and *Oke, T.R.,* 1988: Wind, temperature and stability conditions in an east-west oriented urban canyon. *Atmos. Environ. 22,* 2691–2700
Oke, T.R., 1987: Boundary Layer Climates. (2nd ed.) Routledge, University Press, Cambridge, 435 p.
Petralli, M., Masetti, L., Brandani, G. and *Orlandini, S.,* 2013: Urban planning indicators: useful tools to measure the effect of urbanization and vegetation on summer air temperatures. *Int. J. Climatol. 34,* 1236–1244.
Salamanca, F., Martilli, A., Tewari, M. and *Chen, F.,* 2011: A study of the urban boundary layer using different urban parameterizations and high-resolution urban canopy parameters with WRF. *J. Appl. Meteorol. Climatol. 50*, 1107–1128.
Scharf, L.L., 1991: Statistical signal processing. Vol. 98. Reading, MA: Addison-Wesley, 515 p.
Spagnolo, J. and *de Dear, R.,* 2003: A human thermal climatology of subtropical Sydney. *Int. J. Climatol. 23*, 1383–1395.
Stewart, I.D. and *Oke, T.R.,* 2012: Local Climate Zones for urban temperature studies. *Bull. Am. Meteorol. Soc. 93,* 1879–1900.
Stewart, I.D., Oke, T.R. and *Krayenhoff, E.S.,* 2014: Evaluation of the 'local climate zone' scheme using temperature observations and model simulations. *Int. J. Climatol. 34,* 1062–1080.
Unger, J., Sümeghy, Z., Gulyás, Á., Bottyán Z. and *Mucsi, L.*, 2001: Land-use and meteorological aspects of the urban heat island. *Meteorol. Appl. 8,* 189–194.
URBAN-PATH Project, 2014: Evaluations and Public Display of Urban Patterns of Human Thermal Conditions. http://urban-path.hu/. Last accessed: 20 April 2014.
Watkins, R., Palmer, J., Kolokotroni, M. and *Littlefair, P.,* 2002: The London heat island: Results from summertime monitoring. *Build. Serv. Eng. Res. Technol. 23,* 97–106.